December 1989

FINAL REPORT

for the Period January 1987 - December 1989

ELECTROCHEMICAL INCINERATION OF WASTES

Prepared by

L. Kaba, G.D. Hitchens, and J.O'M. Bockris
Surface Electrochemistry Laboratory
Texas A&M University
College Station, Texas 77843, U.S.A.

Prepared for

NAGW-1779

ELECTROCHEMICAL INCINERATION OF WASTES

L. Kaba, G.D. Hitchens, J.O'M. Bockris

Surface Electrochemistry Laboratory
Department of Chemistry, Texas A&M University
College Station, Texas 77843, U.S.A.

INTRODUCTION

The disposal of domestic organic waste in its raw state is a matter of increasing public concern. Earlier, it was regarded as permissible to reject wastes into the apparently infinite sink of the sea but, during the last 20 years, it has become clear that this is environmentally unacceptable [1,2]. On the other hand, sewage farms and drainage systems for cities and for new housing developments are cumbersome and expensive to build and operate [3,4]. New technology whereby waste is converted to acceptable chemicals and pollution-free gases at site is desirable. The problems posed by wastes are particularly demanding in space vehicles where it is desireable to utilize treatments that will convert wastes into chemicals that can be recycled. In this situation, the combustion of waste is undesirable due to the difficulties of dissipating heat in a space environment and to the inevitable presence of oxides of nitrogen and carbon monoxide in the effluent gases [5,6]. Here in particular, electrochemical techniques offer several advantages including the low temperatures which may be used and the absence of any NO and CO in the evolved gases.

Work done hitherto in this area has been restricted to technological papers, and the present report is an attempt to give a more fundamental basis to the early stages of a potentially valuable technology.

1

THE ELECTROCHEMISTRY OF ORGANIC OXIDATION TO CO_2

Aqueous solutions have an electrode potential window in which substances can be oxidized without competition from oxygen evolution up to about 1.6 V on the normal hydrogen scale in acid solution at 25°C. Correspondingly, the oxidation potentials of some organic compounds found in human waste and chemicals derived from biomass are shown in Table 1. It should be possible, therefore, to carry out a complete oxidation of all the components in fecal wastes, including urea, to CO_2 in aqueous solution. Correspondingly, a number of organic solvents exist that offer an extended potential range for waste oxidation without competition from the oxygen evolution reaction (see Table 2), although the reduced conductivity available in such system (even in the presence of suitable salts) would have to be taken into account [10]; the most anodic potential used in the present work was 1.9 V versus the Normal Hydrogen Electrode (NHE).

On the other hand, if the oxidation of wastes is incomplete in aqueous solution, there is a possibility of introducing them into molten carbonate systems at 650°C and using anodic oxidation under these or similar conditions [11,12]; it may be that a considerable degree of thermal oxidation of the wastes would occur at 650°C with bubbled oxygen in the presence of the typical lithium potassium carbonate mixture without the application of potential.

The temperature coefficients of waste oxidation reactions are important in view of the work of Horri [13], who found that when lowering the temperature to 0°C, during the reduction of CO_2 on Cu, a 90% yield of methane was obtained. At present, little is known about the temperature coefficient of organic oxidation reactions, but in Kolbe-like oxidation reactions of material formed from the dissolution of coal [14], it was found that, (dE/dT)

2

- 4×10^{-3} V/°C and (dI/dT) - 0.1 mA/°C. From considerations of the oxidation of coal product, it seemed that - an expected range for the oxidation of wastes would be around 1.0-1.5 V (vs NHE), thus, not enough to decompose water significantly on platinum.

The electrode materials for waste oxidation in aqueous solutions should be inexpensive, remain un-oxidized under the highly anodic conditions (i.e. be an oxide) and be a poor electrocatalyst for oxygen evolution. Lead dioxide is often used for organic oxidations since it is highly conducting (it is used as a battery material) and has a high overvoltage for oxygen evolution [15,16]. This field is open to new oxide electrodes that have come to be used in recent years [17]. Among these are the perovskites [18], where the addition of 20-30% barium oxide to the materials such as lanthanum nickelate allows a conducting oxide to be used as an electrode which is stable to oxygen attack. In addition, Ebonex (Ti_4O_7) may be used which is an extremely stable anodic or cathodic material in acid environments [19].

Although, electrochemical oxidations are an important means of obtaining high-value chemical feedstocks from waste biomass [20], little information is available on the complete oxidation of carbonaceous material to CO_2. Bockris et al [21] showed that carbohydrates are completely oxidized to CO_2 during electrolysis. Initially, the electrolysis was performed on simple carbohydrates, such as sucrose, cellobiose (β.D-glucose dimer) and glucose, in 40% H_3PO_4 or 5N NaOH at temperatures of 80-100°C. A platinized platinum gauze (52 cm^2) was used as the anode. The reactivity decreased for molecules of increasing complexity. Nevertheless, it was found that cellulose could be broken down to CO_2 with a current efficiency of around 100% and only 2 faradays were involved in the evolution of 1 mol of CO_2 perhaps because of

preliminary hydrolysis reactions. Oxidation reactions of casein have been studied on platinum in 1N NaOH [22].

The electrolysis of waste mixtures can be achieved indirectly by the anodic generation of oxidizing agents which themselves bring about the oxidation of carbonaceous material in the solution. This approach has been utilized for urine purification in regenerative life support systems that were based on the generation of activated chlorine (Cl_2, HOCl and OCl^-) as the oxidants from Cl^- in urine [9,23,24]. These studies showed that close to 100% of the organic material could be removed by electrolysis using planar electrodes. Additional features include the production of OCl^-, a strong disinfectant and bleaching agent. Also, the generation of activated chlorine has been used as an effective means of treating mixtures of urine and fecal waste from humans [10,25]. Through the electrochemical generation of activated chlorine on platinum electrodes, the waste mixture could be decolorized and clarified using a current of 50 mA/cm^2; furthermore, the odor was quickly lost. No quantitative estimates of the products were available, although the evolution of CO_2, O_2 and Cl_2 was detected. An "indirect" electrochemical method of waste treatment has been developed recently by Delphi Research Inc [8]. In this approach, electrodes were used to regenerate redox couples which were circulated to a waste holding tank. The conversion of waste material such as cattle manure and wood chips into a pollution-free effluent which contained no carbon monoxide or oxides of nitrogen was achieved.

The use of new electrocatalysts, organic solvents to increase the range of potentials without interference of oxygen, wider temperature ranges, the use of various flow systems to increase the contact time and eventually

carbonate and other molten salts, belong to a later stage of the investigation.

METHODOLOGY

Electrochemical Cells and Apparatus

Two kinds of cells were used, and are shown in Figures 1 and 2.

The cell shown in Figure 1, was used for all of the work in which acid electrolytes were used. The volume of the anodic compartment was 400 cc's, the volume of the cathodic compartment was 200 cc's. Both the working and counter electrodes were fitted through the top of the cell in ground glass joints. The cell was continuously supplied with nitrogen as a means of sparging the gases from the electrolyte and additional stirring was by a magnetic follower at 6,000 rpm. The outlet gas was carried through a tube packed with glass wool, through a water trap and finally to a barium hydroxide solution. The cell rested on a hot plate, and the temperature was monitored using a thermometer fitted into the anodic compartment using a ground-glass joint. After each experiment, the glass cell was cleaned by treatment in an oven at 500°C in air to eliminate organic waste products, washed with sulfuric acid and washed finally with distilled water.

For experiments involving mixtures of biomass and urine (in the absence of added electrolyte, a U-tube cell was used (Figure 2). The cell had an internal diameter of 3 cm and was 25 cm high. Argon was used to sparge CO_2 from the electrolyte and the off-gases were collected as described above. The electrolyte was stirred with a magnetic follower. The volume of electrolyte was 400 ml. The working electrodes were either a platinum foil (100 cm^2), designed so that it occupied most of the volume of the cell on both sides, or a lead dioxide rod [9]; a Pt counter electrode was used in both cases. the cell was placed on a hot plate.

A Pine Instrument RDE4 potentiostat was used for voltage sweep

experiments and for galvanostatic and potentiostatic electrolysis described below. Current versus potential curves, and current versus time curves were recorded on a Hewlett Packard XY recorder (Model 7044B).

Waste Materials and Solutions

A synthetic mixture of material which represented the main constituents of feces was made up in a supply of 4.6 kg that was sufficient for all the waste experiments and was kept frozen between experiments. Though the nature of sewage and fecal waste [26] can vary considerably, generally, one-third of its contents is made up of microorganisms from the intestinal flora and approximately one-third is made from undigested fiber. The remainder is made up from lipids, and inorganic materials; the waste mixture shown in Table 3 reflects these proportions. The microorganisms Torpulina and E. coli were obtained in powdered form (Sigma Chemical Co) and the remaining contents were obtained from standard chemical suppliers. The mixture had a paste-like consistency and gave off a strong odor. The conversion factor wet waste: dry waste was determined by leaving known samples of waste in the oven at 150°C and the weight was monitored for a number of days until a constant value was obtained: 1g wet weight of waste was shown to be equivalent to 0.39 g dry weight. All amounts of waste are given in terms of dry weight.

For the experiments involving electrolysis in acid electrolytes, the material was weighed and treated in a pestle and mortar to which a small amount of 12 M sulfuric acid was added. The material was further homogenized in a 150-Watt sonicator (Fisher) for 20 minutes to reduce the particle size to 1 μm. Following this treatment, the waste material was transferred to the working electrode compartment containing the electrolytes. Sulfuric acid or 98%

7

phosphoric acid was used at 25-150 °C.

In the experiments involving urine-biomass mixtures, urine was collected from laboratory personnel and mixed with the solid waste material using the procedures described above.

Ultrasonic stirring: Use of ultrasonic devices to increase the limiting current density of waste oxidation on Pt.

Although normal stirring was maintained throughout the experiment at about 6,000 rpm with the magnetic stirrer, ultrasonic stirring was introduced, rather than a rotating disc electrode because of the difficulty of maintaining high speed rotation for prolonged periods in enclosed environments.

The human ear is sensitive to frequencies between 16 Hz and 16 kHz. Beyond 16 kHz lies the region of ultrasound. Typically ultrasonic processing was frequencies around 20 kHz. Ultrasonic inspection on the other hand is done with frequencies up to 20 MHz. The required power and frequency range useful for chemical requirements is generally produced by one or two methods Piezoelectric crystals or magnetostrictive devices. For chemical or electrochemical reactions, ultrasonic irradiation can be introduced in two ways.

The reaction vessel (round bottom flask) is immersed in a liquid usually water in a common laboratory cleaner with acoustic power of 100 watts and generating at a frequency of ca 50 Hz. (30), or a sonic horn generator can be placed directly into the reaction medium. The sonic horn uses a 20 kHz beam with total acoustic power of 100-600 watts (300 watts in our case) and acoustic intensities of 1-600 watts/cm^2 at the surface of the horn.

Ultrasonic Effects

The affect caused by ultrasound can be attributed to two phenomena.
1) There is a rapid movement of fluid caused by variation of sonic pressure which subjects the solvent to compression and rarefaction (reduction of the Nernst diffusion layer).

It is generally accepted that the formation and collapse of microbubbles (cavitation) is responsible for most of the chemical affect observed.

Ultrasonics and Electrochemistry (30, 46, 47, 48)

Several applications for ultrasonics have been found in the field of electrochemistry. These can be divided broadly into three classifications.
1) The effect of ultrasonic waves on electrodes processes.
2) The electrokinetic phenomena involving ultrasonics.
3) The use of ultrasonics as a tool in the study of the structure of electrolytic solutions.

In our work on the electrochemical oxidation of waste, a limiting current of 7 ma/cm^2 (geometric area of the electrode) was obtained by increasing the temperature to 150°C. The solution was a highly concentrated H_2SO_4 (12M). The aim of the use of ultrasounds was to investigate the increase in current density at low temperatures.

A high intensity ultrasonic processor (300 watts model from Sonics and Materials Inc.) was used. The ultrasonic power supply converts 50 - 60 Hz line voltage to high frequency 20 kHz electrical energy. The horn tip was ½" diameter.

A one compartment cell was used. The working electrode was Pt (12.5 cm^2 geometric area). The counter electrode was made of Pt. The reference

electrode was calomel. The solution was H_2SO_4 0.5M (400ml). The concentration of dry artifical fecal waste was 14 g/liter. The experiment was carried out at room temperature. When operating on a continuous mode the temperature of the solution increased. To avoid this phenomenon, the experiments were carried on pulse mode.

The tip of the ultrasonic generator, made of Titanium is put into the solution at various depths, and cyclic voltammogram is run between 0 and 1.6V (saturated calomel electrode) at different sound power output.

Sound Intensity

The sound intensity I is the amount of sound energy passing through a square centimeter in unit time. It is given either in erg/cm^2 or $watts/cm^2$, and may be represented for plane sound waves by the following relation.

$$I = pv/2 \ (\omega A)^2 = Pv/2 \ u^2 = P^2/2Pv = Pu/2$$

A is the maximum amplitude of the vibrating particles of a medium of density p, in which a sound waves of frequency $\omega/2\pi$, travel at the velocity v, P is the amplitude of the oscillating sound pressure and u is the acoustic quickness.

The measurement of sound radiation pressure is made by radiometer. An apparatus of this sort is formed in principle by a sort of torsion balance which carries on one side a mica plate, which is struck by the sound while on the other side there is a small balancing weight.

The intensities given in this report are the ratio of the power output at the surface of the horn, by the Platinum electrode surface area. These values

10

are therefore higher than the real values at the electrode surface.

Product Sampling and Chemical Analysis

Gases were continuously removed from the working electrode compartment as described above. The rate of CO_2 production was determined through back-titration of the $Ba(OH)_2$ with HCl solution. Gas samples were removed for gas chromatographic analysis through a septum placed in the gas flow immediately downstream from the reaction cell but before the water trap. Samples were taken up in a syringe and transferred to the gas chromatograph.

A VARIAN (model 3400) gas chromatograph with a carbo sieve II column with a thermal conductivity detector was used for the gas analysis. Helium or argon was used as the GC carrier-gas at a flow rate of 30 ml/min. Chromatograms were recorded using a HP3390A integrator which provided digital readouts of the retention times and integrated areas of the different peaks. The rate of CO_2 evolution was also monitored by gas chromatography and compared with the amount measured from the barium hydroxide trap. Calibration curves for CO_2 were performed on a regular basis. The CO_2 calibration graph gave a slope of 4.62×10^{-11} μl CO_2 per integrated count; this is equivalent to 2.06×10^{-4} moles of CO_2 per integrated count. The rate of CO_2 production measured by the GC was within 1-2% of that given by the barium hydroxide method. Gas chromatography was used to assay the off-gases for detection of carbon monoxide and methane. The procedure involved the addition of standard amounts of each of these gases to determine their retention time.

Determinations of NO and NO_2 in the gas stream were made using a Matheson-Kitagawa Model 8014.400A Toxic gas detector with Kitagawa Precision gas detection tubes; gas samples were taken from the sample port in the gas

stream as described above.

Molecular nitrogen analysis of the electrolyte was performed using a Perkin Elmer Elemental Analyzer which involves heating 1-3 mg of the sample at a temperature of $900^\circ C$ causing the sample to be volatilized. A helium gas stream transfers the vapor to separate detectors for H_2, N_2 and CO_2.

THE CHEMISTRY OF CARBONATE SYSTEMS (42,43,44) EQUILIBRIUM CONSIDERATION

Equilibrium Consideration

Carbon dioxide is widely used in gas absorption experiments owing to relative ease with which convnetional wet chemistry methods can be used to determine the liquid phase concentration.

In a strict sense CO_2 absorption into water is not a purely physical process because the carbonic acid (H_2CO_3) formed from the absorbed CO_2 dissociates into various ionic species until equilibrium obtains.

The reactions involved are as follows:

$$CO_2 \ (gas) = CO_2 \ (aqueous) \tag{1}$$

$$CO_2 \ (aqueous) + H_2O = H_2CO_3; \qquad k \tag{2}$$

$$H_2CO_3 \rightarrow H^+ + HCO_3^- \qquad k_1 = 4.3 \times 10^{-7} \tag{3}$$

$$HCO_3^- = H^+ + CO_3^{2-} \qquad k_2 = 4.7 \times 10^{-11} \tag{4}$$

$$H_2O = H^+ + OH^- \qquad k_w = 1 \times 10^{-14} \tag{5}$$
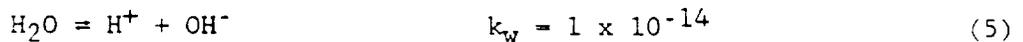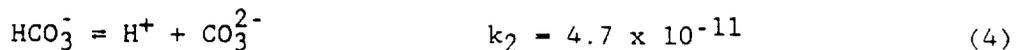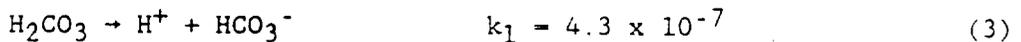
Since the concentration of CO_2 in solution and H_2CO_3 are tied together by the equilibrium relation

$$k = \frac{[H_2CO_3]}{[CO_2]} \tag{6}$$

It is not necessary to identify both species separately and it is costumary to use the term "carbonic acid" for the dissolved carbon dioxide present in a non-ionized form. From the relative values of the equilibrium constants, i.e., $k_1 \gg k_2 \gg k_w$, it is evident that the ionization reaction equation (3) is dominant provided some H_2CO_3 remains.

Now let us calculate the concentration of bicarbonate ions HCO_3^- amd the pH of the carbonic acid solution. for the reaction, equation (3).

$$k_1 = \frac{[H^+] \, [HCO_3]}{[H_2CO_3]} = 4.3 \times 10^{-7}$$

Since we can ignore other sources of the H^+ ion, we can put

$$[H^+] = [HCO_3]$$

solving for $[H^+]$ or $[HCO_3]$ we obtain

$$[H^+] = [HCO_3] = \sqrt{k_1 (H_2CO_3)}$$

and $r = \dfrac{[HCO_3]}{[H_2CO_3]} = \sqrt{\dfrac{k_1}{[H_2CO_3]}}$

when $[H_2CO_3]$ is 0, 001 M (typical concentration at the liquid-gas interface and bulk inlet in the present work) the corresponding mole ratio r of HCO_3^- is 0.65%. This means that only a very small fraction of absorbed carbon dioxide dissociates into the bicarbonate ion, and we can treat the system as if it is pure physical absorption.

From Eq. (7)

$$pH = -\log [H^+] = 3.2 - \frac{1}{2}\log [H_2CO_3]$$

so that the pH of saturated carbonic solution at 1 Atm and room temperature (0.034M) is 3.94. From the reaction given by equation (3) and (4) and ignoring the hydrolysis of water, equation (5) it is straigtforward to calculate the fraction of total carbonate present as H_2CO_3, HCO_3^- amd CO_3^{2-} as a functionof the pH of the mixed carbonate system at equilibrium. Fig. 49 shows the result in graphical form. It can be seen that the reaction (3) and (4) are complete at a pH of about 4 and 8.3 respectively.

G.2 <u>Titration of Carbonid Acid and Bicarbonate Ion</u>

Typical titration curves of carbonic acid with a strong base (curve a) and of the bicarbonate ion with a strong acid (curbe b) are shown in Figure 50. The H_2CO_3 equivalence point (pH = 8.3) correspond to the completion of reaction (3) and (4) respectively. The sharp pH change at the H_2CO_3 equivalence point was used for standardization of the HCl solution and in the present work using accurately weighed $NaHCO_3$.

The color change from violet to yellow at the end point of the titration was sharp when Phenol red indicator was used. Such procedures are standard and described in common quantitative analysis textbooks [42, 43]. The same method was employed to analyze the CO_2 from the waste oxidation reaction. From reaction (3) it follows that:

$$C_{HCO_3^-} = \frac{V_{HCl} \cdot C_{HCl}}{V_{H\,CO_3^-}}$$

where $C_{HCO_3^-}$ and V_{HCO_3} are the HCO_3^-concentration and volume of sample liquid, respectively, and C_{HCl} and V_{HCl} are the concentration and volume of HCl

solution consumed.

The CO_2 concentration can be determined using the HCO_3^- equivalence point (pH - 8.3) by titration with H or OH solution at the phenolyhtaein endpoint but the pH change is not sharp enough to give an accuracy of greater than 5%. A better method is to remove all the CO_3^{2-} ions by precipitation with $BaCl_2$ solution and back titrate the excess OH^- with standardized HCl solution to the phenolyhtalein endpoint. The overall reaction is:

$$CO_2 + 2OH^- = CO_3^{2-} + H_2O$$

$$CO_3^{2-} + Ba^{++} = BaCO_3$$

$$OH^- + H^+ = H_2O.$$
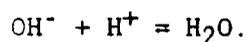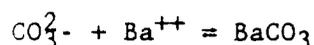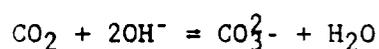
The solubility of CO_2 in water at 20°C is 0.04 mole liter^{-1}. the CO_2 formed during the anodic oxidation of waste is displaced from the anolyte by purging the solution with N_2 or Argon, in a solution of $Ba(OH)_2$. The amount of CO_2 produced is determined by back titration of the excess OH^- with HCl.

Chlorine Analysis

In the analysis of mixtures of fecal wastes and urine, chlorine evolution was examined by collecting the off-gases in the water trap described above.

Chlorine is easily dissolved under these conditions. The water was transferred to the trace analysis unit at Texas A&M and chlorine was determined by neutron activation analysis.

Neutron Activation Analysis (45)

Radioactive nuclei decay at a rate ($-dN/dt$) proportional to the number of nuclei present N

$$- \frac{dN}{dt} = \frac{0.693}{t_{\frac{1}{2}}} N$$

where $t_{\frac{1}{2}}$ is the half-life of the nuclide (time in which one half of the radioactive nuclei decay).

Radioactive isotopes (radionuclides) are produced artificially by exposing nuclei to neutrons from a neutron source, usually a nuclear reactor. For example, manganese, which occurs naturally as the manganese 55 isotope, is conveted by irradiation with neutron, designated $i_0 n$ to radioactive manganese -56.

$$^{55}_{25}Mn + ^{1}_{0}n \rightarrow ^{56}_{25}Mn$$
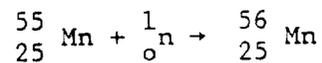
in this equation the superscript is the mass number of the species and the subscript is the atomic number. The managanese -56 product decays with a half life of 26 hours and emits γ rays with an energy of 0.85 million electron-volts (Mev). If Ni is the number of nonradioactive manganese nuclei present in the sample (Manganese -55 nuclei) the rate of production of radioactive P is given by the formula

$$P = f\sigma Ni$$

where f is the neutron flux (particles/cm^2/sec) and σ is the cross section ov

16

the isotopic being activated. The cross section expresses the tendency of the inactive nuclei to absorb neutrons and become activated. A high cross section increases the resistivity of the activation analysis of a particular nucleus.

Cl which occurs naturally as the Cl 37 is converted by irradiation to radioactive ^{38}Cl.

$$^{37}_{17}Cl + ^{1}_{o}n \rightarrow ^{38}_{17}Cl$$
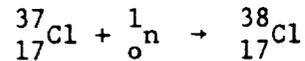
The ^{38}Cl decays with a half life of ~ 30 min, and emits gamma rays with energies of 1642 Mev and 2167 Mev.

Neutron activation analysis consists of three steps:

(1) Irradiating a sample with neutrons to produce radionuclides.

(2) Determining the activities of the radionuclide products

(3) Relating the activities to the quantities of the elements originally present in the sample.

Neutron Activation Analysis Sensitivity and Specificity

Neutron activation analysis in very sensitive technique. As little as 1 x 10^{-7}g of an element can be analyzed readily by neutron activation. Factors that contribute to high sensitivity are high cross section and high isotopic abundance of the potent isotope; low atomic weight; high neutron flux; and high detection efficiency. Cross section is the most important of these characteristics and varies by a factor of over 10^6 for various isotopes.

Although many elements can be determined by direct analysis of the gamma-ray spectrum of the sample after irradiation, a radiochemical separation is frequently necessary prior to "counting" the desired radionuclide.

This leads to another substantial advantage of neutron activation

analysis use of carriers. After the irradiation is completed, the total number of radionuclides of an element remaining at any given time is determined only by their half lives and not by any chemical reactions. Therefore, large quantities of the sought for element maybe added as a carrier after activation to facilitate chemical separation.

Specificity is a big advantage with NAA Radiochemical properties, half-life, gamma-energy, and beta energy are all properties that are used to distinguish elements analyzed by neutron activation analysis. Thus it is relatively easy to determine the element, and even the particular parent isotope of that element.

The calculation of the quantity of an element in a sample from all the factors contributing to the measured radioactivity (neutron flux, isotope cross section, counter efficiency) is feasible in principle, but very difficult in fact. Therefore, a standard consisting of a known quantity of the element being determined is almost always used in activation analysis.

Chlorine Analysis by NAA

In the analysis of mixtures of fecal wastes and urine, chlorine evolution was examined by collecting the off-gases in the water trap described above. Chlorine is easily dissolved under these conditions. The water was transferred to the trace analysis center at Texas A&M and chlorine was determined by neutron activation analysis.

About 2 ml of water sample is sealed into a 3.5 cc polyethylene vial. Standard solutions of known chlorine content are handled in the same ways (as well as an independent quality control check sample).

Standard samples and quality controls are sequentially analyzed by

irradiation in the Texas A&M University 1MW TriGa research reactor at a neutron flux of about 2×10^{13} neutrons cm^{-2} s^{-1} for ten (10) minutes. Following irradiation, the material are drawn from the vial using a syringe and a portion (~1.0 g) weighed into another (2/3 diam) polyethelene vial. After a delay of about five minutes (from end irradiation), the sample is placed in a high resolution lithium germanium [Ge(Li)] gamma ray detector. Characteristic gamma from the reaction product ^{38}Cl of 1642 and 2167 kev are detected and used for quantification. Sample are compared to standard materials to compute chlorine content. Detection limits in a water matrix are less than 0.1 ppm. A nuclear data 9900 multichannel pulse analyzer is used to accumulate nuclear spectra. The detector is a Camberra Ge(Li), resolution $\cong$ 1.8 kev ^{60}Co 1332 kev line, efficiency $\cong$ 12%.

TOTAL ORGANIC CARBON

Total Organic Carbon analysis of the electrolyte was determined by means of a Model 700 TOC Analyzer Infrared instrument in conjunction with a persulfate oxidation CO_2 trapping technique (EPA method 415). These measurements were made by O.I. Corp., College Station, Texas.

Total Carbon (TC)

Defined as all carbon in a sample, including inorganic, organic, and volatile carbon, as they may be present. TC is reported in terms of total mass of carbon per unit of sample (mg/l).

Total Inorganic Carbon (TIC)

Defined as that carbon is a sample which is converted to carbon dioxide

19

after acidification of the sample. TIC includes all dissolved carbon dioxide, bicarbonate, and carbonate species and is reported in terms of total mass of carbon per unit of sample (mg/l).

Total Organic Carbon TOC

Generally defined as that carbon in organic compounds which is converted to carbon dioxide by oxidation, after inorganic carbon has been removed or subtracted.

Dissolved Organic Carbon DOC

Defined as that organic carbon which is determined by analysis of aqueous sample which have been filtered through 0.45 μ filters. DOC is reported in terms of total mass of carbon per unit of

ppm: parts per million carbon

Defined as mass units of carbon for million sample mass units (μg/g). In aqueous samples this is generally taken to be the same as mgC/liter.

ppb: parts per billion carbon

Defined as mass units of carbon per billion sample mass units (ng/g). In aqueous samples this is generally taken to be the name as μC/liter.

Biochemical Oxygen Demand BOD

Defined as, an empirical that measures oxygen uptake by bacteria over a 3 - 5 day period.

Disadvantage of BOD.

1) Value is influenced by rapidly decomparable organic matter.

2) Value is influenced by rapidly decomparable inorganic substances

(chemical or biological activity)

3) Some organics are not decomposed in the 3 - 5 day test period (humics).

Chemical Oxygen Demand (COD)

Defined as oxygen consumed by a strong oxidant usually dichromate.

SPECTRUM OF WATER

ultra pure water	drinking water	waste water
5 - 20 ppb	10 ppm	100 ppm
		municipal
		industrial

Total Organic Carbon Measurement (TOC)

TOC is determined by the measurement of carbon dioxide released by chemical oxidation of the organic carbon in the sample. After the sample, has been acidified and purged of TIC, potassium fersulfate ($k_2S_2D_8$), a strong oxidizer, is added. This oxidant quickly reacts with organic carbon in the sample at 100°C to form carbon dioxide. When the oxidation reaction is complete, the carbon dioxide is purged from solution concentrated by trapping them desorbed and carried into a non dispersive infrared analyzer (NDIR) which has been calibrated to directly disply the mass of carbon dioxide detected. The resulting carbon mass in the form of carbon dioxide is equivalent to the mass of organic carbon originally in the sample.

EXPERIMENTAL RESULTS

A: ELECTROCHEMICAL REACTIONS OF BIOMASS COMPONENTS

A preliminary investigation of the general electrochemical reactions of biomass components was performed using each of the main constituent materials present in the artificial waste mixture i.e., oleic acid, cellulose, casein, and a microbial biomass consisting of Torpulina. These experiments were carried out in 12 M sulfuric acid.

(1) Oleic acid

Fig. 3 shows sweep voltamograms were performed for oleic acid at 150°C in vigorously stirred sulfuric acid using platinum electrodes. Fig. 4 shows that the limiting current increases with concentration up to a concentration of 3 g l^{-1}. At this point, the limiting current has attained a maximum value corresponding to the maximum solubility of oleic acid in sulfuric acid which is in the order of 0.01 M at 150°C.

Fig. 5 shows potential sweep curves as a function of electrolyte temperature which shows the potential region in which oxidation of oleic acid occurs at a reasonable rate. It is noteworthy that there are two limiting currents manifested on this curve. Finally, co-evolution of O_2 occurs when the potential reaches c. 1.8V.

Fig. 6 shows the limiting current plotted as a function of 1/T. The energy of activation is approximately 8.0 kcal $mole^{-1}$.

Fig. 7 shows a plot of the log current density as a function of potentials. These are not Tafel relationships in the normal sense, because the region being investigated is partly controlled by diffusion.

22

Finally, in Fig. 8, CO_2 is plotted as a function of time of electrolysis.
The reaction for the complete oxidation of oleic acid is given below.

$$C_{17}H_{38}COOH + 34H_2O \rightarrow 18CO_2 + 102\ H^+ + 102e^-$$
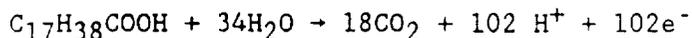
The current efficiency was calculated from the amount of CO_2 produced per hour
and the current as shown below.

CO_2 yield assuming 100%   = $\dfrac{I_L \times t \times 18}{102F}$ moles
current efficiency

where I_L is the limiting current in amps, t is time of electrolysis in

seconds, n is the number of electrons taking part in the reaction (102) per

molecule and F is the Faraday constant on coulombs. The current efficiency

calculated on this basis was around 200%.

(2) <u>Cellulose</u>

Fig 9 shows potential sweep measurements as a function of amount of

cellulose added to the electrolyte.

The limiting current density for the electrolysis as a function of added

cellulose is shown in Fig. 10. The limiting current does not increase after 7

$g\ 1^{-1}$.

Fig. 11 shows the current-potential curves as a function of the

electrolyte temperature. The limiting current occurs in the vicinity of 1.4

volts.

Log (i) as a function of 1/T is shown in Figure 12. The heat of

activation corresponds to about 7 kcal $mole^{-1}$.

Fig 13 shows a plot of the potential versus log current density. The

23

early part of this line, below the limiting current, shows a Tafelian behavior. The Tafel slope at 80° is c. 0.3.

In Fig. 14 shows the gross amount of CO_2 produced as a function of time at 150°C. After 20 hours the rate of evolution of CO_2 declines, corresponding to the exhaustion of carbonaceous material from the solution.

It is known that in acid conditions, cellulose is hydrolysed to glucose, thus, the following reaction was used in determining the Faradaic efficiency:

$$C_6H_{12}O_6 + 6H_2O \rightarrow 6CO_2 + 24H^+ + 24e^-$$

The results showed that for each CO_2 molecule, 2.8 electrons are required [cf. ref. 2]. It is likely that, in addition to hydrolysis, some oxidation had occurred to remove carbon atoms from glucose [see e.g. 21]. Faradaic efficiency was, thus, recalculated based on the following reaction:

$$C_5H_8O_7 + 3H_2O \rightarrow 5CO_2 + 14H^+ + 14e^-$$
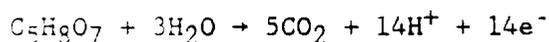
In this scheme, 2.8 electrons would be required for each CO_2 evolved which is consistent with the experimental results. The efficiency of 100% at 80°C is, however, exceeded at higher temperatures. At 150°C, similar calculation gives a current efficiency of around 300%, probably due to more extensive thermal degradation. At these higher temperatures, an efficiency of around 100% is obtained by assuming cellulose has undergone acid hydrolysis to oxalic acid which undergoes oxidation according to the following reaction:

$$H_2C_2O_4 \rightarrow 2CO_2 + 2H^+ + 2e^-$$
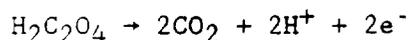
(3) <u>Casein</u>

Fig 15 shows potential sweep measurements as a function of the concentration of added material. From Fig. 16, the limiting current is seen to reach it maximum at about 6 grams per liter.

Fig. 17 shows potential sweep measurements as a function of temperature. Fig. 18 shows log i as a function of 1/T which gives an activation energy of about 6 k cal mole^{-1}. These curves are plotted in a log form in Fig. 19 and the lowest part of these curves gives a Tafel line which has a slope of about b = ¯0.2. Finally, Fig 20 shows the moles of CO_2 as a function of time and indicates a higher rate at the beginning, slowing to a constant rate after about ten hours.

(4) <u>Yeast (Torpulina)</u>

Potential sweep measurements as a function of yeast concentration are shown in Figure 21. The corresponding plots in Fig. 22 indicates a solubility, in terms of grams per liter, that is many times those of the other substances, i.e., the saturation value of the limiting current density occurs at about 20 grams per l^{-1} and the limiting current density is much higher than those of the other substances, i.e., c. 6 ma cm^{-2}.

Fig. 23 is a plot of i against V at various temperatures. The corresponding log i_L versus 1/T plot is shown in Fig 24; the heat of activation is 7 k cal per mole.

The corresponding log plots are given in Fig. 25, and yield a Tafel slope for the low regions of c. 0.2.

The plot of the evolution of CO_2 as a function of time over the first 22 hours is shown in Fig. 26.

Finally, in **Fig. 27** is a collection of the data for the four components examined shown on a log scale.

PHENOMENOLOGICAL CONCLUSIONS FROM THE ELECTROLYSIS OF INDIVIDUAL COMPONENTS

1) The limiting currents, in amps cm^{-2}, increased with the increase of the size of the molecule concerned.

2) The energies of activation are about the same (c. 6 ± 1 kcal $mole^{-1}$) for all the substances examined.

3) The i-V curves have a limiting current plateau around 1.4 V for cellulose, casein and yeast, and 1.7 V for oleic acid.

4) The Tafel lines have slopes of c. 0.2 - 0.3.

B: ELECTROCHEMICAL REACTIONS OF FECAL WASTES

Platinum Electrodes:

Fig 28 shows the i-V behavior for concentrations of added waste material

between 4.6 and 23.4 g l^{-1}. The limiting currents are in the range 1.7 and

3.5 mA cm^{-2}.

Fig. 29 shows limiting current densities as a function of waste

concentration. The maximum solubility appears to be in the region of 20 g l^{-1}

in 12 M sulfuric acid at 150 ^{o}C.

The temperature variation of the limiting current, in both sulfuric and

phosphoric acid, is seen in log scale in Fig. 30. The heat of activation is

c. 7 kcal $mole^{-1}$ in H_3PO_4 and 9 kcal $mole^{-1}$ in H_2SO_4.

Fig. 31 shows the log i-V curves for a concentration of 14 grams per

liter at three temperatures. The limiting plateau occurs between 0.1 and

about 4 ma per cm^{-2}.

In similar experiments on the electrolysis of dissolved products from

coal, it was found by Murphy and Bockris [14] that addition of cerric

compounds was effective in increasing the current density. similar work has

been performed by Su Moon Park and colleagues [27].

For the present case, the addition of ceric compounds increases the

apparent limiting currents at 150°C for the various concentrations. Fig. 32

shows that the increase is c. 5 times that obtained for the oxidation without

the ceric compound.

However, in Fig. 33 is shown the net electrochemical CO_2 yield as a

function of time in the absence of ceric. Comparing the apparent increase in

limiting current (Fig. 32) with the increase in CO_2 (Fig. 33), the 5-fold

increase in current does not give an equivalent increase in CO_2: the CO_2 produced increased by only 1.4-fold in the presence of cerium.

Thus, the apparently excellent increase in current of Fig. 32 is due largely to oxidation of the cerous ion, and the concomitant take-up of the oxidation of the fecal wastes in the solution by the ceric is less than the increase in the limiting current. Thus, the coupling of the chemical oxidation of the wastes by Ce^{4+} in solution is clearly inadequate to keep up with the more rapid oxidation of the cerous ions at the electrode.

Effect of Ultrasonication

The electrode was irradiated with ultrasound using a 1/2 inch diameter horn tip. Fig 34 shows that the current flow could be increased approximately 2.5 times compared to the unagitated solution. The linearity of the limiting current density with the power output per cm^2 (Fig. 35) suggests that it is reasonable to expect that a current flow increase with a more powerful sonicator.

Lead Dioxide Electrodes:

Figure 36 is the i-V behavior for different amounts of added waste at lead dioxide electrodes.

The variation with temperature of the i-V curves is shown in Figure 37. The limiting current versus 1/T is shown in Figure 38 and gives a heat of activation of approximately 5 kcal mol^{-1}.

In Fig. 39, the ratio of the yield of CO_2 at a constant time (say, 10 hours) in the presence and absence of ceric ions is only about 1.2. It is thus seen that the yield of CO_2 after ten hours is about twice times on lead

dioxide than on the platinum.

TOC levels

During the electrolysis, TOC in the electrolyte was reduced by 95% as shown in Fig. 40. Between the start and end of the electrolysis, considerable visible change in the nature of the waste solution ocurred. The material started as a dark black solution where particulate material could easily be distinguished but as the electrolysis proceded, the solution become transparent to light.

PHENOMENOLOGICAL CONCLUSIONS

1. The limiting currents for the fecal solid wastes were c. 3 ma per cm^{-2} at 150°C, and were obtained with a dissolved concentration of 25 grams per liter. Yeast makes the greatest contribution at about 5 ma per cm^{-2}.

2. The energies of activation for limiting currents were greater in sulfuric acid than in phosphoric acid, however, all other information shows sulfuric acid to be a more effective medium for electrolysis.

3. The limiting current plateaus occur at c. 1.4 V for the artificial waste fecal mixture, just as they do for most of the components. The Tafel slopes are c. 0.3 and the heat of activation ⁻ 7 k cal $mole^{-1}$.

4. The addition of ceric ions increases the real current density for the oxidation by c. 1.4 times.

5. Lead dioxide is a better electrocatalyst than platinum by a factor of about PPP.

6. The total organic carbon decreased by about 95% after 96 hours.

7. Carbon monoxide, nitrogen dioxide, nitrous oxide, ammonia and methane could not be detected in the gaseous effluent.

C.   ELECTROLYSIS OF SOLID WASTE & URINE MIXTURES

The results here concern the electrolysis of the artificial solid waste mixture described above in the presence of urine. The solid waste concentration was 30 grams per liter of urine.

In these experiments, 7 g of artificial waste was dissolved in 10 ml of urine and homogenized for 5 minutes using ultrasonication. A total of 230 ml of urine was then added to the homogenized mixture; the total volume of the electrolyte was 240 ml containing 7g of solid waste.

As shown in Fig. 41, during electrolysis over 72 hours, the pH of the mixture decreased from 6 to 2. The current-voltage curve (Fig. 41) shows that the peak, that corresponds to the limiting current region occurring at 1.4 V, is shifted to somewhat more anodic regions at the pH drops as would be expected for organic oxidation reactions. The return cathodic sweep does not correspond to the anodic sweep because of diffusion of products into the bulk solution.

In Fig. 42 is the CO_2 production as a function of time at 37°C and 60°C. The area of the electrode is c. 100 cm^{-2}, i.e. the current density is c. 8 ma cm^{-2}. (ie about double the current densities that were obtained in the absence of urine.)

Fig. 43 shows pH as a function of time, and Fig. 44 show the production of chlorine. A total volume of 3 cc's of chlorine was produced in 48 hours. It was difficult to detect the odor of chlorine in the off-gas. The corresponding production of CO_2 is about 600 c.c, therefore chlorine represents considereably less than 1% of the off gas by volume.

Fig. 45 shows the nitrogen remaining in the solution as a function of time. The decline in the nitrogen content is around half that of the total

31

organic carbon content.

Fig. 46 shows the production of CO_2 on lead oxide compared with that on platinum (Figure 42).

TOC levels

In Fig. 47 is the decrease in the total carbon present with time at 37°. It is seen that this decrease in 72 hours is about 78%. A carbon mass balance calculation was performed that showed a 90% correlation between CO_2 evolved and the decrease in TOC during the reaction. Fig. 48, however, shows a corresponding result on lead dioxide, and it is seen that there is a more even decline in TOC. After 96 hours of electrolysis, 82% of the TOC carbon had been eliminated from the electrolyte.

PHENOMENOLOGICAL GENERALIZATION (SOLID WASTES-URINE MIXTURES)

1. After c. 12 hours, the mixtures had become colorless, and had lost all fecal odor.

2. The pH shift for the voltametric peaks was around RT/F per pH unit.

3. The pH decline of the mixture began after about 48 hours of electrolysis.

4. The chlorine evolved was about 0.1% by volume of the evolved gases.

5. CO_2 production volume leveled off after about 48 hours, and at about double this time 80% of the TOC had been removed to form CO_2.

6. Carbon monoxide, nitrogen dioxide, nitrous oxide, ammonia and methane could not be detected in the gaseous effluent.

32

DISCUSSION

The limiting currents for waste oxidation in H_2SO_4 were in the region of 8 mA cm^{-2} (geometric area) on platinum and 20 mA cm^{-2} on lead dioxide electrodes. The heat of activation for these reactions were 6-7 kcal mol^{-1} which is characteristic for a diffusion controlled reaction. A plateau was observed in the potential sweep measurements in the region of 1.4-1.7 V, thus, it is likely that a reversible potential for waste exists in the region of 0.9 V and an additional voltage is due to an activation overpotential. The Tafel lines are not well developed though they have gradients of around 0.25 that are not exceptional for complex systems in the presence of a large amount of impurities.

By assuming that the reversible potential is in the region of 0.8V an approximate estimation of the exchange current density can be made using the following relationship:

$$\eta = 0.25 \log i/i_0$$

Where η is the overpotential, i is the average current in the limiting region $(5.10^{-3}$ A $cm^{-})2$, an i_0 of 3.10^{-6} A cm^{-2} was calculated at 150°C. It is noteworthy that if the temperature could be increased a further 25°C the limiting current would be increased 1.5 times and achieve a value of 7.5 mA cm^{-2}.

A flow-through electrode in which the dissolved organic compounds have to be recirculated over a large electrode area, has several advantages over stationary electrodes. The advantage is primarily connected with the substantial or almost total decrease of mass transport limitation. One consequence of using such electrode is that interior mass transfer and ohmic

33

resistance effect may lead to a non-uniform potential distribution, thereby, affecting the selectivity which might otherwise be achieved. A flow through electrode greatly increases the ratio of electrode area to solution volume therefore give a large reaction rate. Based on a semi-empirical model, Sioda [41] found that the limiting current obtained on a flow through porous electrode is expressed by the following equation.

$$I = nFC_oVR$$

n is the number of electrons transferred per molecule of the electroactive species, F is the Faraday constant, Co in the initial concentration, v is the flow rate, and R is the limiting degree of conversion of the electroactive species. The limiting degree of conversion is given by the following equation

$$R = 1 - \exp(-jsa^{1-\alpha} v^{\alpha-1} L)$$

where s is the specific internal surface, a is the cross section area, L is the length of the porous electrode and j and α are constants, α being a fraction of 1.

Ceric ions enhanced the current density and enhanced the rate of breakdown of waste to CO_2. Mediators have been shown to play an important role in the breakdown and upgrading of coal slurries [27 29]. Redox mediators were used based on the notion that they would have a lower i_0 than that of the organic materials and carry out homogeneous oxidation of the materials in solution. However, the increase in current density of only 1.5 was rather disappointing. The standard redox potential of Ce^{3+}/Ce^{4+} reaction is 1.45 V,

34

consequently, the overpotentials used in the experiments were insufficient to oxidize these redox mediator at high enough rates to greatly enhance the oxidation of material in solution. Possibly, it would be advantageous to use mediators with redox potentials lower than that of Ce^{3+}/Ce^{4+}, such as Fe^{2+}/Fe^{3+} (0.69V in 1M H_2SO_4) or Br_2/Br^- (1.08V). The combinations of catalysts such as Co^{2+} with Fe^{2+}/Fe^{3+} for the oxidation of wood waste and V^{5+} with Fe^{2+}/Fe^{3+} for cattle waste and sewage sludge oxidation, have been used by Dhooge [8].

Lead dioxide was more effective at waste oxidation that platinum presumably due to reduced competition from oxygen on lead dioxide although this approach would benefit from the use of advanced electrocatalytic materials. A substoichiometric oxide of titanium known commercially as EBONEX with Ti_4O_7 as the predominant material is of interest in the context of the present work. This electrocatalytic material exhibits high chemical stability in both acid and alkaline environments and can function alternately as an anode and a cathode without degradation. The material has a high surface porosity and has an overpotential for oxygen evolution of 1.7 V in 1M H_2SO_4. The principal use for this material at present is in the formation of OCl^- from Cl^- without the formation of deposits and electrode poisoning effects, thus, it use may be important in the approach involving the treatment of solid waste and urine mixtures by the hypochlorite route.

For a rotating electrode, the limiting current for a reversible reaction controlled only by mass transfer is given by the Levich equation.

$$i_L = 0.62 \times n \times F \times D^{2/3} \, \upsilon^{-1/6} \times C \times \omega^{1/2}$$

Assuming that the kinematic viscosity is 0.04 cm^2/s, $D = 10^{-4}$ cm^2/s and $C = 10^{-2}M$, to get a limiting current value of 8 mA/cm^2 ω should be equal to 10,000 rpm. To increase the current density 10 times, would require 10^5 rpm which is unrealistic. Alternativly, the use of ultrasonics is attractive for the purpose of increasing the limiting current. The action of ultrasound, up to 7 W cm^{-2} increased the current density of waste oxidation 2.5 times (see Figure 34). The increase in current density was linear with power output and, thus, it is reasonable to expect a greater increase in current density could be attained at greater ultrasound intensities. Huck et al [30] showed that ultrasound at 2 W cm^{-2} increased the limiting current by one order of magnitude for the electrochemical reactions of Fe^{2+}/Fe^{3+} and $[Fe(CN_6)]^{3-}$/$[Fe(CN)_6]^{4-}$ due to cavitation. A further investigation is therefore required to determine if increased power output per electrode area can substantially increase the current density for waste oxidation.

Electrolysis of solid waste-urine mixtures appears to be a highly effective means of waste treatment. Immediately after the start of electrolysis the mixture was decolorized and the characteristic odor of the waste was eliminated. This process operates through an activated chlorine mechanism involving the generation of either OCl^- or $HOCl$ at the anode from Cl^- from urine. Relatively little chlorine was evolved during the electrolysis. This process does not require expendable chemicals or the use of strong acids and elevated temperatures, thus, is attractive for use in CELSS and further development of this processing technique is warranted.

An immediate goal in the development of this process is the investigation of electrocatalysts for both the anode a cathodic reactions. Candidate electrodes for the formation activated chlorine in aqueous saline solutions

consist of a mixture of ruthenium dioxide and titanium dioxide metal base; further examples are given in a recent review [17].

Maintaining the electrodes in an active form will require attention since the electrodes will tend to poison with time. Pulse techniques and electrode regeneration [31] have the capability to reduce this problem.

An assessment of the operational parameters of a waste electrolysis subsystems can be made based on the experiments described above and from information on solid waste production in closed life support systems. Information on the later is given by Wydeven [32] who estimated solid waste production, including urine solids to be 128 g dry weight man day^{-1} and this value has been used in calculations of the operational parameters of a waste electrolysis subsystem. In the experiments described above (see e.g. Fig. 47) electrolysis using an electrode with a geometric area of 220 cm^2 (real area) resulted in a decrease in TOC of 4.8 g over a 24 hour period. Calculations show that to oxidize 128 g TOC over a 24 hour cycle an electrode of 0.5 m^2 is required. Through the use of electrodes such as platinized platinum which have roughness factors usually in the range of 100, about 53 cm^2 would be necessary.

Power requirements for a electrolysis subsystem operating on a 24 hour cycle are calculated below using a current density of 4 mA cm^{-2}, and assuming the cell voltage to be 2 V.

Total current = 0.004 x 5000

= 20 A

Power = 20 x 2

= 40.0 W

Under the conditions used in these experiment approximately 200 liters of hydrogen will be evolved from the cathode. If the evolved hydrogen is recycled in a fuel cell operating at 60% efficiency, approximately 34% of the electrical energy utilized in the electrolysis can be generated.

Particular advantages of waste electrolysis using activated chlorine over combustion are the low operating temperatures and apparent absence of carbon monoxide and oxides of nitrogen detected in the effluent gas. Carbon dioxide is the predominat gas in the effluent although N_2 may be present inaddition to O_2 formed from the competing oxygen evolution reaction. Carbon dioxide can be utilized for the regeneration of oxygen in closed life support system using for instance the Sabatier [33] Bosch [34] or CO_2 reduction on solid oxide electrolyte cells [35]. In addition, CO_2 is a valuable resources for food generation using plants or for cell protein on long-duration space missions [36,37].

REFERENCES

1. A.F.M. Barton, "Resource Recovery and Recycling" John Wiley and Sons, New York, (1979).

2. J.O'M. Bockris, ed., "Electrochemistry of Cleaner Environments", Plenum Press, New York (1972).

3. L. Lessing, Fortune July (1973) 133.

4. R.M.E. Diamant, in: "Environmental Chemistry" (ed., J.O'M. Bockris) Plenum Press, New York, p 95 (1977).

5. W. Strauss, in: "Environmental Chemistry" (ed., J.O'M. Bockris) Plenum Press, New York, p 179 (1977).

6. D.J. Spedding, in: "Environmental Chemistry" (ed., J.O'M. Bockris) Plenum Press, New York, p 213 (1977).

7. D.F. Putnam and R.L. Vaughan, SAE Life Support and Environmental Control Conference, San Francisco, California, July 12-14 (1971).

8. P.M. Dhooge, J. Space Manufacturing, Proceedings of the 8th Princeton/AIAA/SSI Conference, American Institute of Aeronautics and Astronautics Washington DC. (1987).

9. R.G. Tischer, P.P. Tischer, L.R. Brown and J.C. Mickelson, Dev. Ind. Microbiol. 4 (1963) 253.

10. F. Goodridge and C.J.H. King, in: "Technques of Electroorganic Synthesis Part 1", (eds., N.L. Weinberg) John Wiley and Sons, New York, p 7 (1974).

11. J. Greenburg, U.S. Patent Feb 15 , 3,642,583 (1972).

12. D.H. Kerridge, Pure Appl. Chem. 41(3) (1975) 355.

13. Y. Hori, N. Kamida, and S. Suzuki, J. Faculty Eng. Chiba Univ. 32 (1981) 37.

14. O.J. Murphy, J.O'M. Bockris and D.W. Later, Int. J. Hydrogen Energy 10 (1985) 453.

15. H. Sharifian and D.W.Kirk, J.Electrochem. Soc. 133 (1986) 921.

16. V. Smith de Sucre and A. P. Watkinson, Can. J. Chem. Eng., 59, 52 (1981).

17. S. Trasatti, ed., "Electrodes of Conductive Metal Oxides" Elsevier Scientific Publishing Co. Amsterdam (1981).

18. J.O'M. Bockris and T. Otagawa, J. Phys. Chem. 87 (1983) 2960.

19. M. Marezio and P.D. Dernier, J. Solid. State Chem., 3 (1971) 340.

20. H.L. Chum and M.M. Baizer, "The Electrochemistry of Biomass and Derived Materials" ACS Monograph 183, American Chemical Society, Washington D.C. (1985).

21. J.O'M. Bockris, B.J. Piersma and E. Gileadi, Electrochim. Acta 9 (1964) 1329.

22. C. Kiderov and G. Musaev, Electrochimiya 21(5) (1985) 698.

23. Lockheed Missles and Space Co. NASA Report CR-151566 (1977).

24. J.C. Wright, A.S. Michaels and A.J. Appleby, AIChE Journal 32(9) (1986) 1450.

25. R.G. Tischer, L.R. Brown and M.V. Kennedy, Dev. Ind. Microbiol. 6 (1965) 238.

26. A.C. Guyton, "Textbook of Medical Physiology" 6th Edition, McGraw Hill, New York (1981).

27. P.M. Dhooge, D.E. Stillwell and S-M Park, J. Electrochem. Soc. 129 (1982) 1719.

28. N.C. Taylor, C.Gibson, K.D. Bartle, D.G. Mills and G. Richardson, Fuel, 64 (1985) 415.

29. R.L. Clark, P.C. Foller and A.R. Wasson, J. Appl. Electrochem. 18 (1988) 546.

30. H. Huck, Bunsenges, Phsy. Chem. 91, 648, (1987).

30. J. Ghoroghchian and J.O'M. Bockris, Int. J. Hydrogen Energy, 10 (1985) 101.

31. S.J Yao, S.K. Wolfson, M.A. Krupper and K.J. Wu, in: "Charge and Field Effects in Biosystems" (M.J. Allen and P.N.R. Usherwood, eds.) Abacus Press Tunbrigde Wells U.K. (1985) 415.

32. T. Wydeven, NASA Technical Memorandum 84368 (1963).

33. R.K. Forsythe, C.E. Verostko, R.J. Cusick and R.L. Blakely, SAE Technical Paper 840936 14th ICES Conference, San Diego, California July 16-19 (1984).

34. K. Otsuji, O. Hanabusa, T. Sawada, S. Satoh and M. Minemoto, SAE Technical Paper 871517 17th ICES Conference, Seattle July 13-15 (1987).

35. A.O. Isenberg and R.J. Cusick, SAE Technical Paper 881040, 18th ICES Conference, San Francisco, July 11-13 (1988).

36. H.G. Schlegel, in, "Fermentation Advances", Academic Press, New York (1969).

37. G.R. Peterson, B.O. Stokes, W.W. Schubert and A.M. Rodriquez, Enz. Microb. Tech. 5 (1983) 337.

38. N.L. Weinberg, ed., "Techniques of Electroorganic Synthesis Part 2", John Wiley and Sons, New York (1975)

39. T. Matsunaga, Y. Namba and T. Nakajima, Bioelectrochem. Bioenerg. 13 (1984) 393.

40. R.K. Thauer, K. Jungermann and K. Dekker, Bacteriological Revs. 41 (1977) 100.

41. B. E. Sioda, **Anal. Chem.**, _46_, 964 (1974).

42. A. R. C. Olson, C. W. Koch and G. C. Pimcantel. Introductory
    Quantitative Chemistry, 219 W. H. Freeman and Co., San Francisco, 1956.

43. W. C. Pierce, E. L. Haenish and D. T. Sawyer, Quantitative Analysis, John
    Wiley and Sons, Inc., New York, 1958.

44. P. K. Munjal, Ph.D. dissertation, University of California (Berkeley).
    University Microfilms, Ann Arbor, MI, Pub. 67.6126, 1966.

45. Stanley E. Manahan. Environmental Chemistry, 4th Edition, PWS Publishers,
    1984.

Figure 1

GC

GCMS

A Purge Gas Inlet
B Purge Gas Inlet
F Glass Frit
G Sample Gas Outlet
CW Cold Water Inlet
W Water Outlet
RE Saturated Calomel Reference Electrode
WE Working Electrode
CE Counter Electrode
M Magnetic Stirring Bar
T Solution Exit Trap
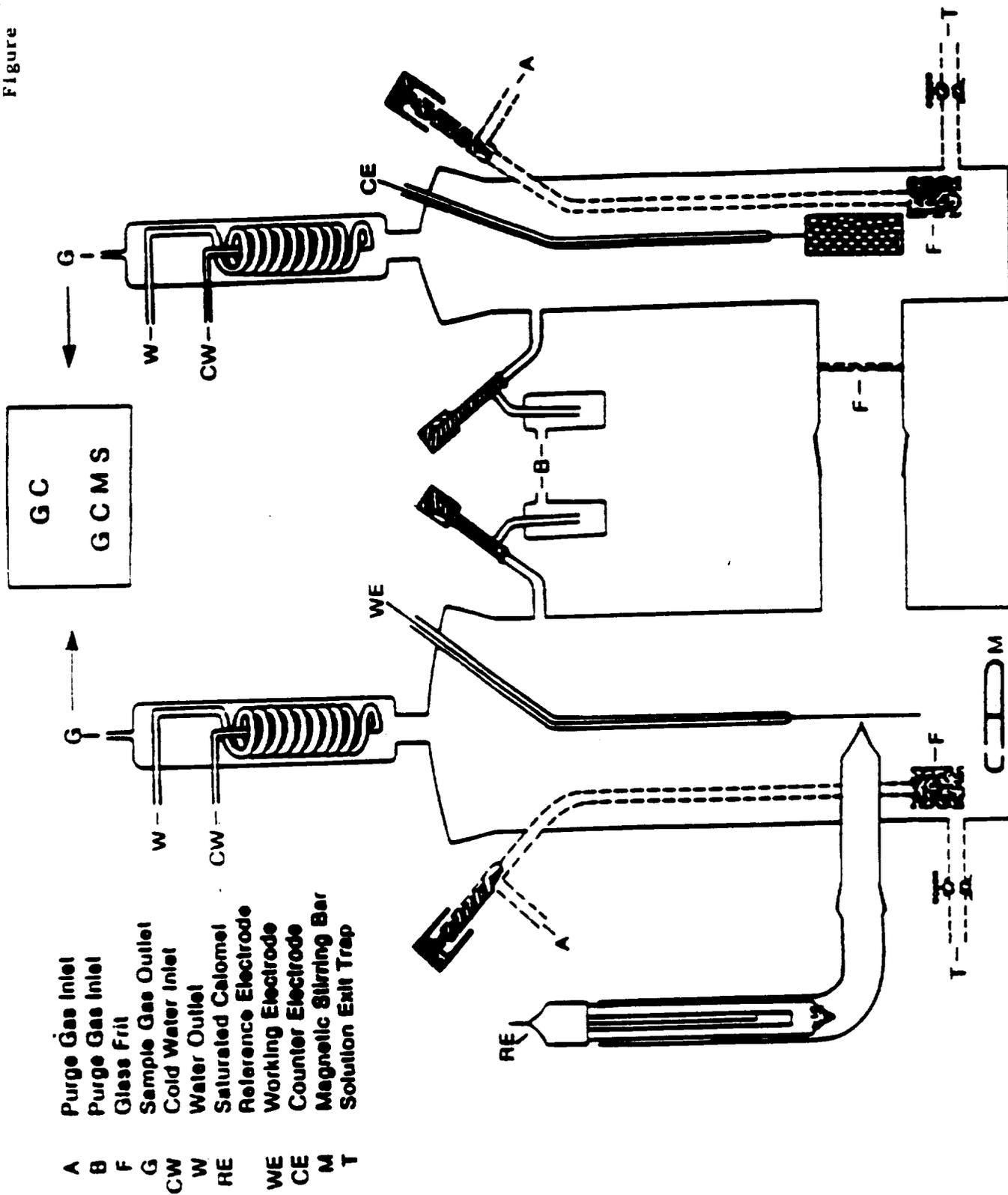
Schematic Diagram of the Electrolysis Cell

Figure 2: Schematic diagram of the U tube cell used for the electrolysis of the mixture of artificial fecal waste (AFW) and urine.
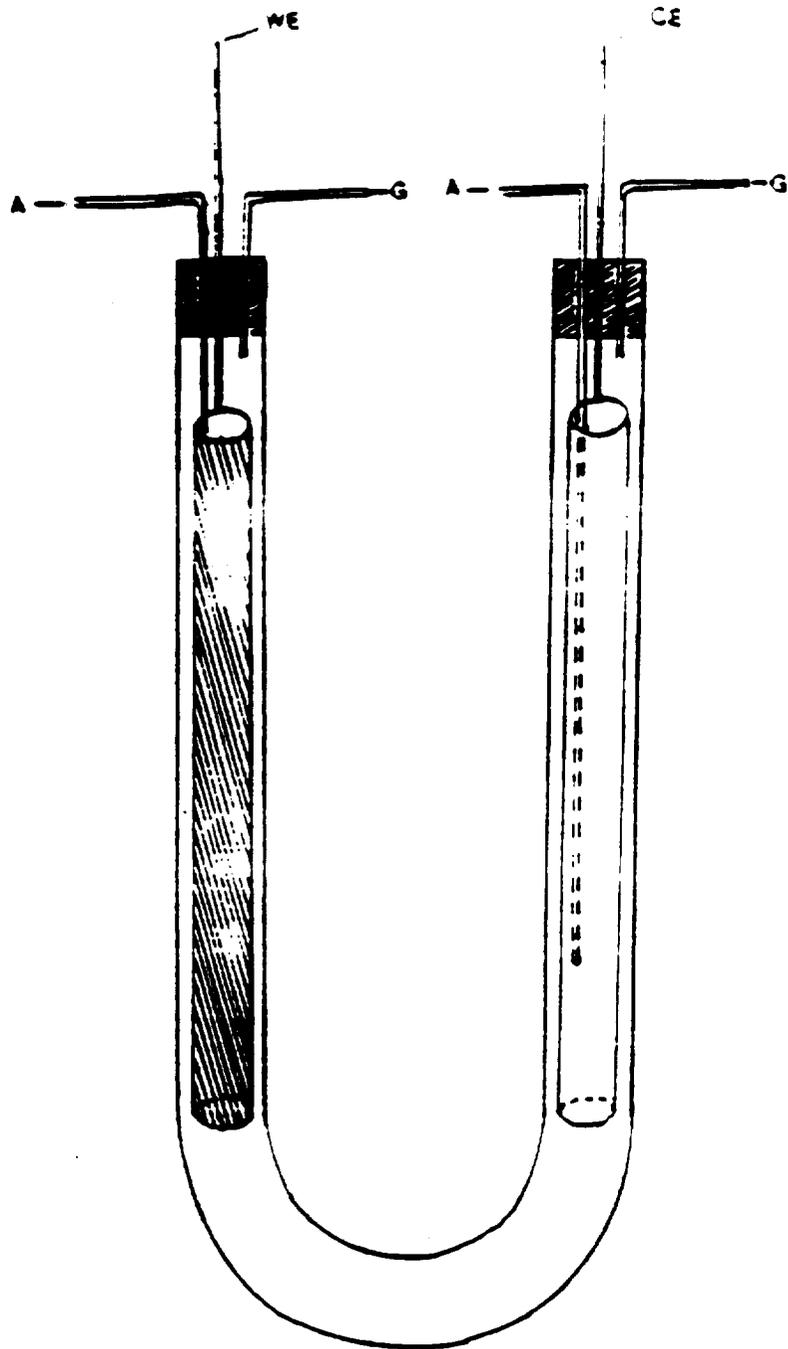
A   Purge Gas Inlet
G   Sample Gas Outle
WE   Working Electro
CE   Counter Electroc
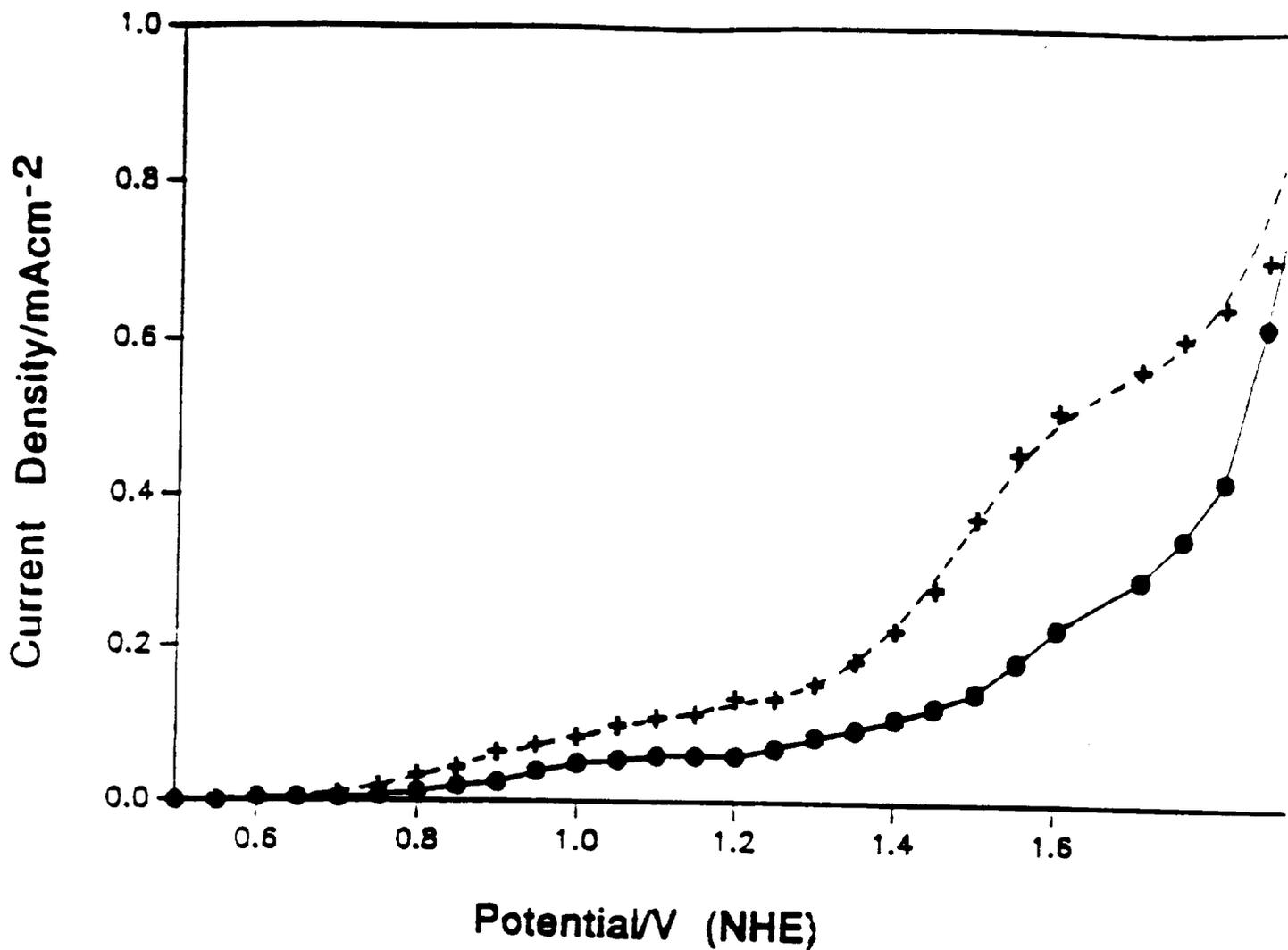
Figure 3: Current-Potential curves for oxidation of oleic acid in 12M H_2SO_4 for different concentrations of oleic acid (● 1 g/liter) (+ 2 and 4 g 1^{-1}). Potential limits 0.5 - 2.0 V (NHE). Scan rate 1 mV/s.
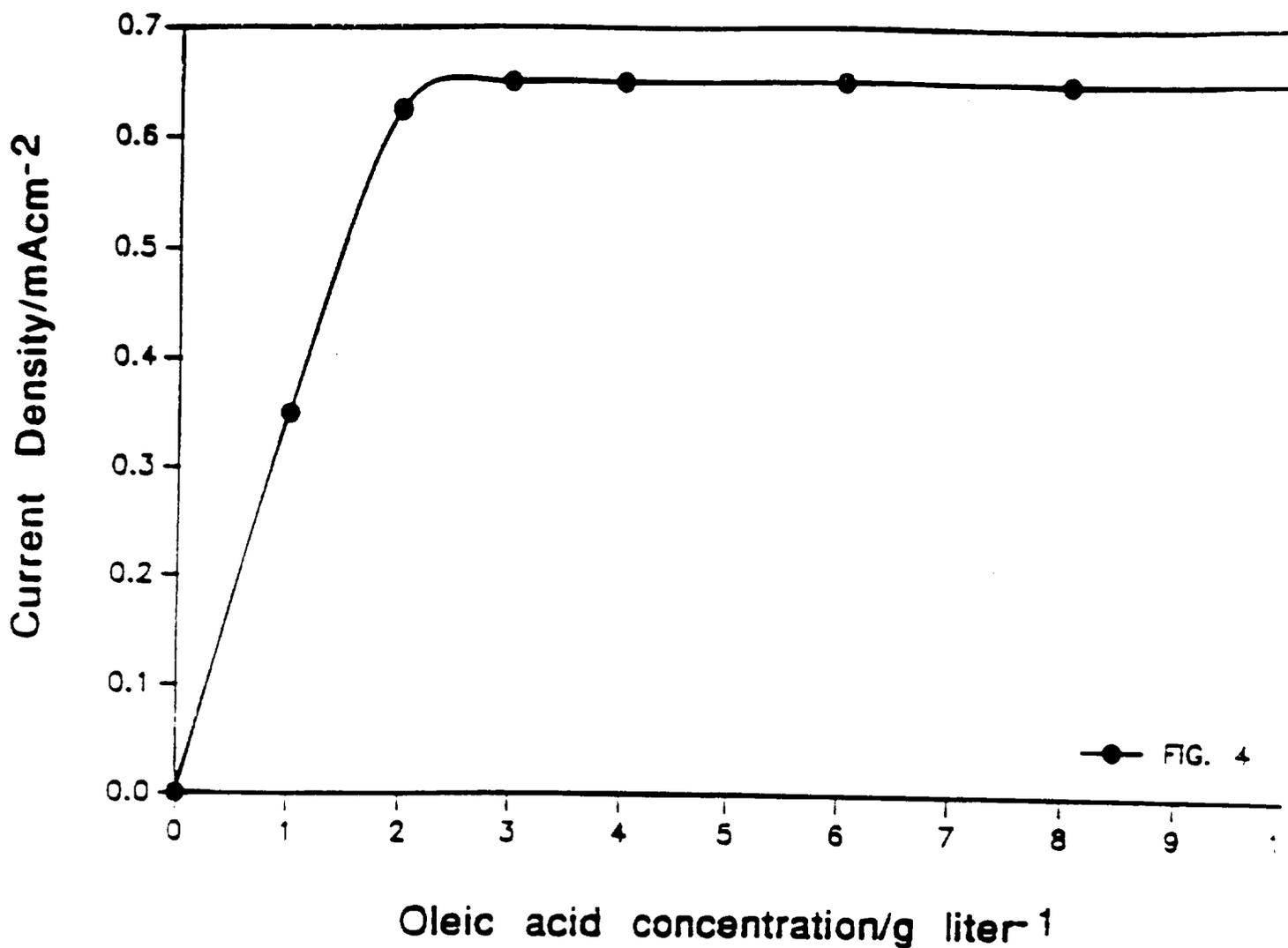
Figure 4: Effect of oleic acid concentration on the anodic limiting current density at 150°C in 12M H_2SO_4 from the voltammetric behavior at Pt electrode. Potential limits 0.5 - 2.0 v (NHE). Scan rate 1mv/s.
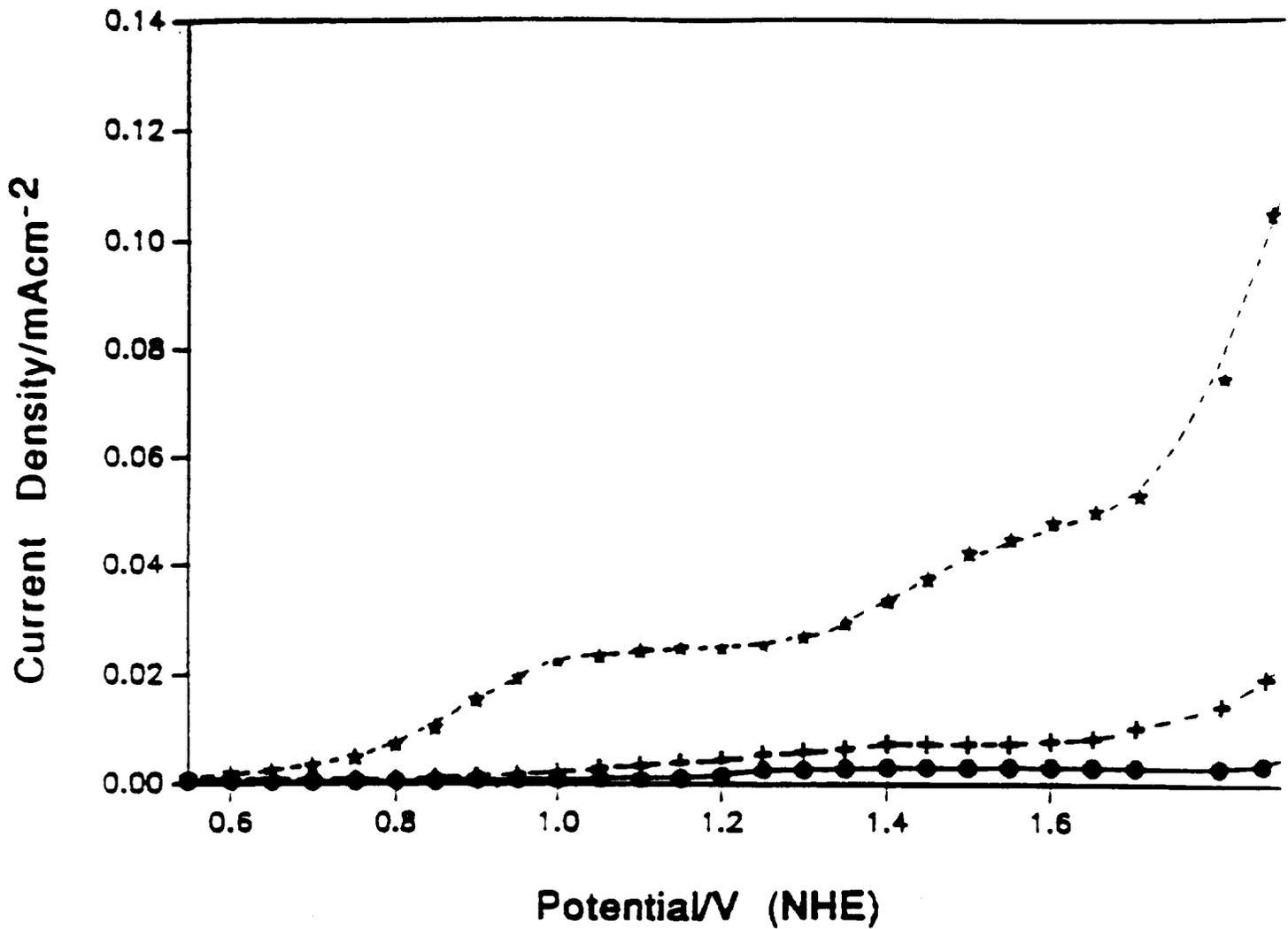
Figure 5: Current potential curves for oxidation of oleic acid in 12M H_2SO_4 at different temperatures. (◯ 25°C, ✚ 80°C, ◆ 120°C). Potential limits 0.4 - 2.0 v (NHE). Scan rate 1 mv/s. T - 150°C. Oleic acid concentration 14 g/liter.
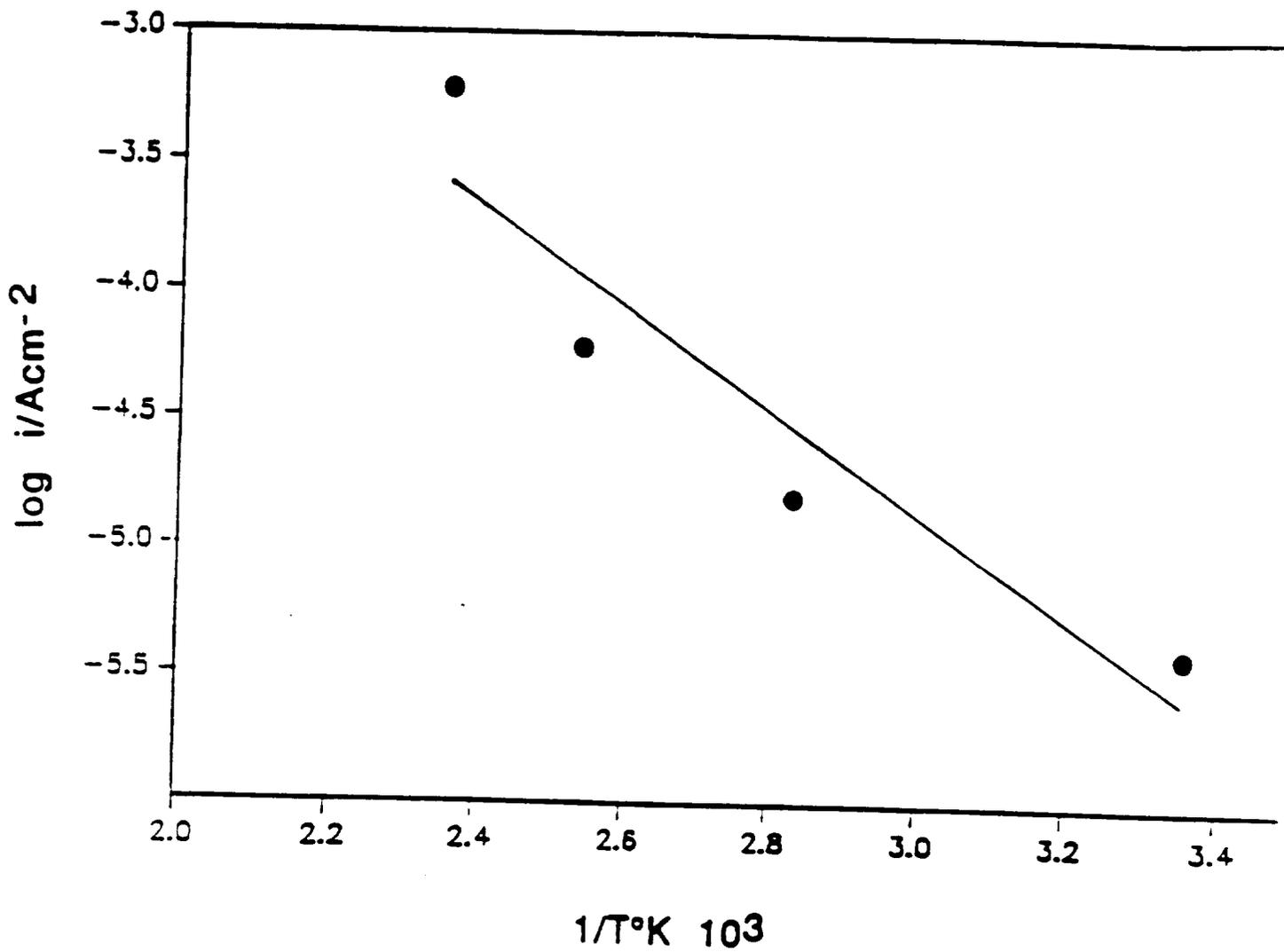
Figure 6: Variation of the limiting current density as function of temperature. Oleic acid concentration 14 g/liter.
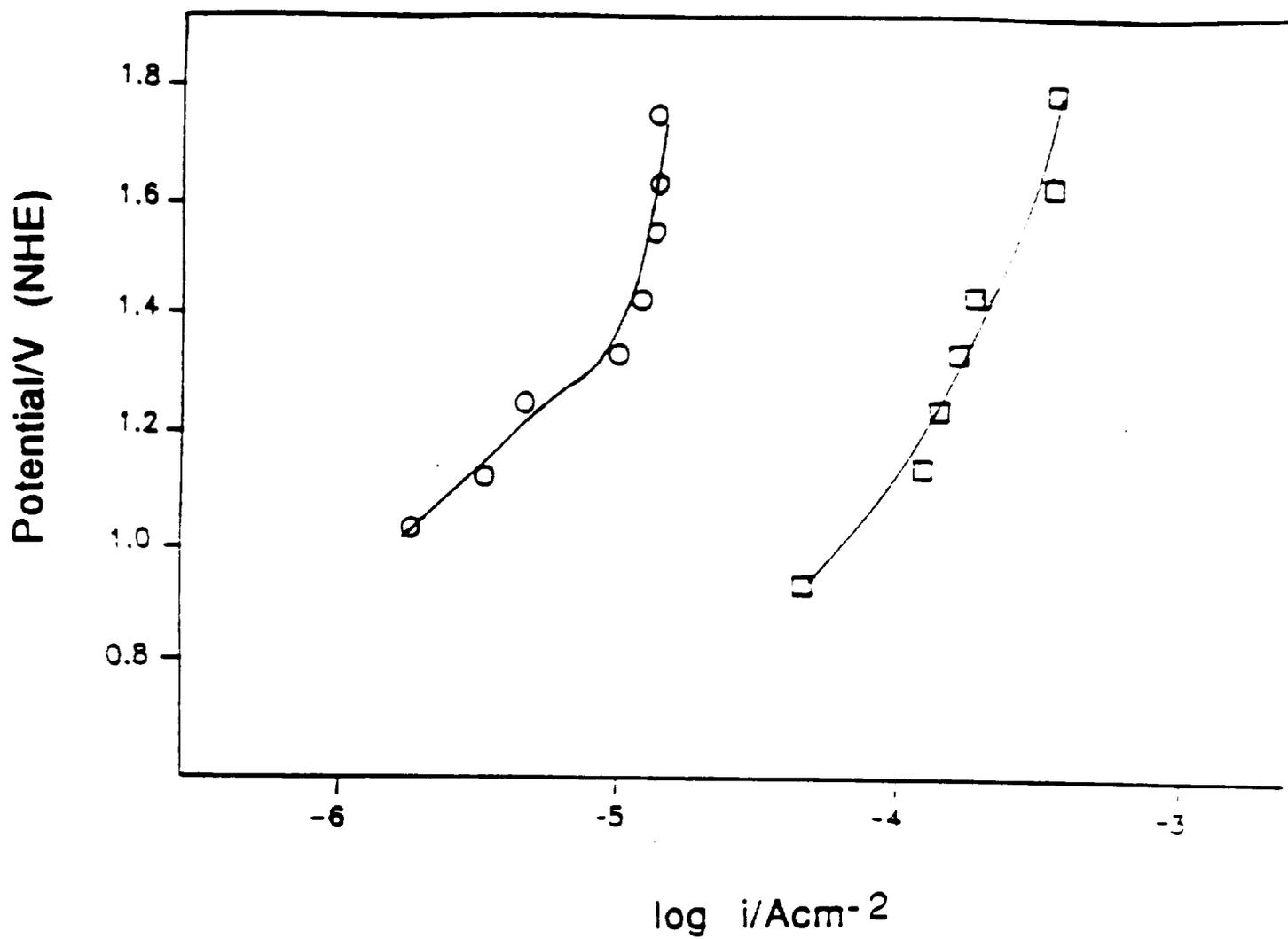
Figure 7: Current/Potential relationship at 80 (O) and 150°C (☐) for oleic acid in 12M H_2SO_4 oleic acid concentration 14 g/liter.
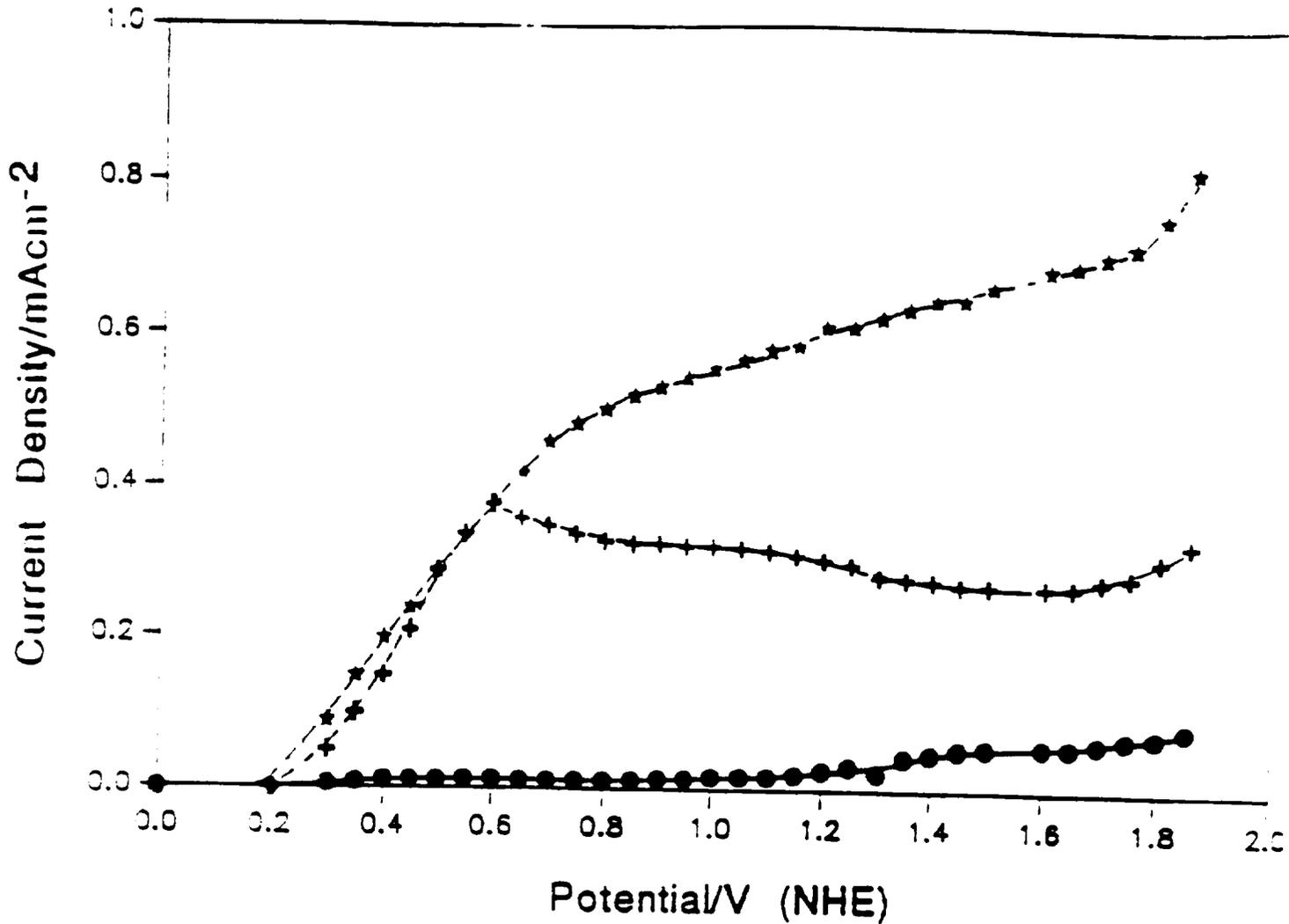
Figure 17. Current-Potential curves for the oxidation of artificial fecal waste on PbO$_2$, at different temperatures. Potential limits 0.2 - 2.0 v. Scan rate 1 mv/s. Waste concentration 24 g/liter. (○ 25°C; + 80°C; ★ 130°C).
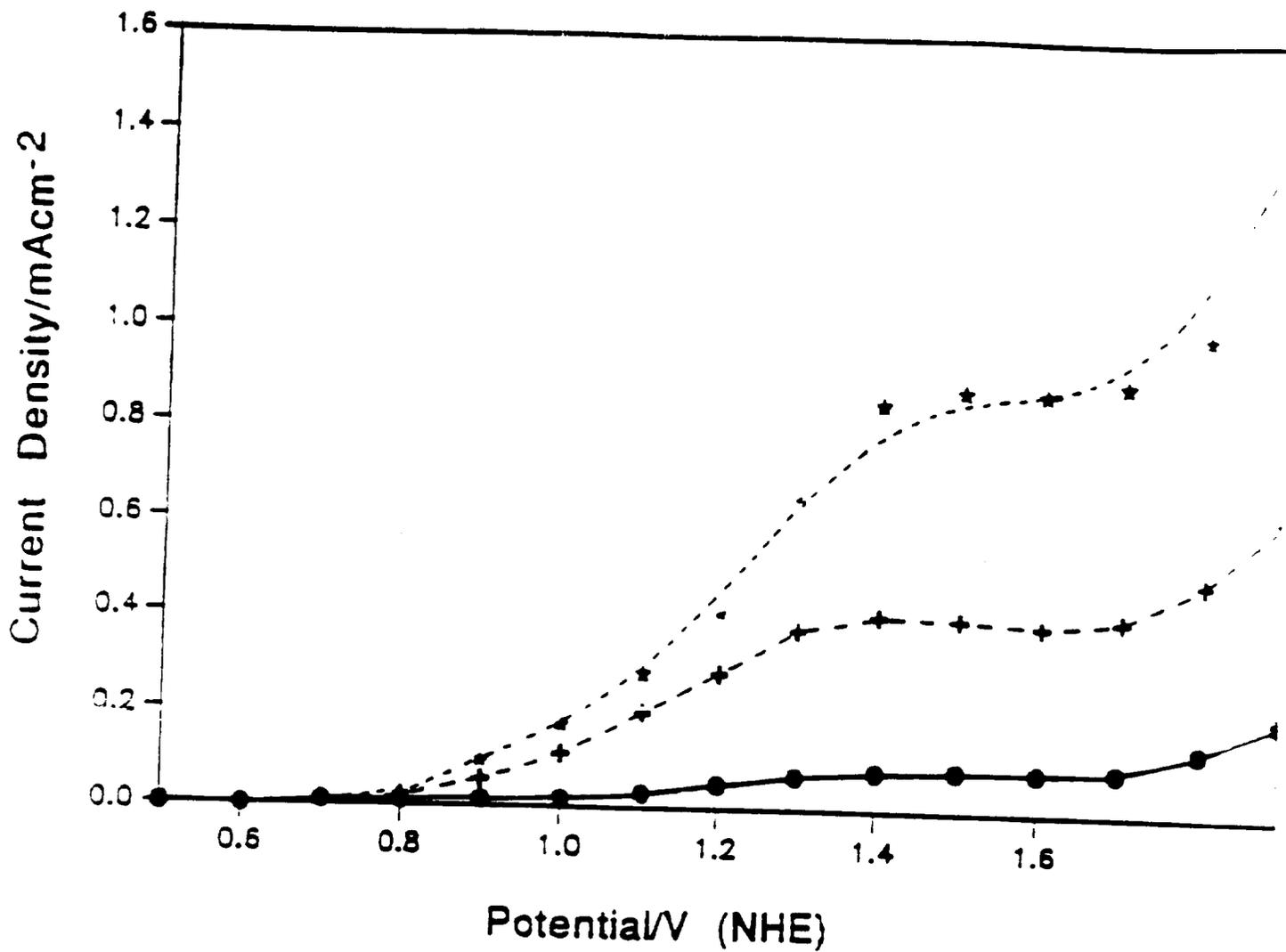
Figure 9: Current potential curves for oxidation of cellulose in 12 M H_2SO_4 for different concentrations of cellulose. (● 1 g/liter; + 2 g/liter; ✶ 5 and 10 g/liter). Potential limits 0.5 - 2 v. Scan rate 1 mv/s. T = 150°C.
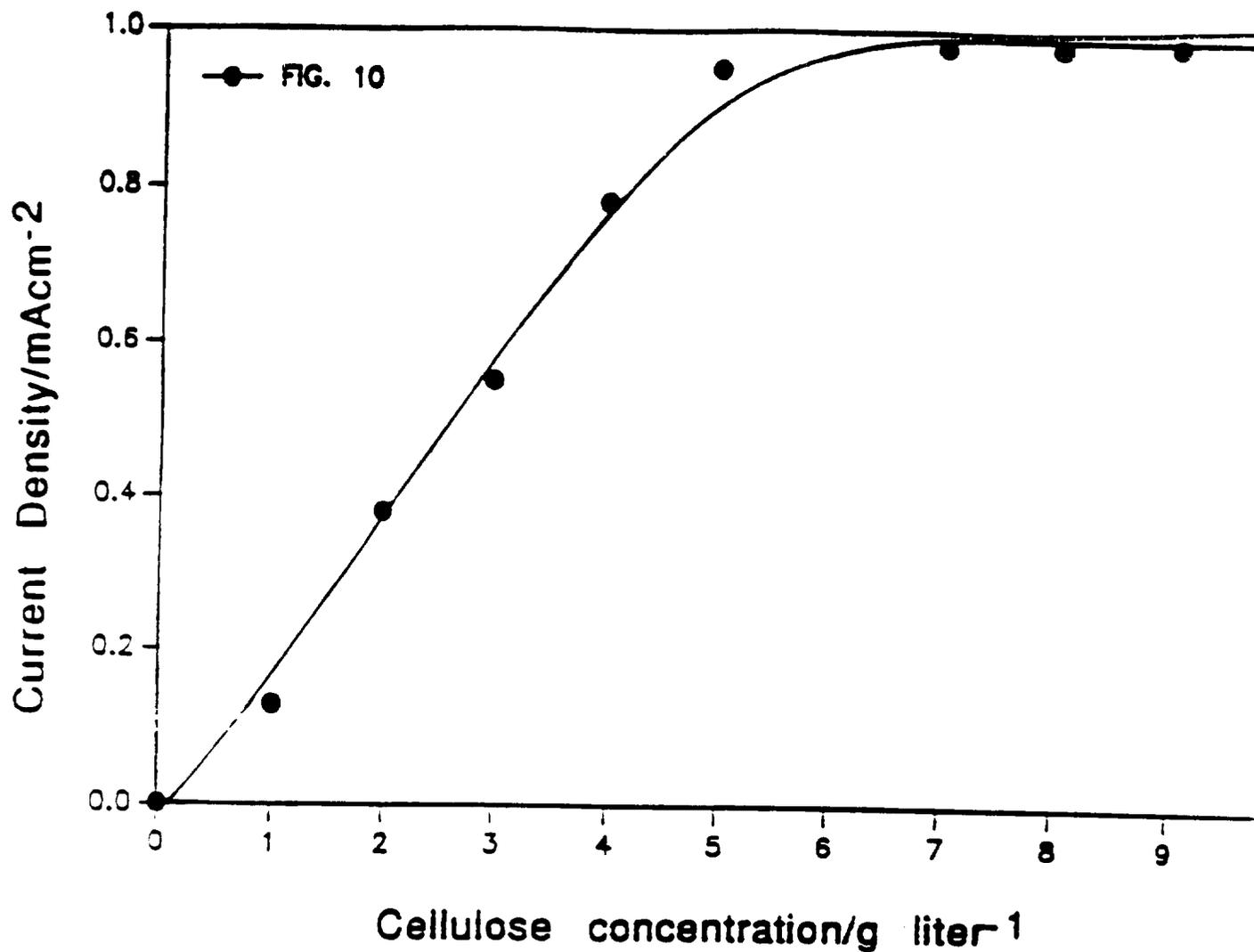
Figure 10: Effect of cellulose concentration on the limiting current density at 150°C in 12 M H_2SO_4 from the voltammetric behavior at Pt electrode. Potential limits 0.5 - 2 v (NHE). Scan rate 1 mv/s.
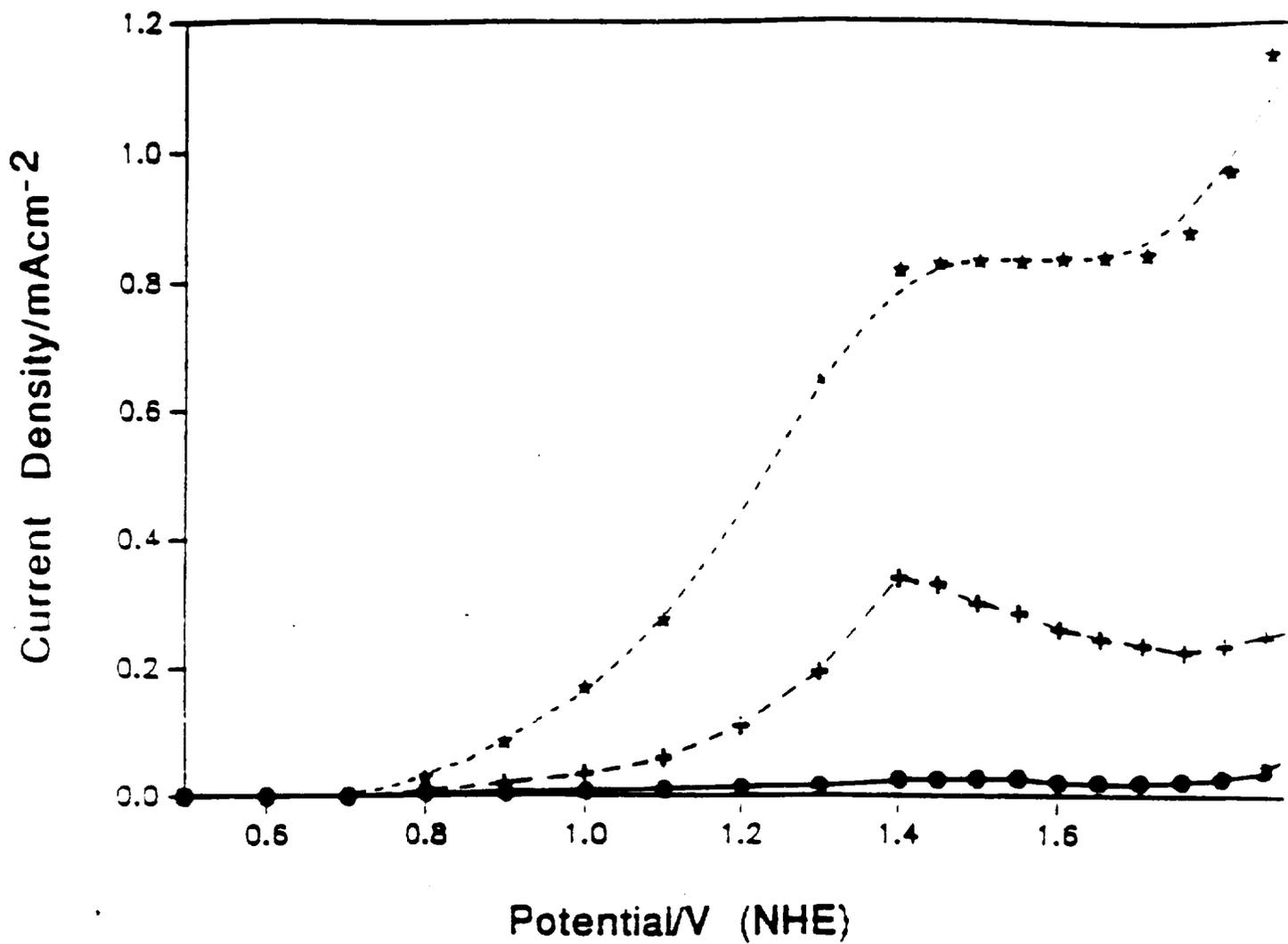
Figure 11: Current potential curves for oxidation of cellulose in 12 M H$_2$SO$_4$ at different temperatured (● 25°C, ✛ 80°C, ★ 150°C). Potential limits 0.5 - 2.0 v (NHE). Scan rate 1 mv/s. T - 150°C. Cellulose concentration 14 g/liter.

Figure 12: Variation of the limiting current density as a function of temperature. Cellulose concentration 14 g/liter.
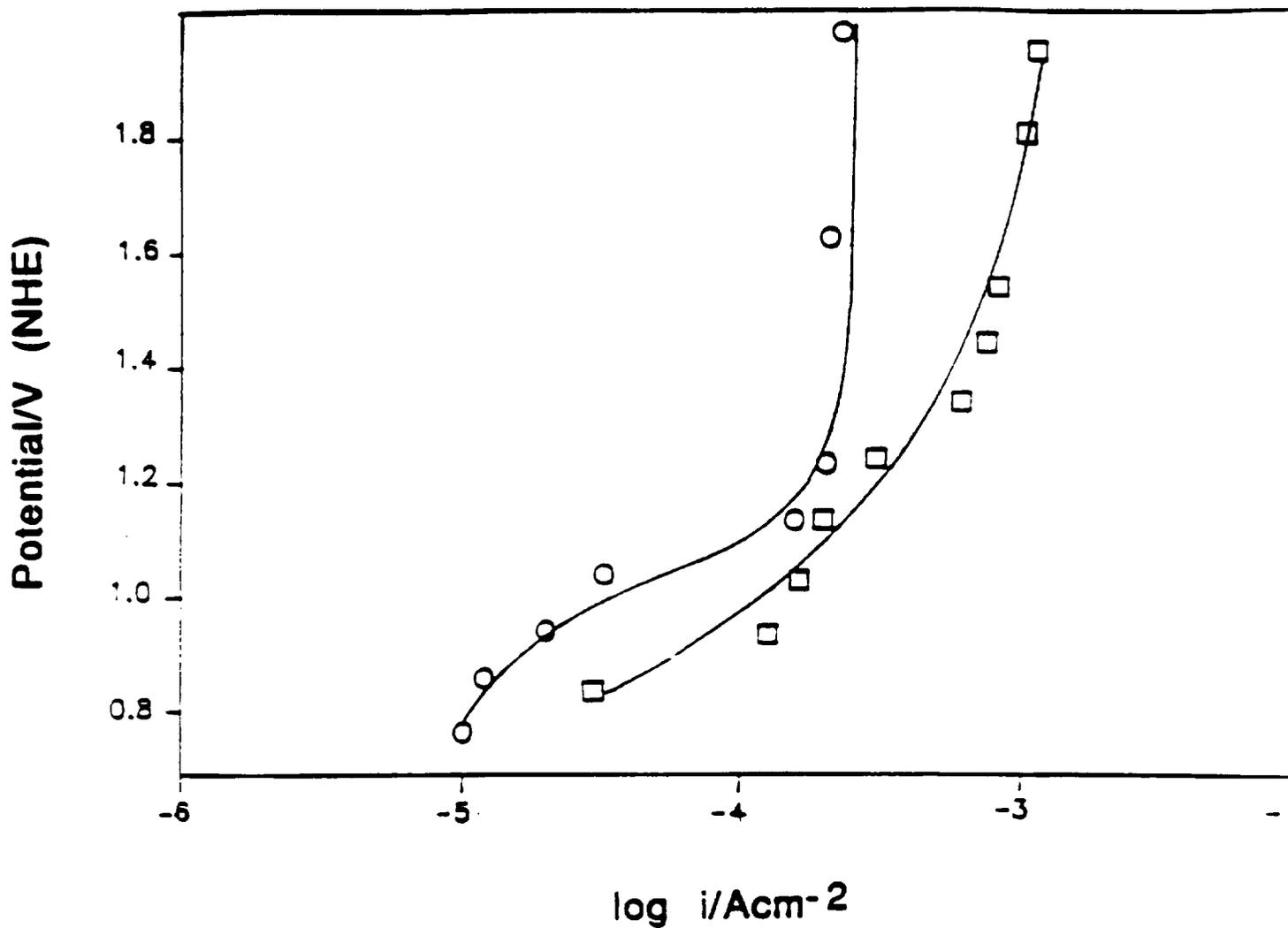
Figure 13: Current/potential relationship at 80°C and 150°C. for cellulose in
12 M H$_2$SO$_4$. Cellulose concentration 14 g/liter.
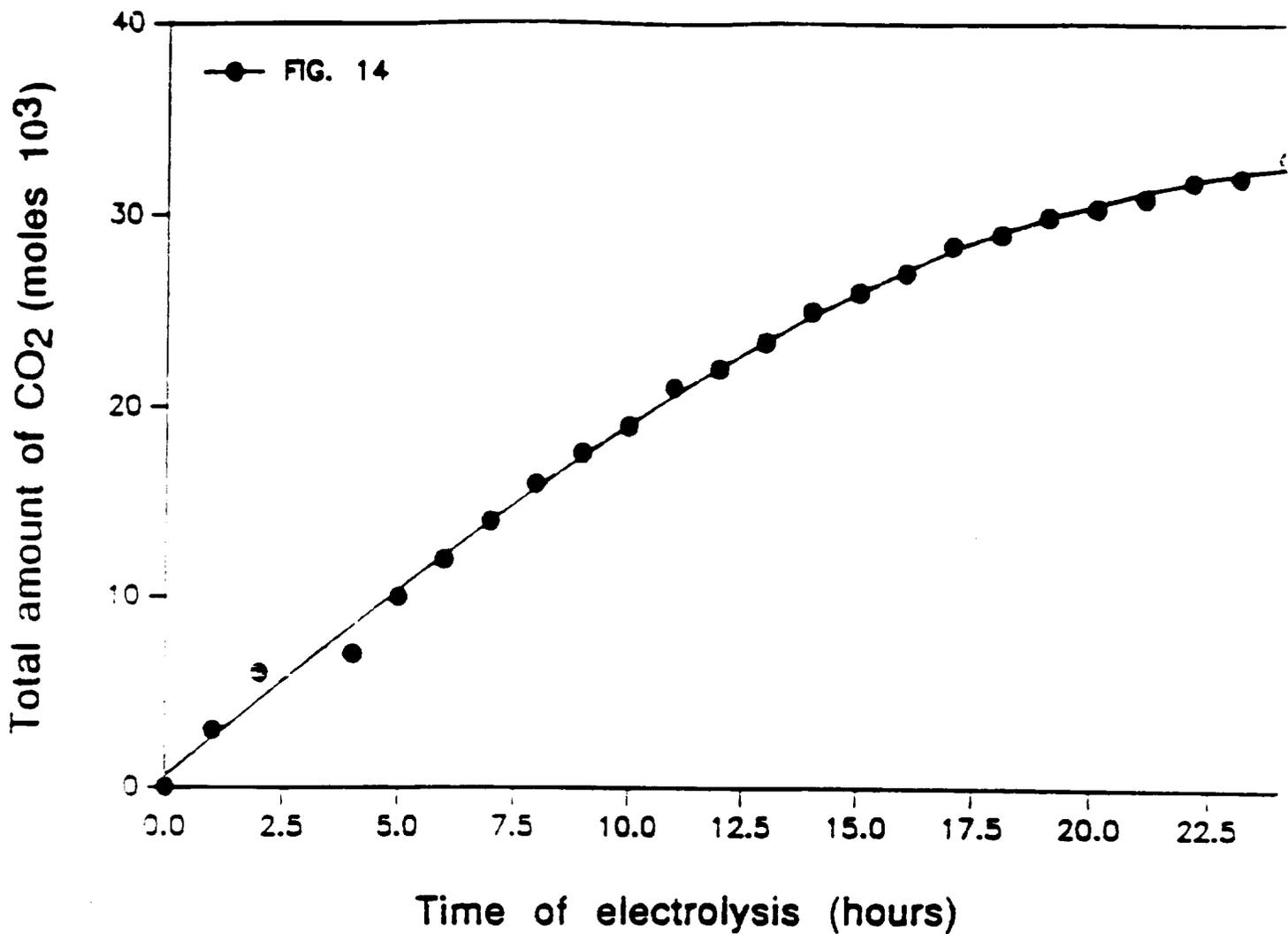
Figure 14: Electrochemical production of CO_2 during cellulose electrolysis in 12 M H_2SO_4 using a Pt electrode at 150°C. Cellulose concentration 14 g/liter.
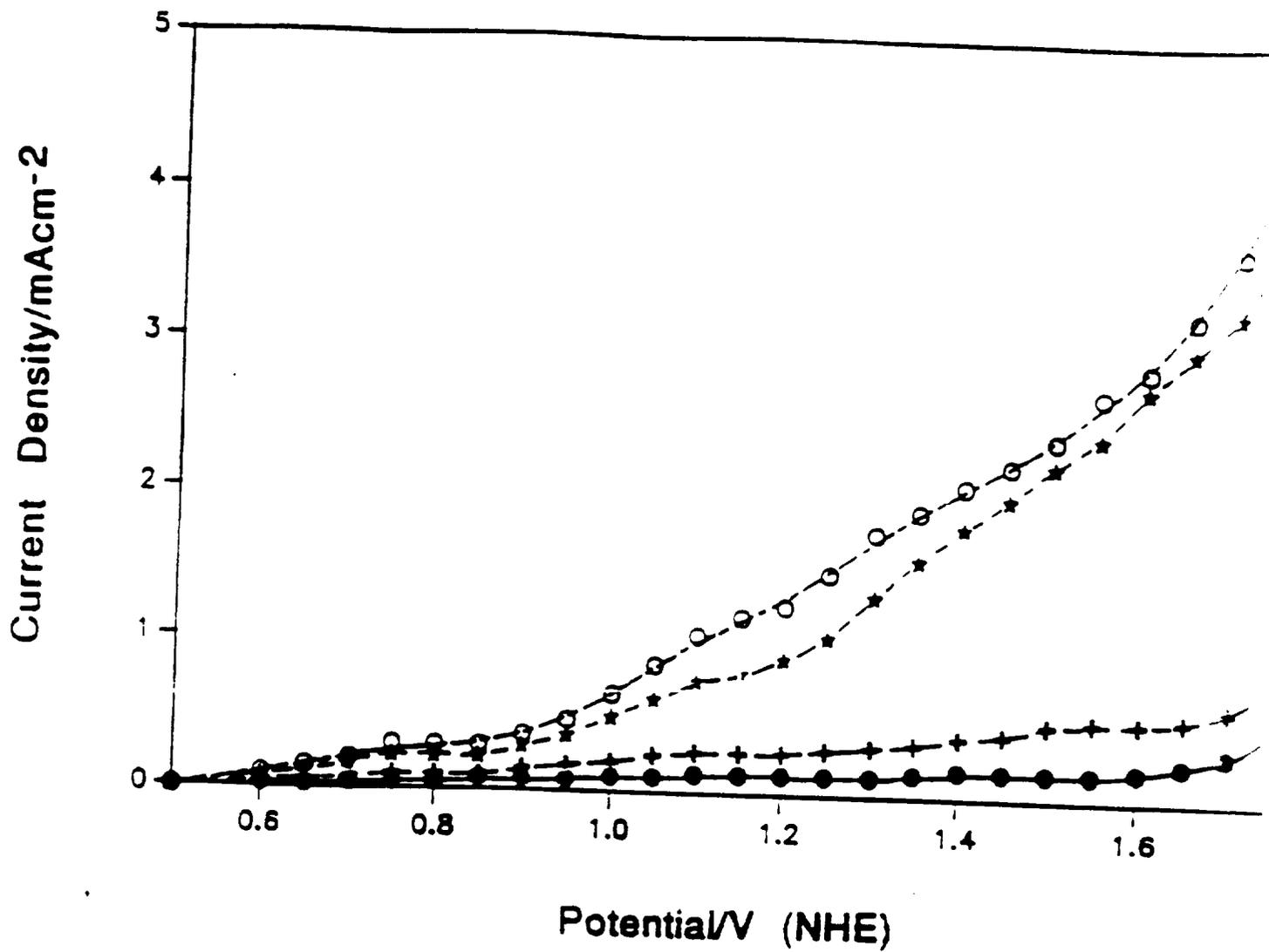
Figure 15: Current-Potential curves for oxidation of casein in 12 M H_2SO_4 for different concentrations of casein (● 2 g/liter; ✝ 4 g/liter; ★ 6 g/liter, ○ 10 g/liter). Potential limits 0.5 - 2 v (NHE). Scan rate 1 mv/s. T = 150°C.
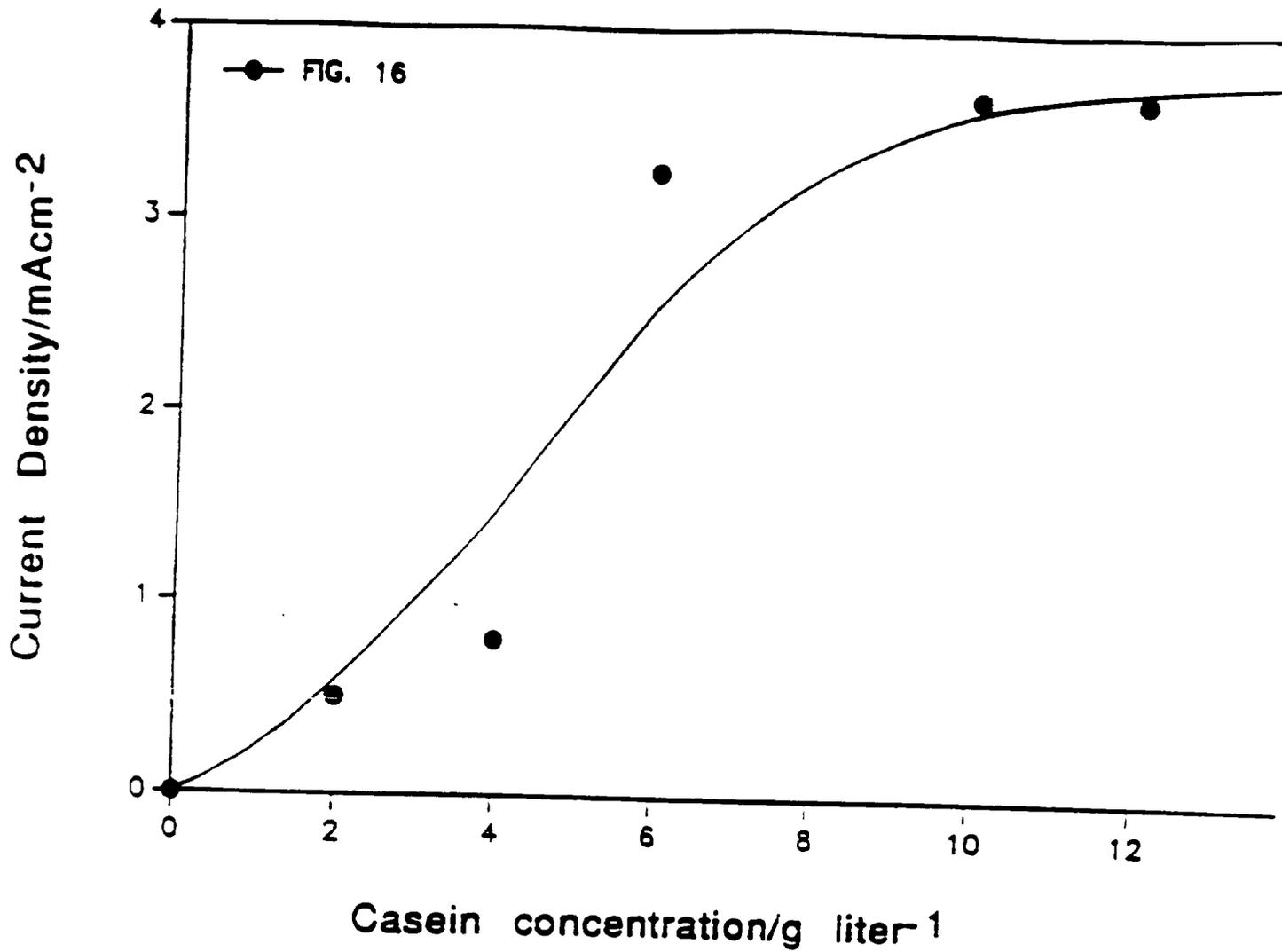
Figure 16: Effect of casein concentration on the anodic limiting current density at 150°C in 12 M H_2SO_4 from the voltametric behavior at pt electrode-potential limit 0.5 - 2.0 v (NHE). Scan rage 1mv/s.
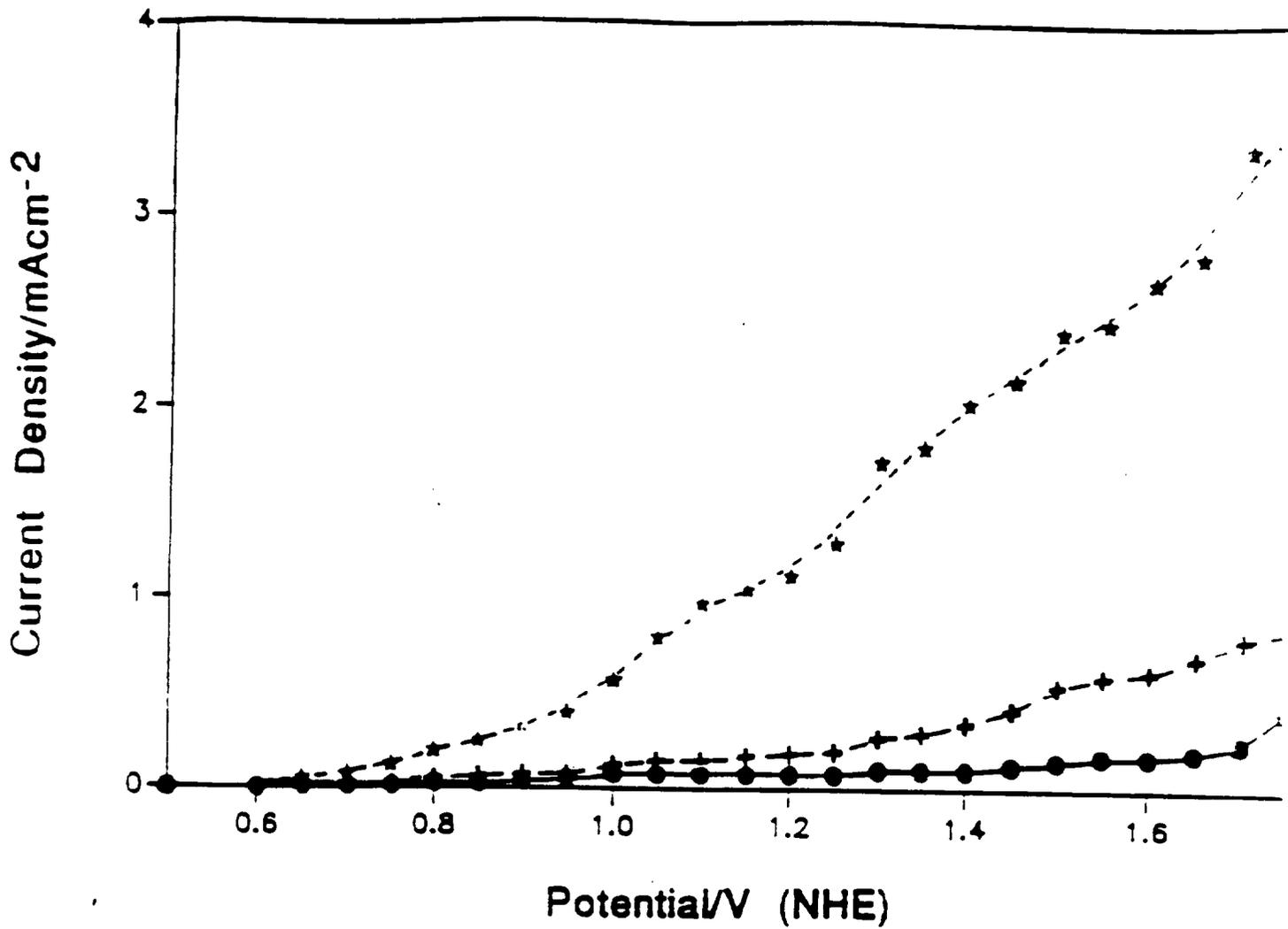
Figure 17 Current-potential curves for exidation of casein in 12 M H_2SO_4 at different temperatures. (● 25°C; ✛ 80°C; ★ 150°C). Potential limits 0.5 - 2 v (NHE). Scan rate 1 mv/s. Casein concentration 14 g/liter.
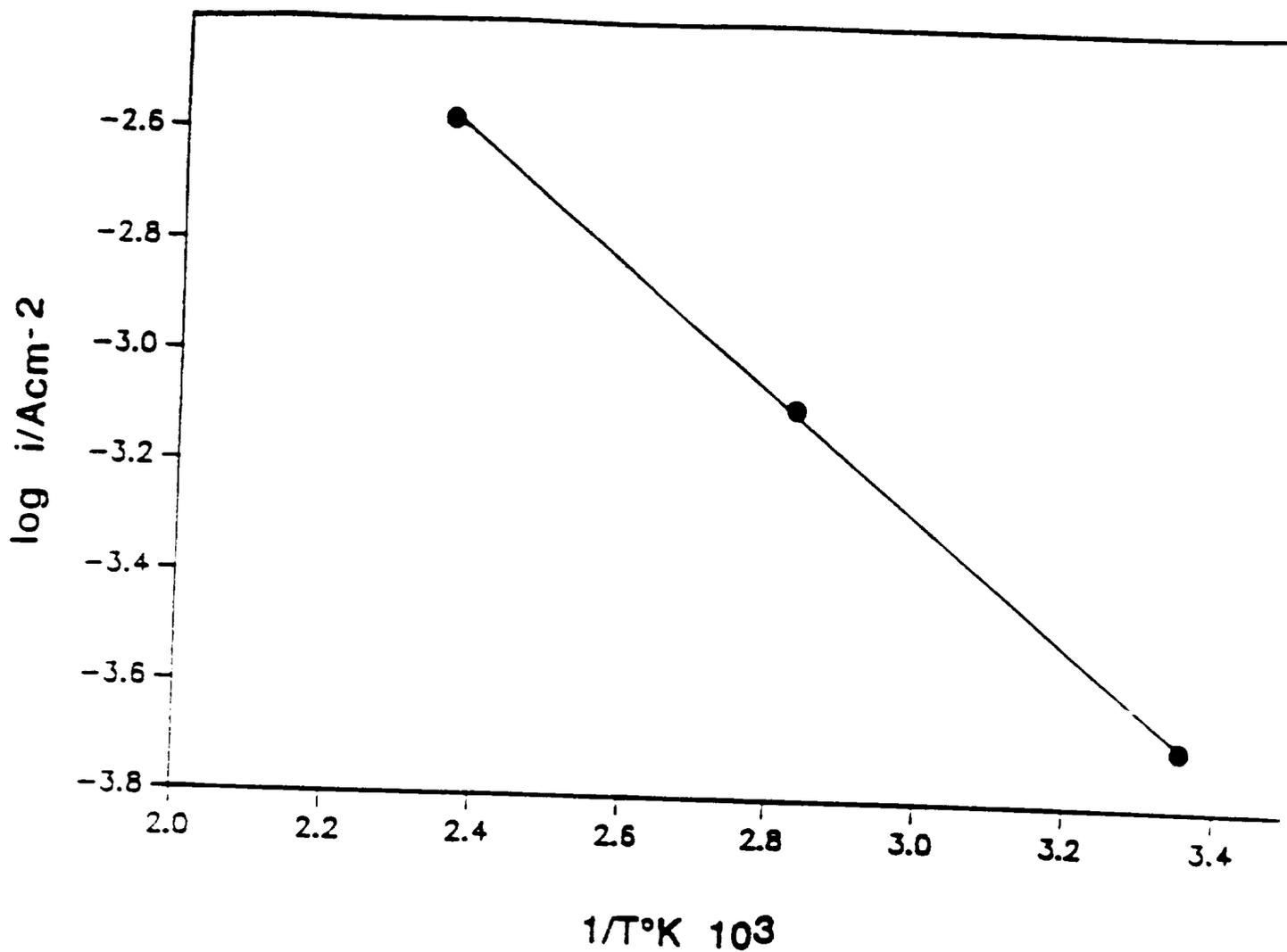
Figure 13: Variation of the limiting current density as function of temperature. Casein concentration 14 g/liter.
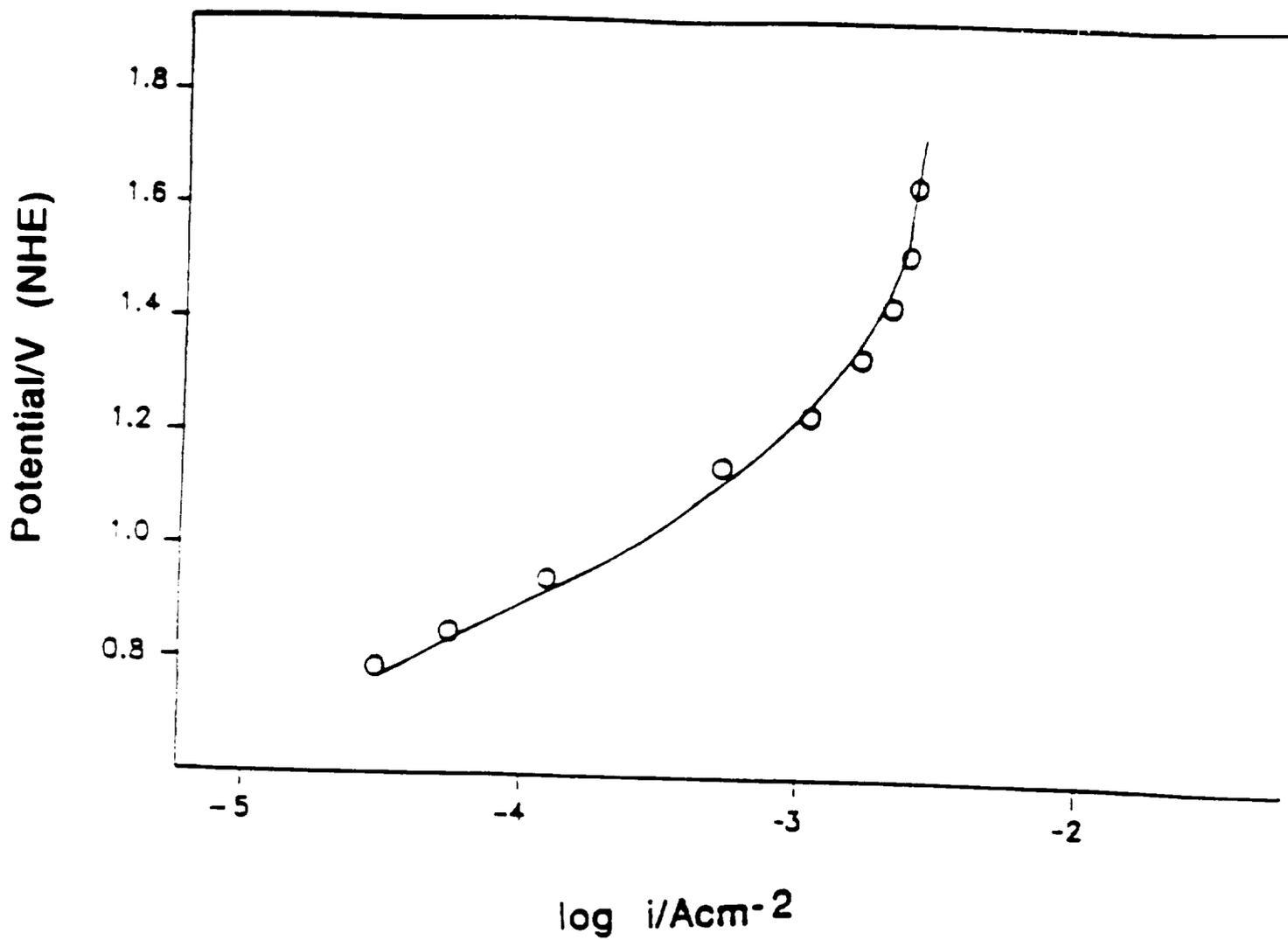
Figure 19: Current/Potential relationship at 150°C for casein in 12 M H_2SO_4. Casein concentration 14 g/liter.
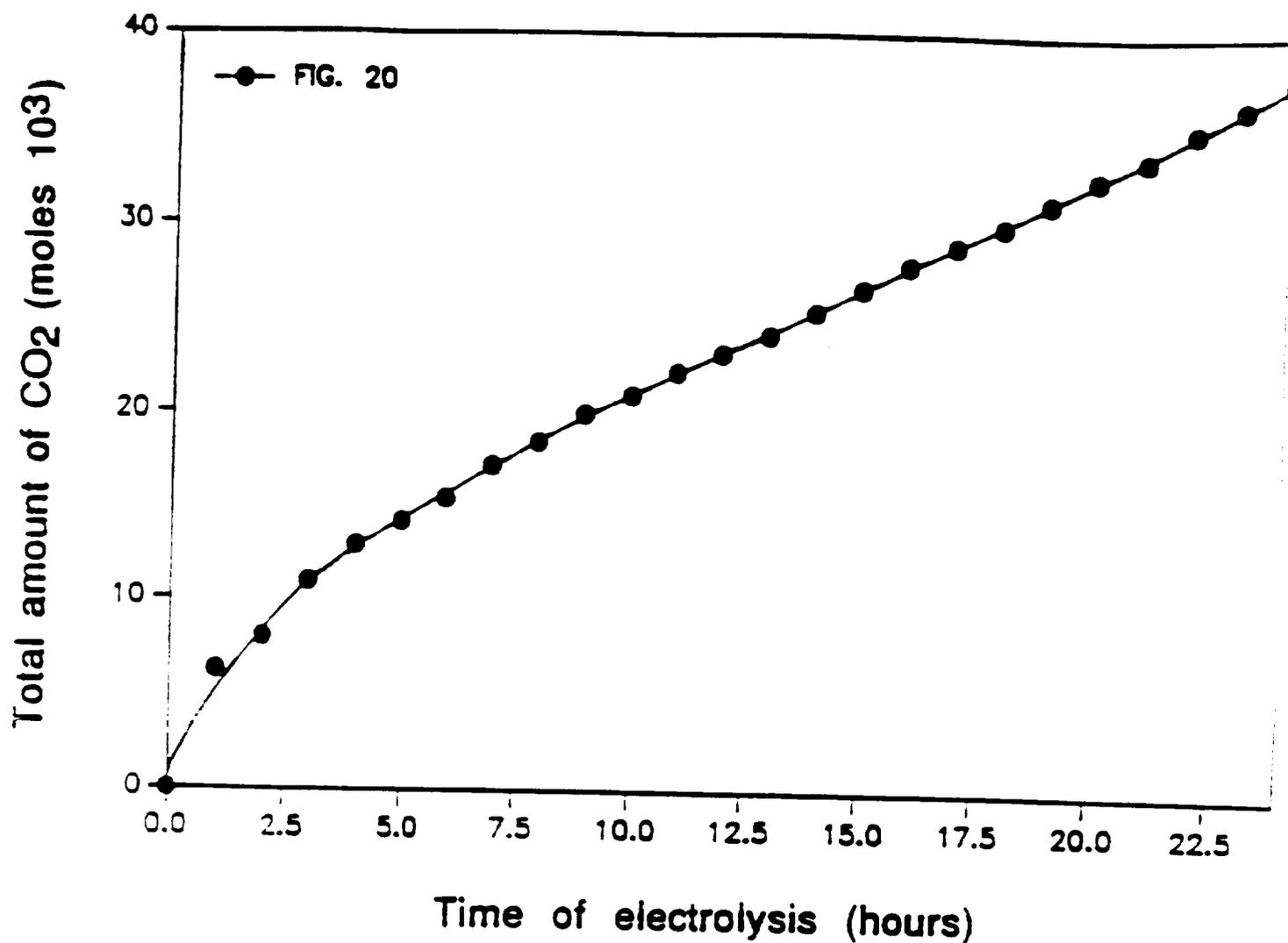
Figure 20: Electrochemical production of CO_2 during casein electrolysis in 12 M H_2SO_4 using a Pt electrode at 150°C. Casein concentration 14 g/liter.
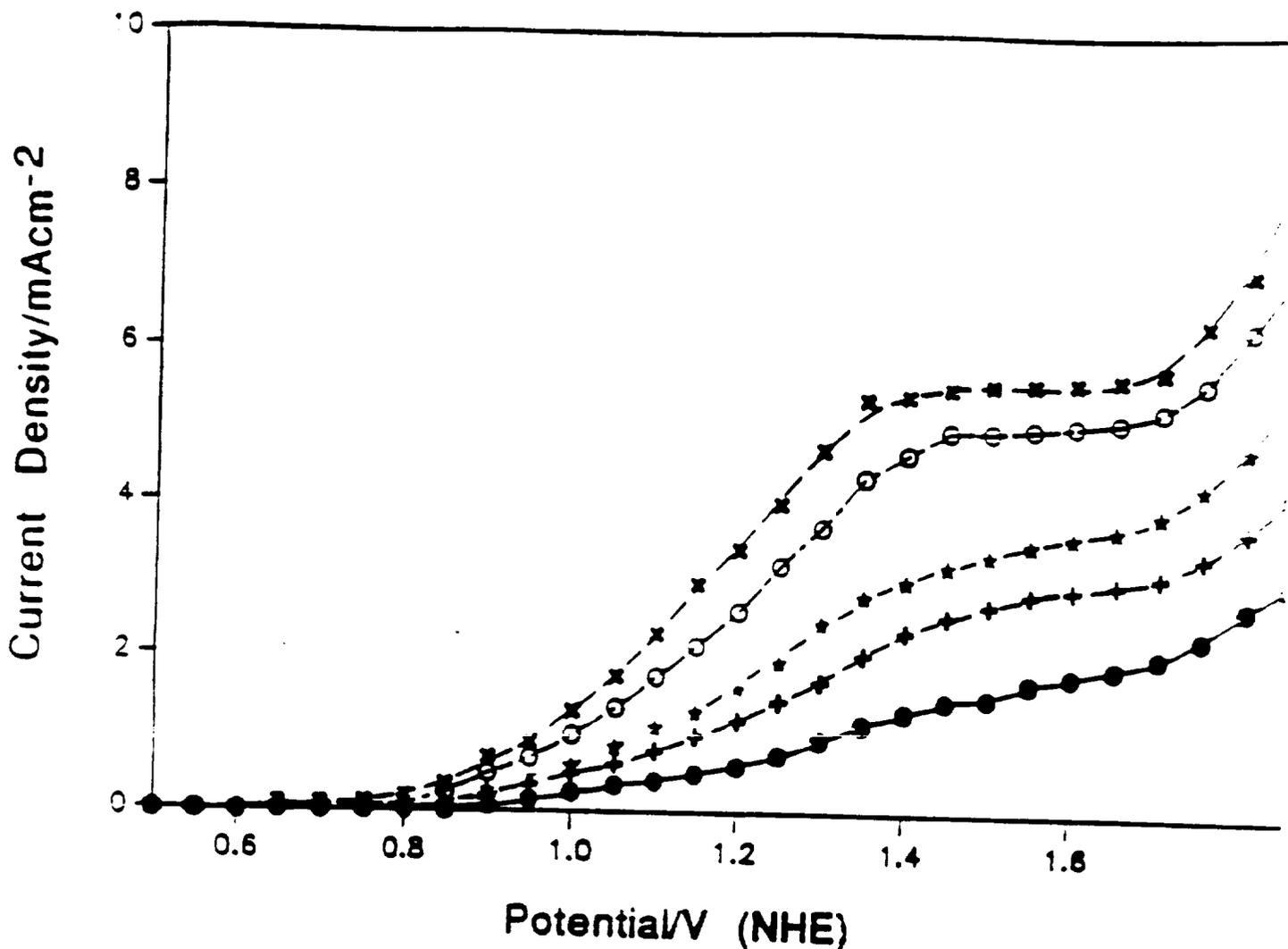
Figure 21: Effect of yeast concentration on the anodic limiting current density at 150°C in 12 M SO$_4$ from the voltammetric behavior at Pt electrode. Potential limits 0.5 - 2 v (NHE). Scan rate 1 mv/s. (● 2.5 g/liter; 5 g/liter; ★ 7.5 g/liter; ○12.5 g/liter; ✕17.5 and 35 g/liter).
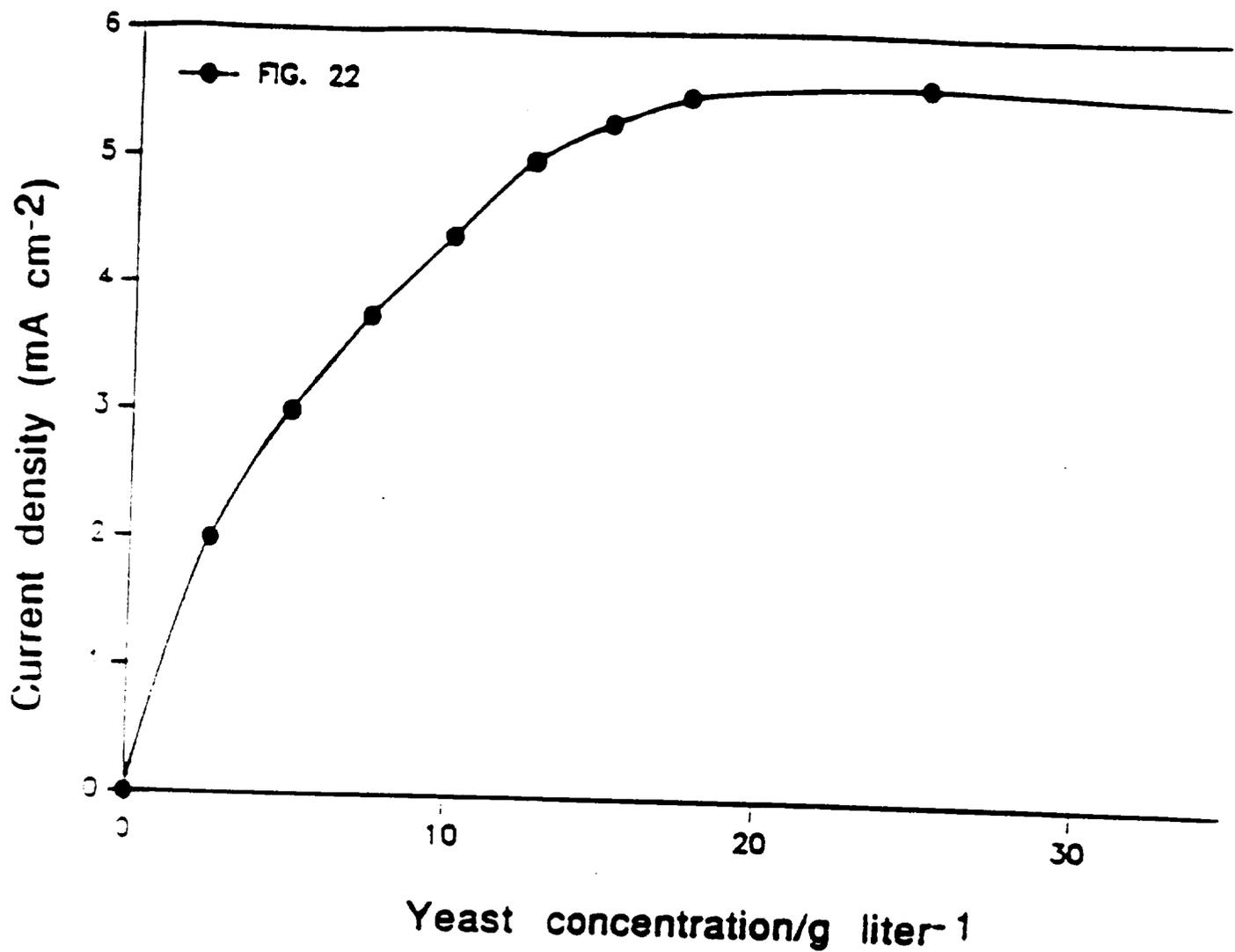
Figure 22. Effect of yeast concentration on the anodic limiting current density at 150°C in 12 M SO$_4$ from the voltammetric behavior at Pt electrode. Potential limits 0.5 - 2.0 v (NHE). Scan rate 1 mv/s.
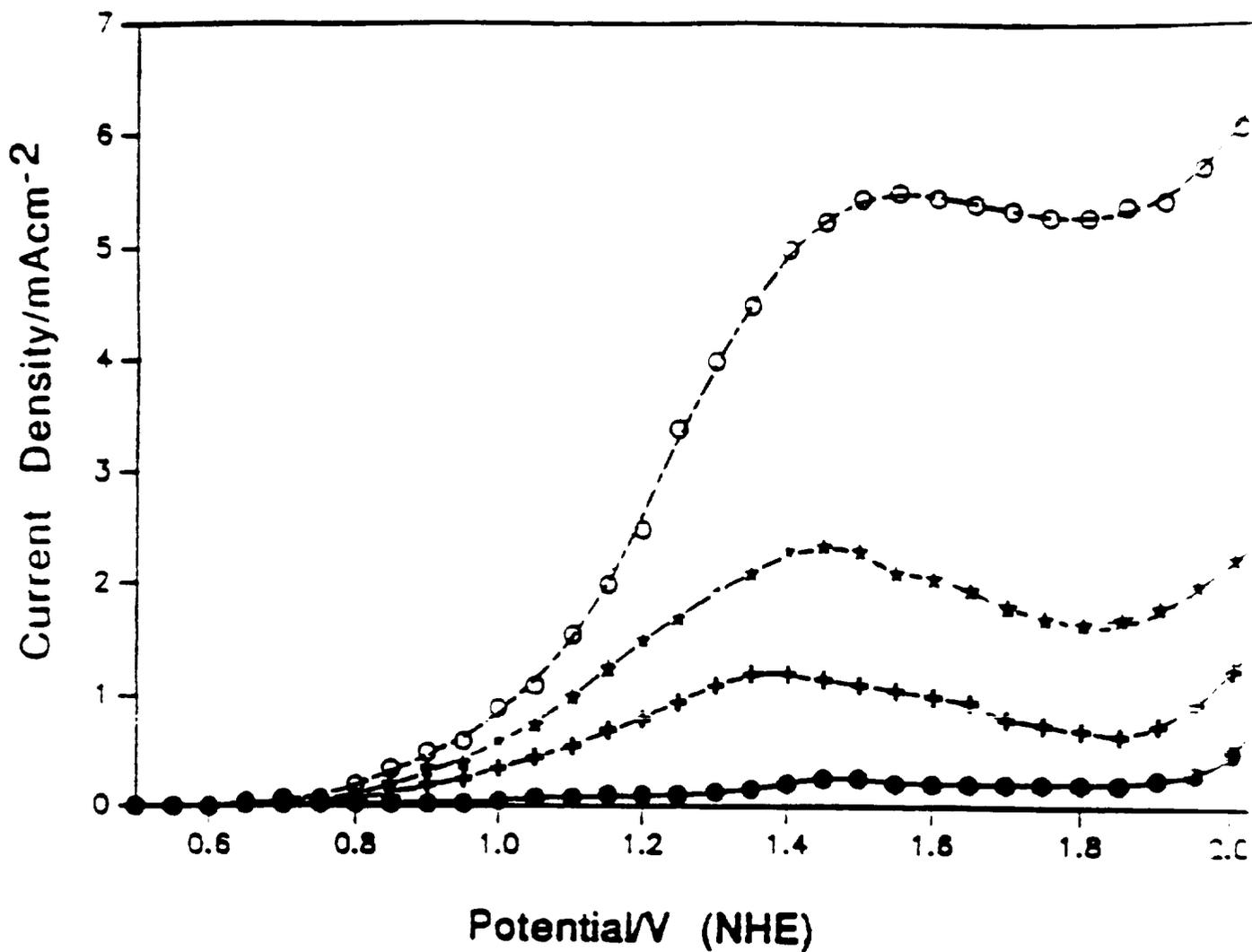
Figure 23: Current-Potential curves for oxidation of yeast in 12 M H_2SO_4 at different temperatures. Potential limits 0.5 - 2.0 v (NHE). Yeast concentration 14 g/liter. (● 25°C; ✦ 80°C; ★ 120°C; ○ 150°C).
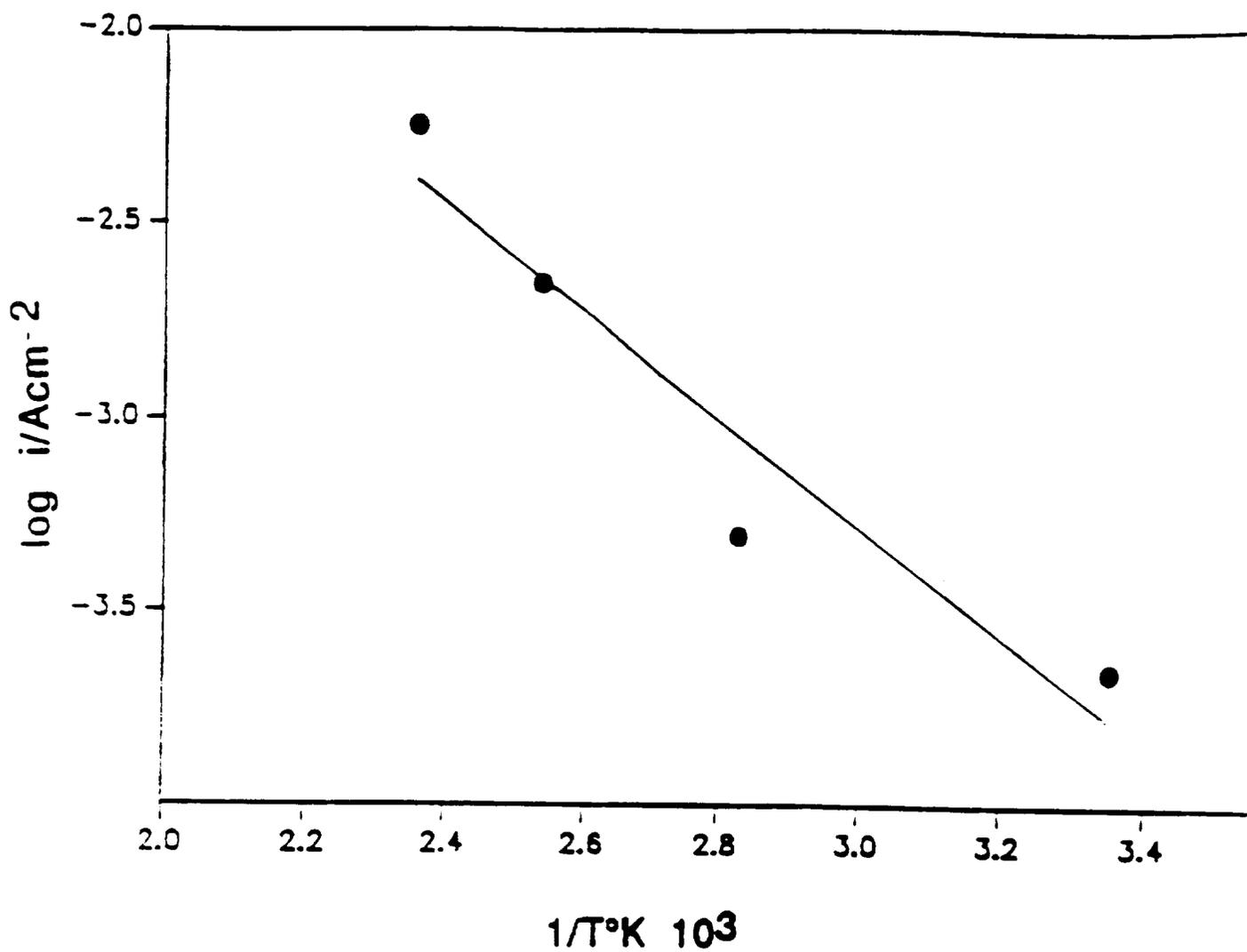
Figure 24. Variation of the limiting current density as function of temperature. Yeast concentration 23.4 g/liter.
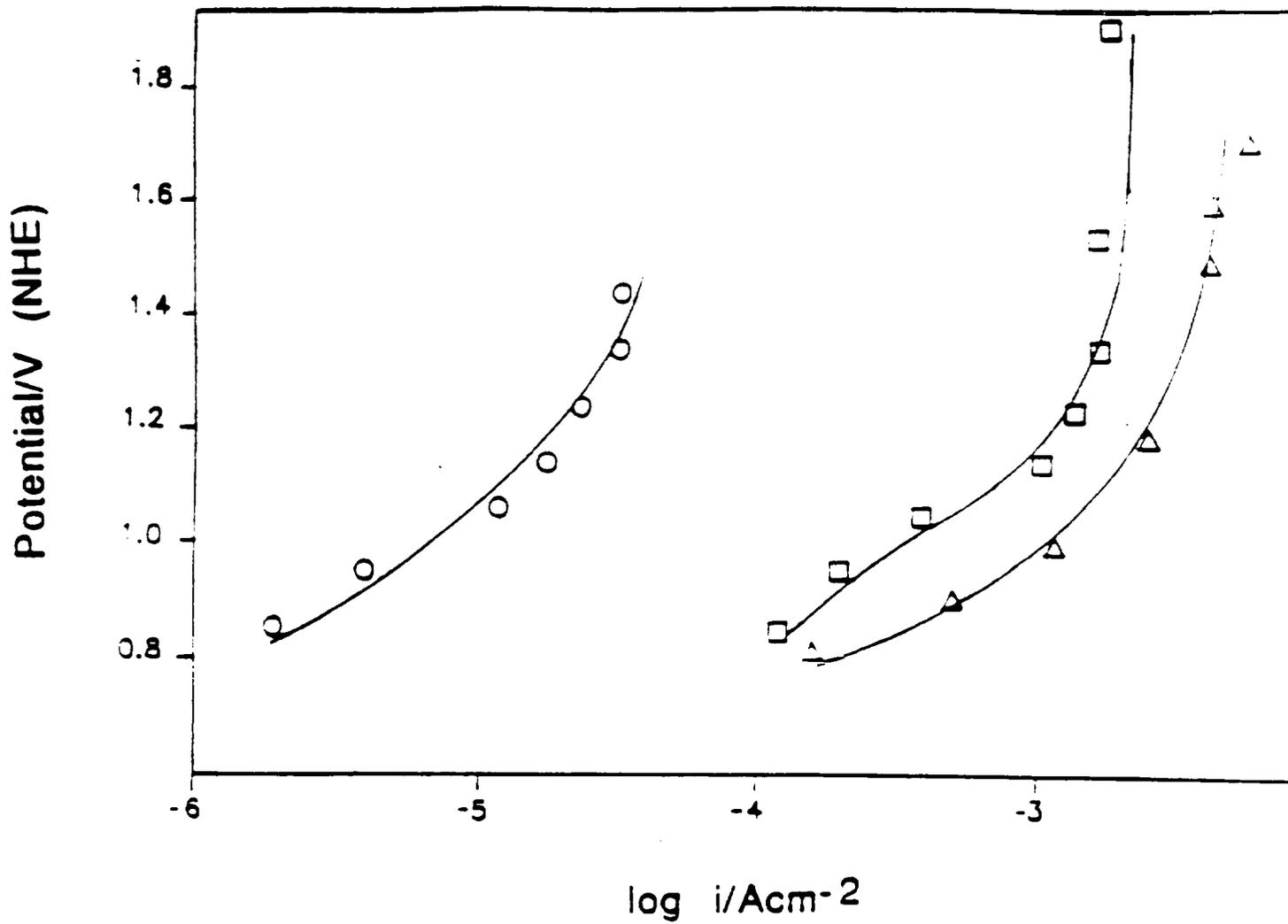
Figure 25: Current/Potential relationship at 80°C (◯), 120°C (☐), 150°C
(△), for yeast in 12 M H_2SO_4. Yeast concentration 23.4 g/liter.
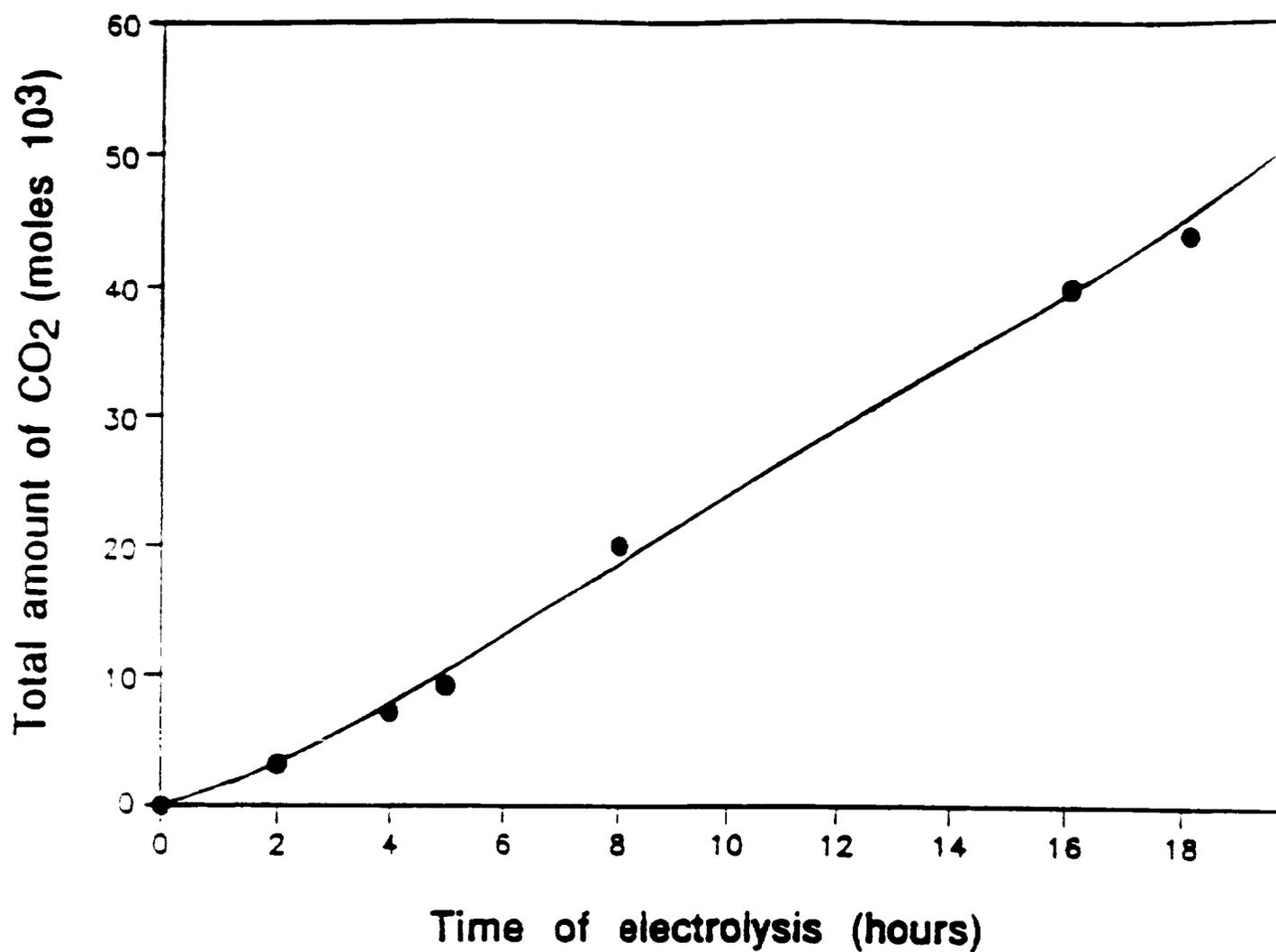
Figure 16: Electrochemical production of CO_2 during yeast electrolysis in 12 M H_2SO_4 using a Pt electrode at 150°C. Yeast concentration 14 g/liter.
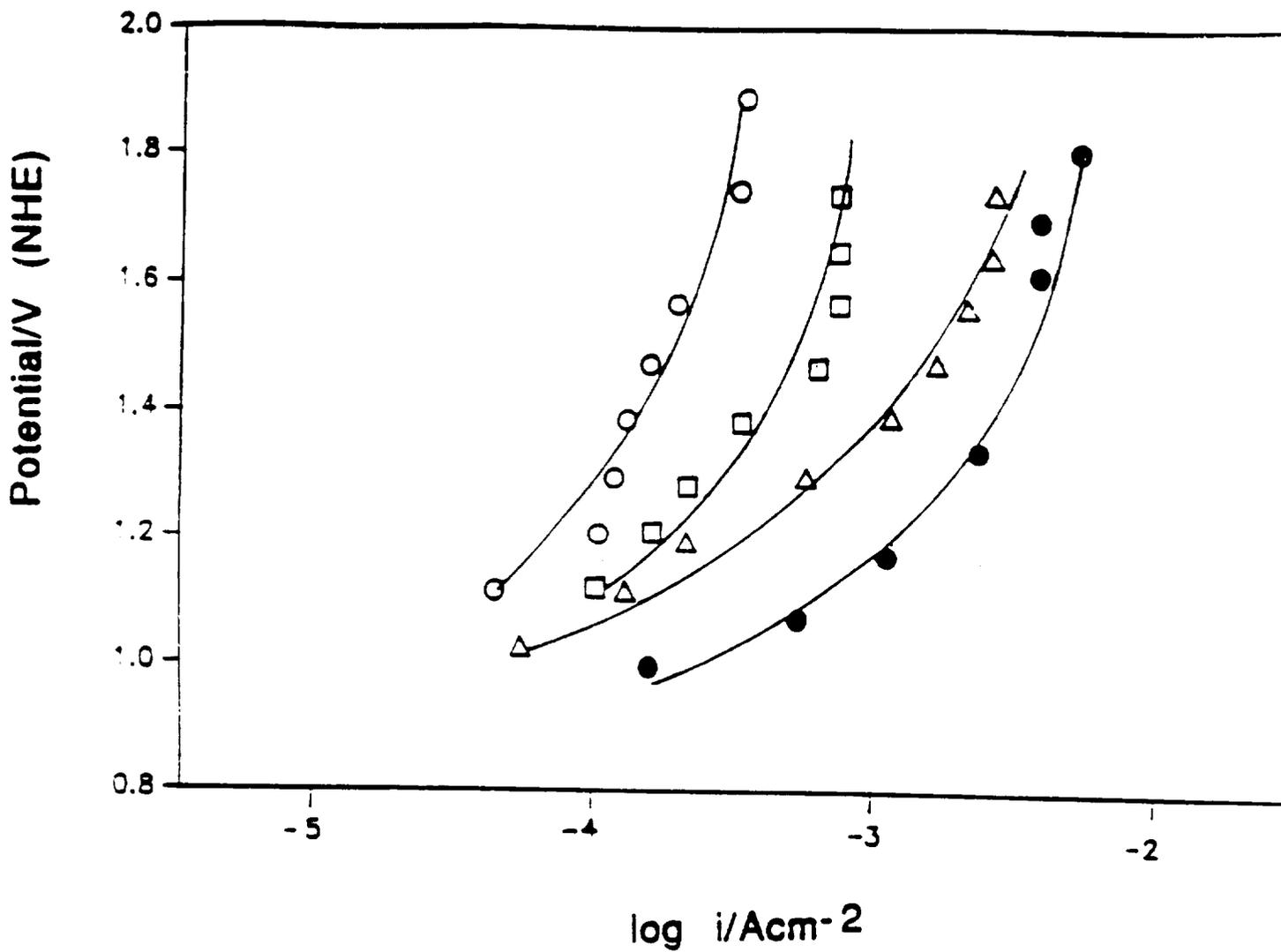
Figure 27: Current/potential relationship at 150°C for oleic acid (O),
cellulose (□), casein (△), and yeast (●) in 12 M H_2SO_4.
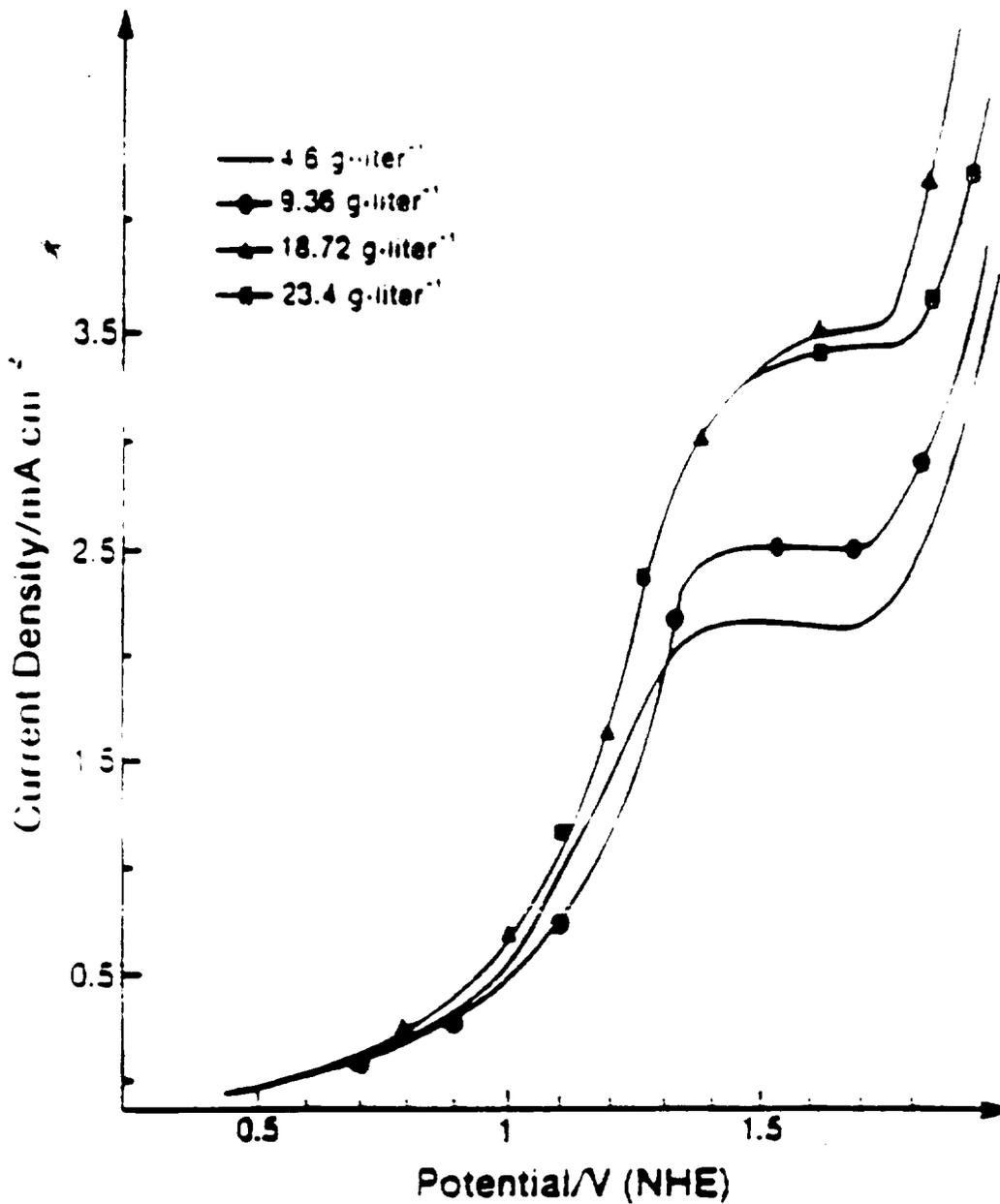
Figure 28: Current-potential curve for the oxidation of artificial fecal waste in 12 M H₂SO₄ on Pt for different concentrations of waste. Potential limits 0.5 1.8 v (NHE). Scan rate 1 mv/s. T = 150°C.

Figure 29
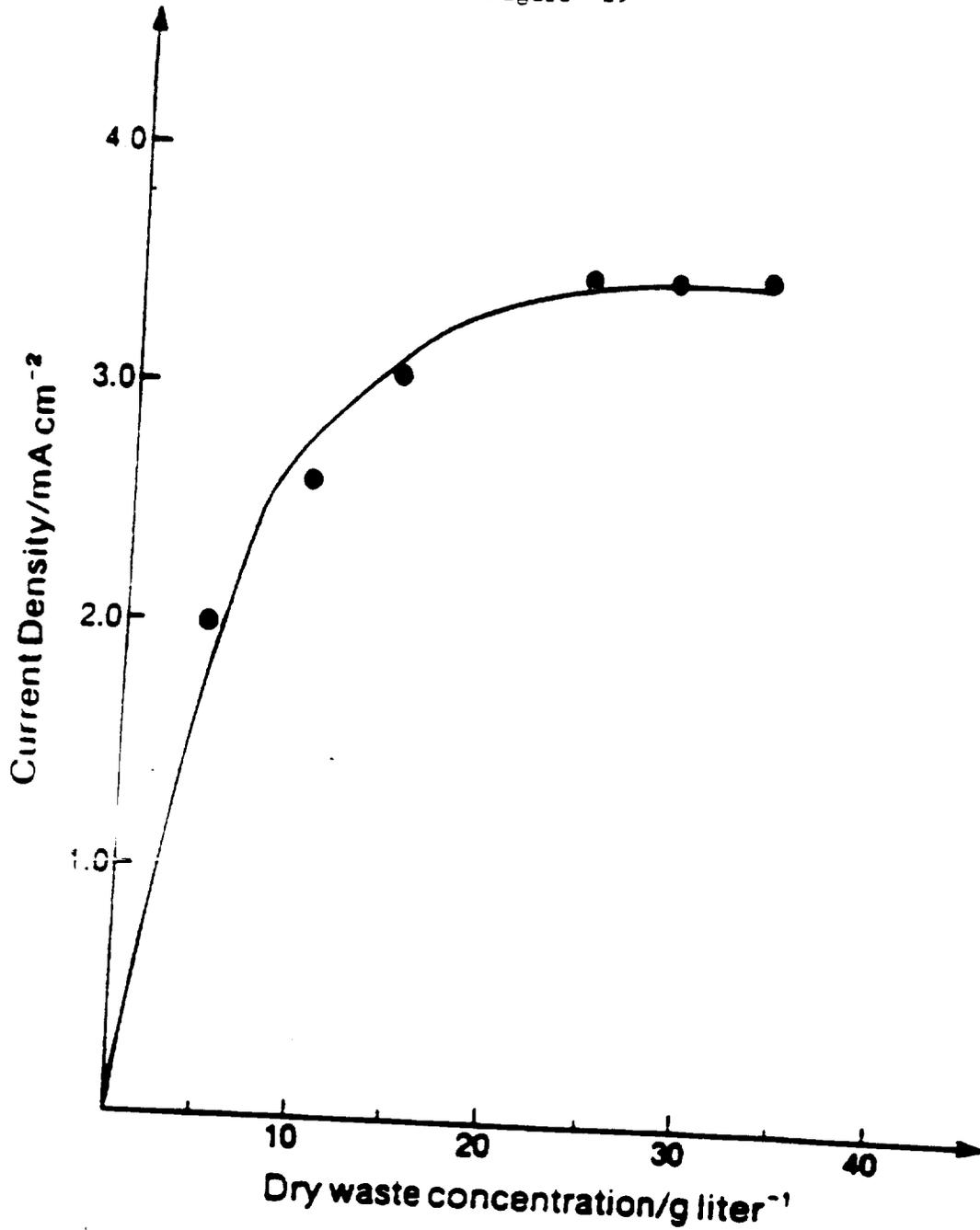
Figure 29: Effect of dry waste concentration on the anodic limiting current density at 150°C in 12 M H_2SO_4, from the voltammetric behavior at Pt. electrode. Potential limits 0.5 - 1.8 v (NHE). Scan rate 1 mv/s.
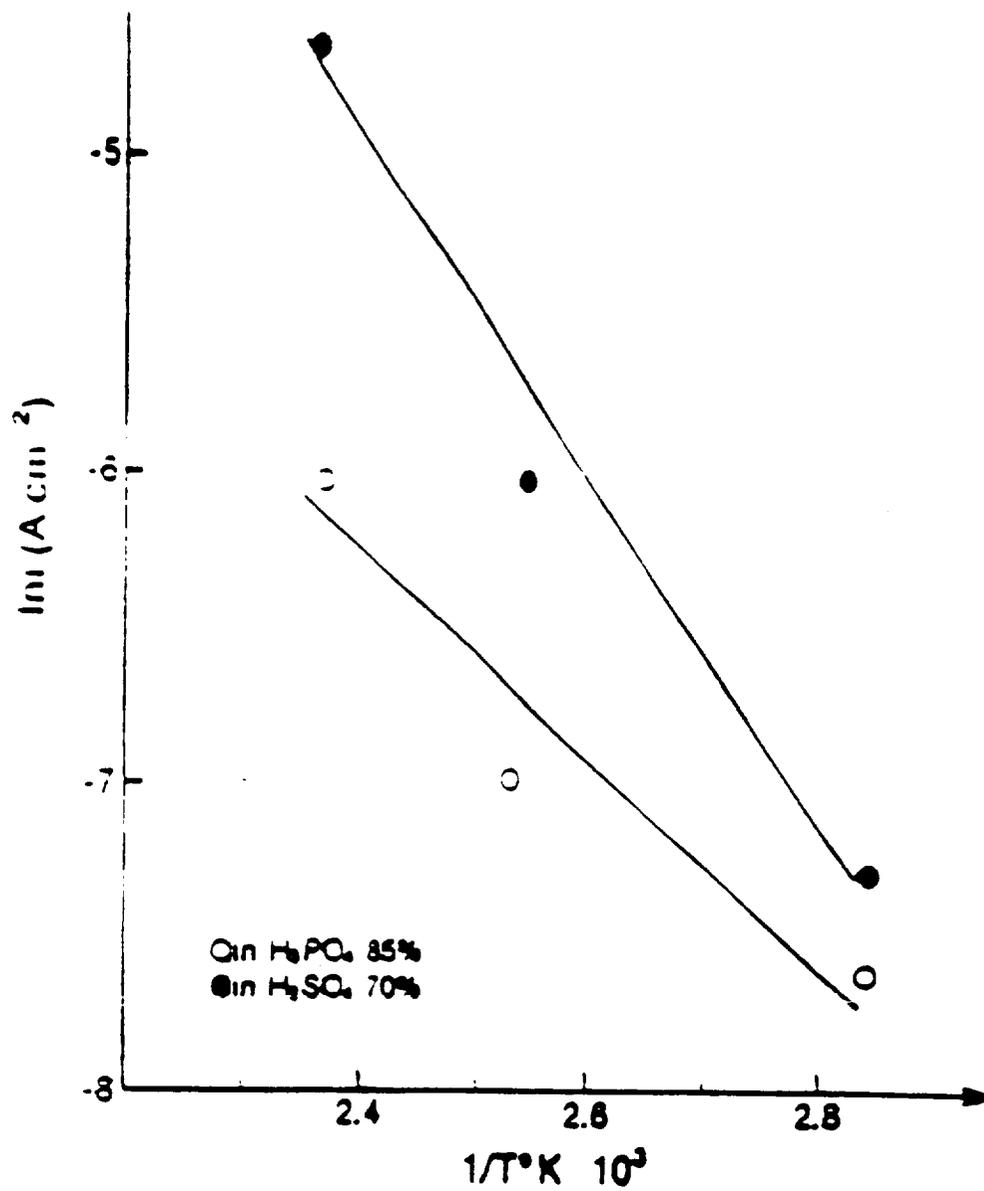
Figure 30: Variation of the anodic limiting current density as a function of temperature on Pt. Waste concentration 23.4 g/liter.
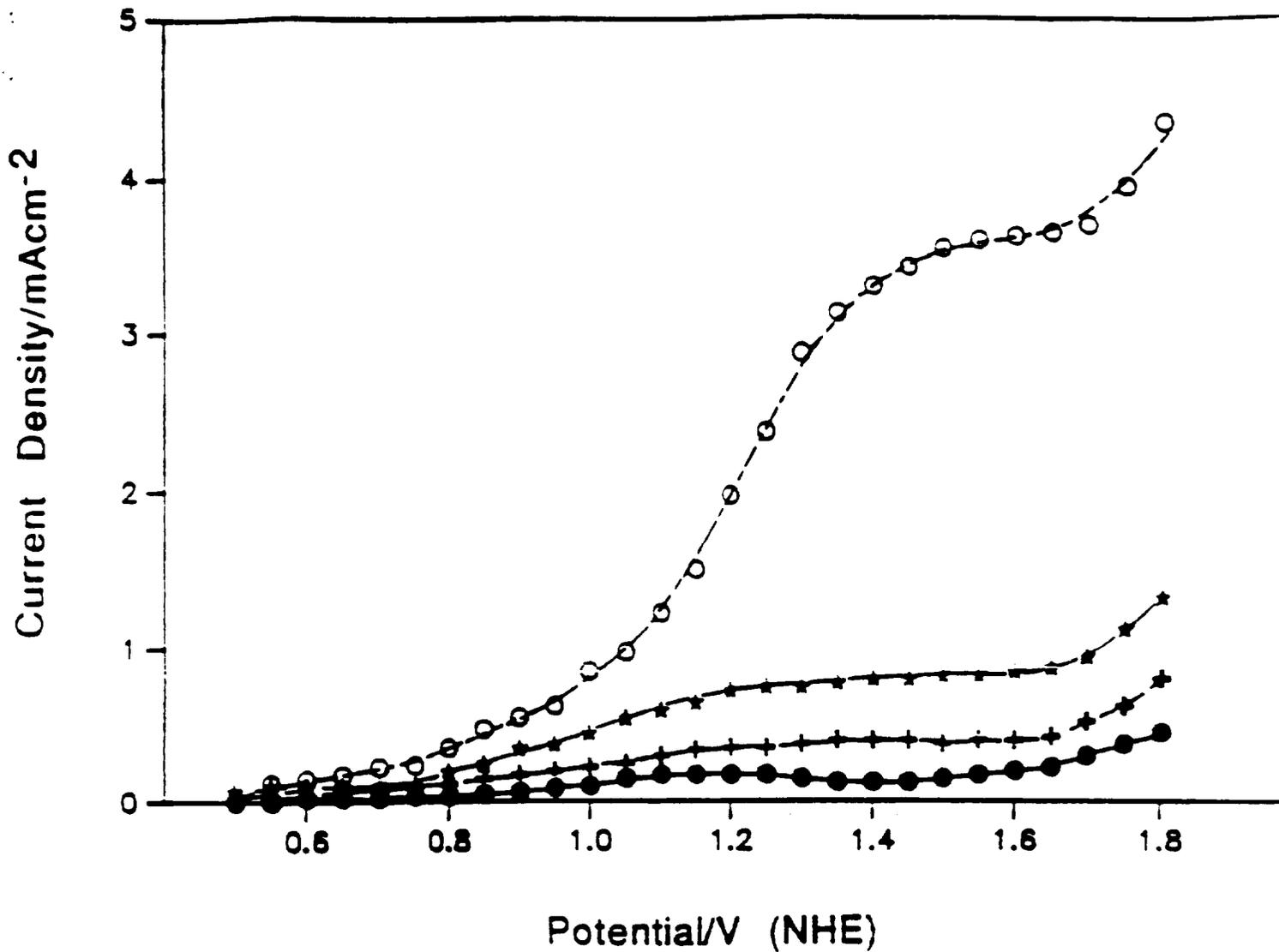
Figure 31: Current potential curves for oxidation of artificial fecal waste at different temperatures on Pt. Potential limits 0.5 - 2.0 v (NHE). Artifical waste concentration 23.4 g/liter. (● 25°C; + 80°C; ★ 120°C; ○ 150°C).
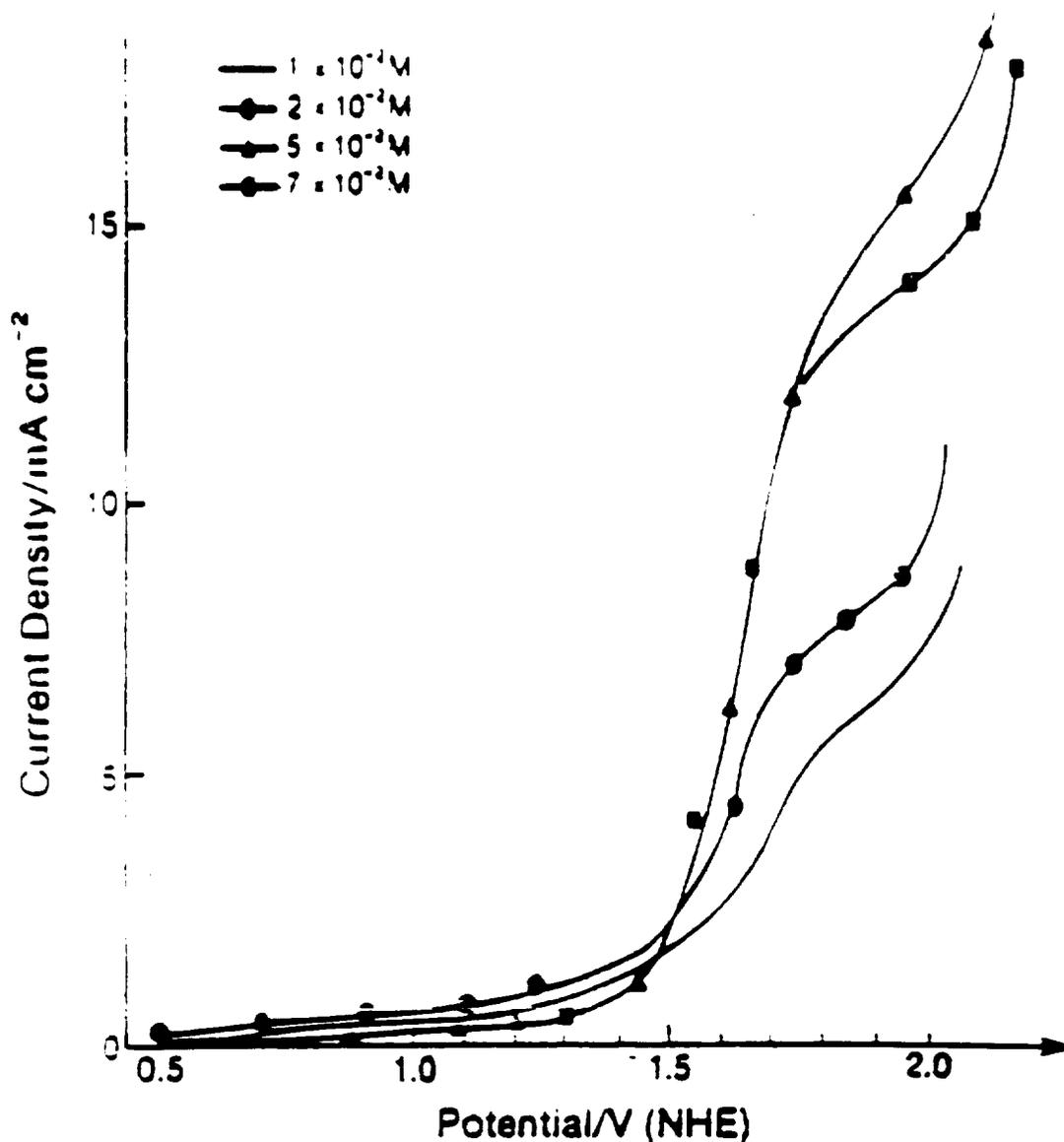
Figure 22. Current-Potential curves for oxidation of artificial fecal waste in 12 M H_2SO_4 using a Pt electrode for different concentrations of Ce^{4+}. Sweep rate 1 mv/s.
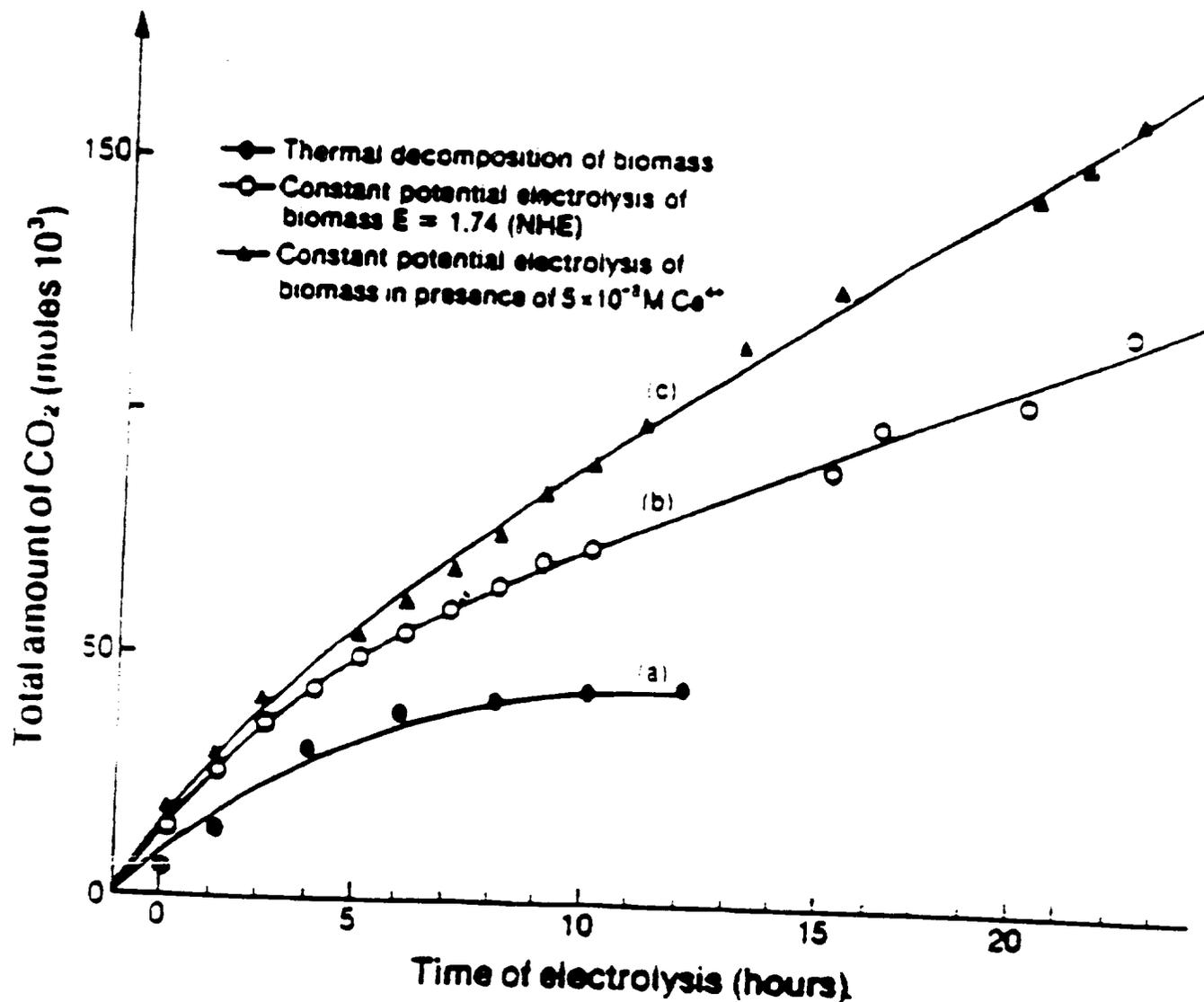
Figure 33: CO_2 production during biomass electrolysis in 12 M H_2SO_4 using a Pt electrode at 150°C. Biomass concentraton 14.04 g/liter.
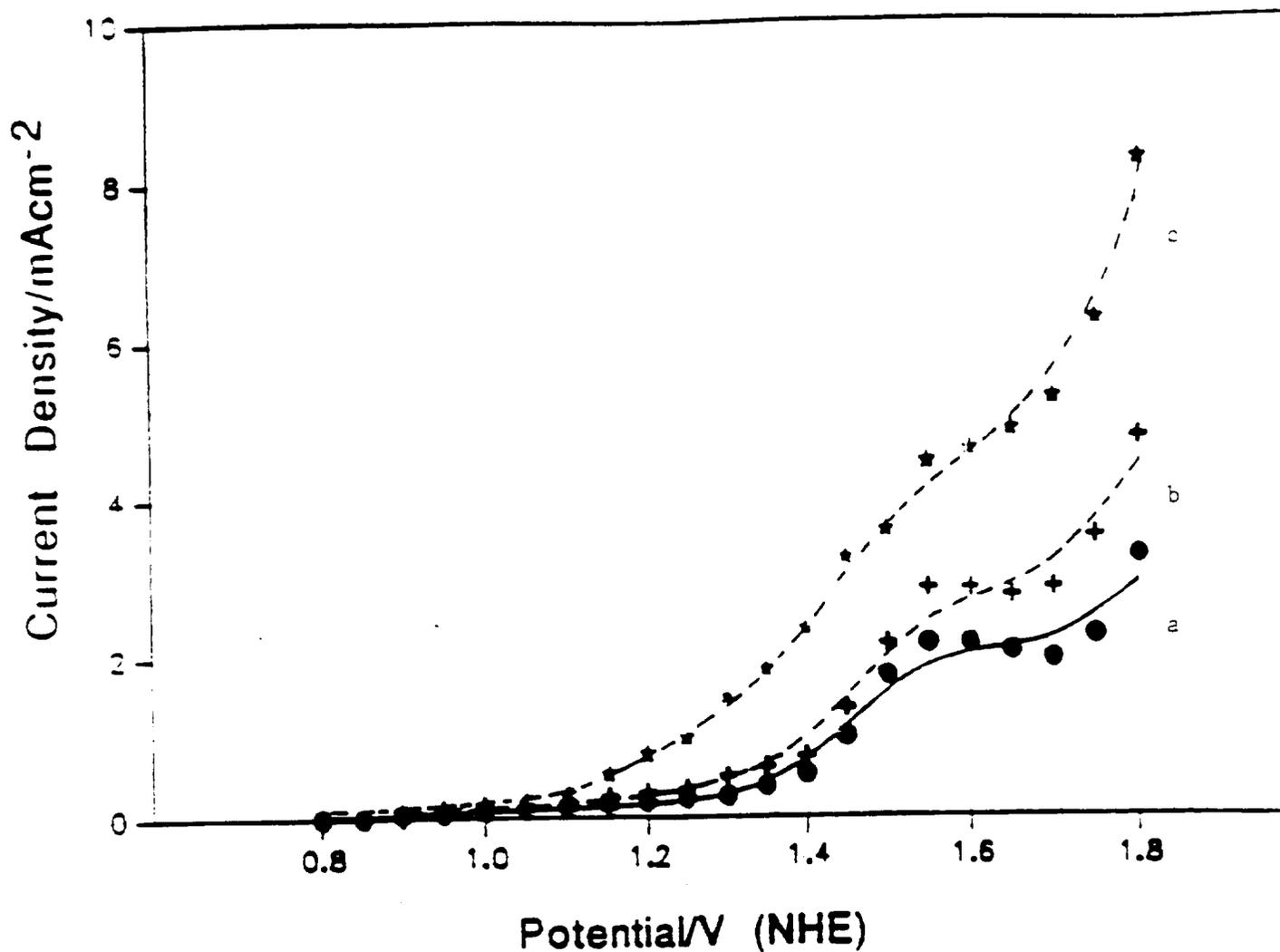
Figure 34: Effect of ultrasound intensity on the voltammetric behavior of
artifical fecal waste in 0.5M H_2SO_4 on Pt. Artificial waste
concentration 14 g/liter. Scan rate 10 mv/s. Temperature 25°C.

(a) No stirring

(b) Stirring with a magnetic stirrer at 6000 rpm.

(c) Ultrasonic stirring at 7 watts/sq. cm.
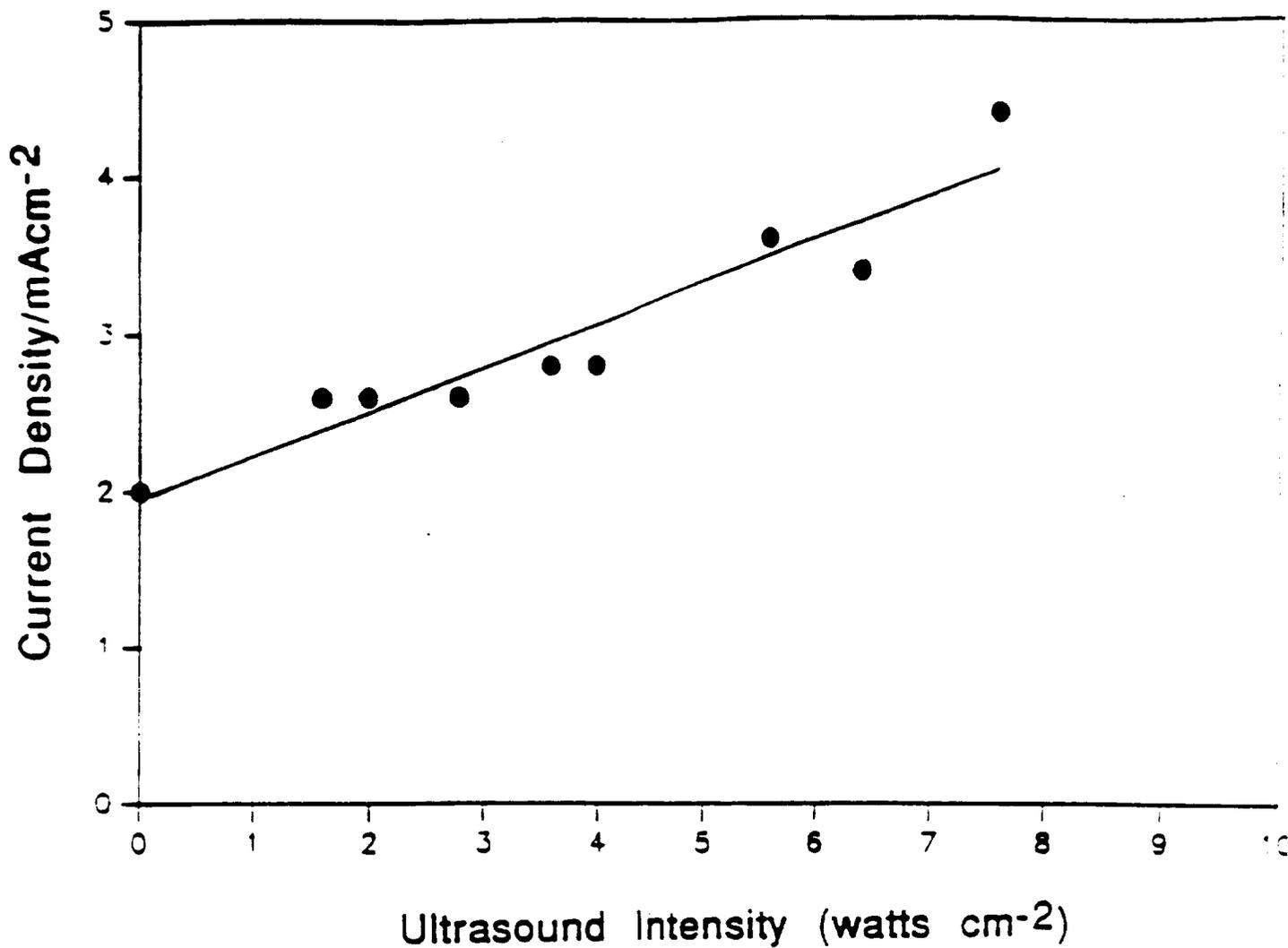
Figure 35

Figure 35: Effect of ultrasound intensity on the limiting current density from the voltammetric behavior of artificial fecal waste in 0.5 M H_2SO_4 on Pt. Artificial waste concentration 14 g/liter.
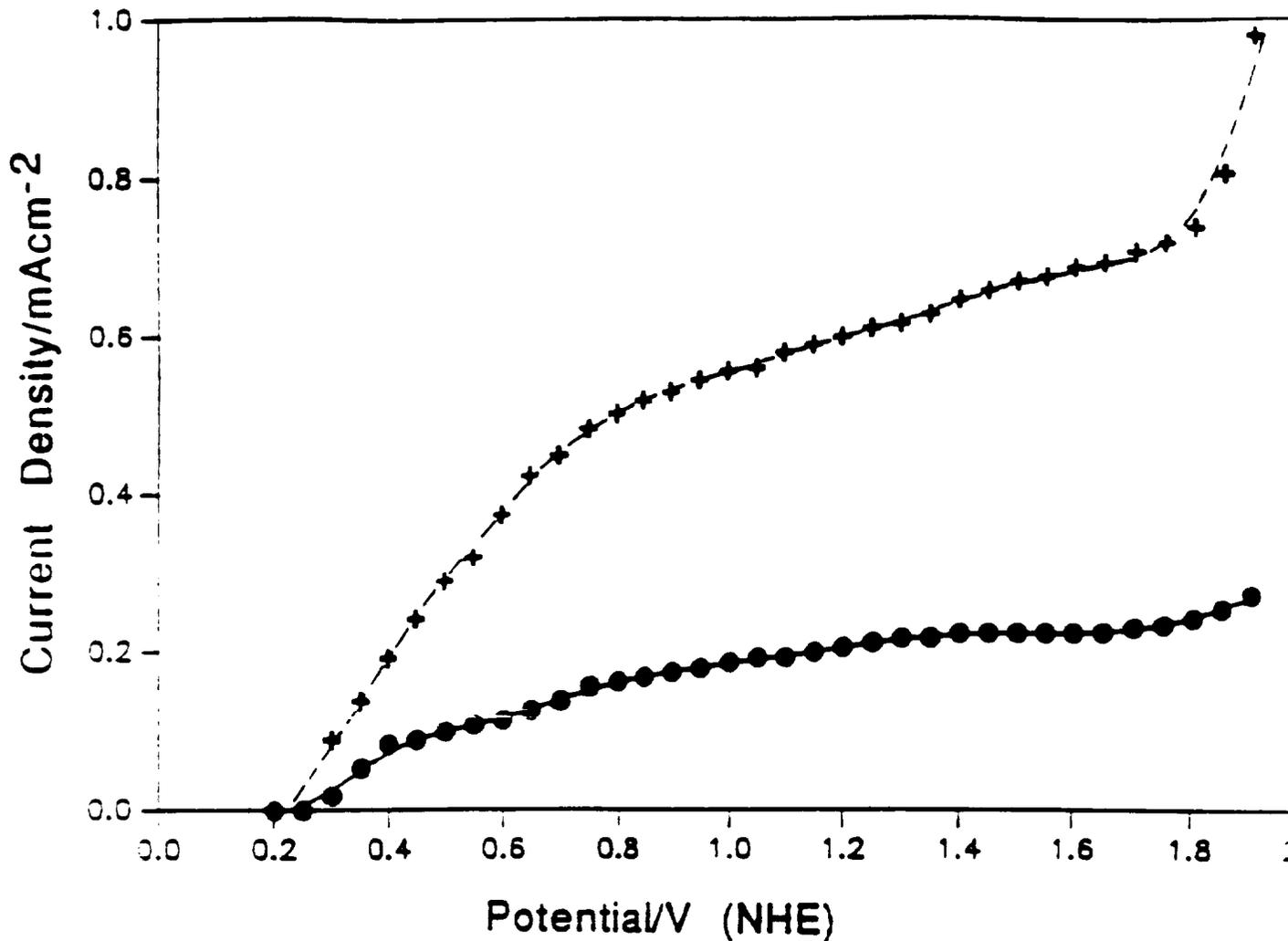
Figure 36: Current/Potential curves for the oxidation of artificial fecal waste in 12 M H_2SO_4 on PbO_2 for different concentrations of waste. Potential limits 0.2 - 2.0 v (NHE). Scan rate 1 mv/s. T = 150°C. (● 4.8 g/liter; ✦ 9.2 and 24 g/liter).
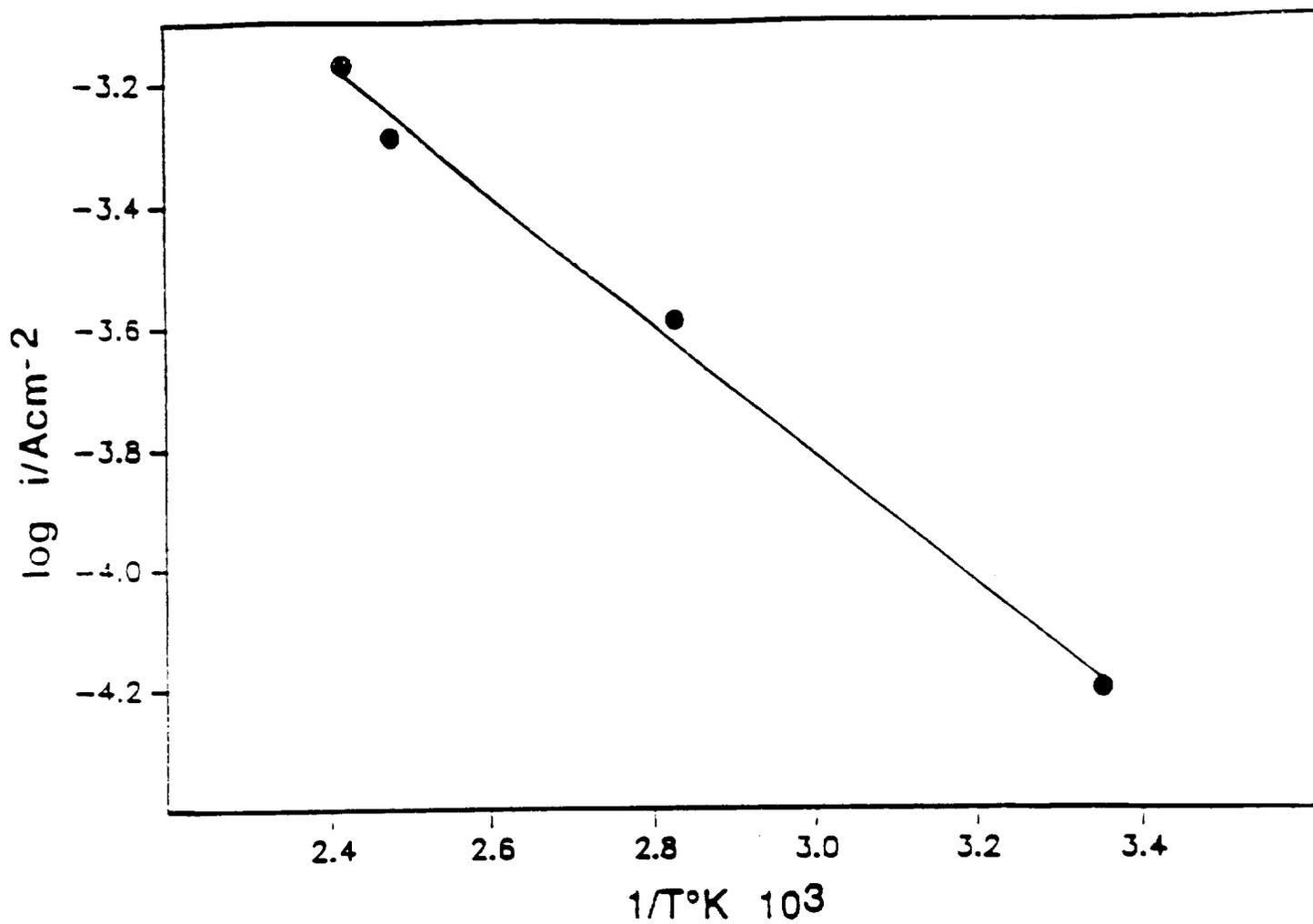
Figure 38: Variation of the anodic limiting current density as a function of
temperature on PbO_2. Waste concentration 24 g/liter.
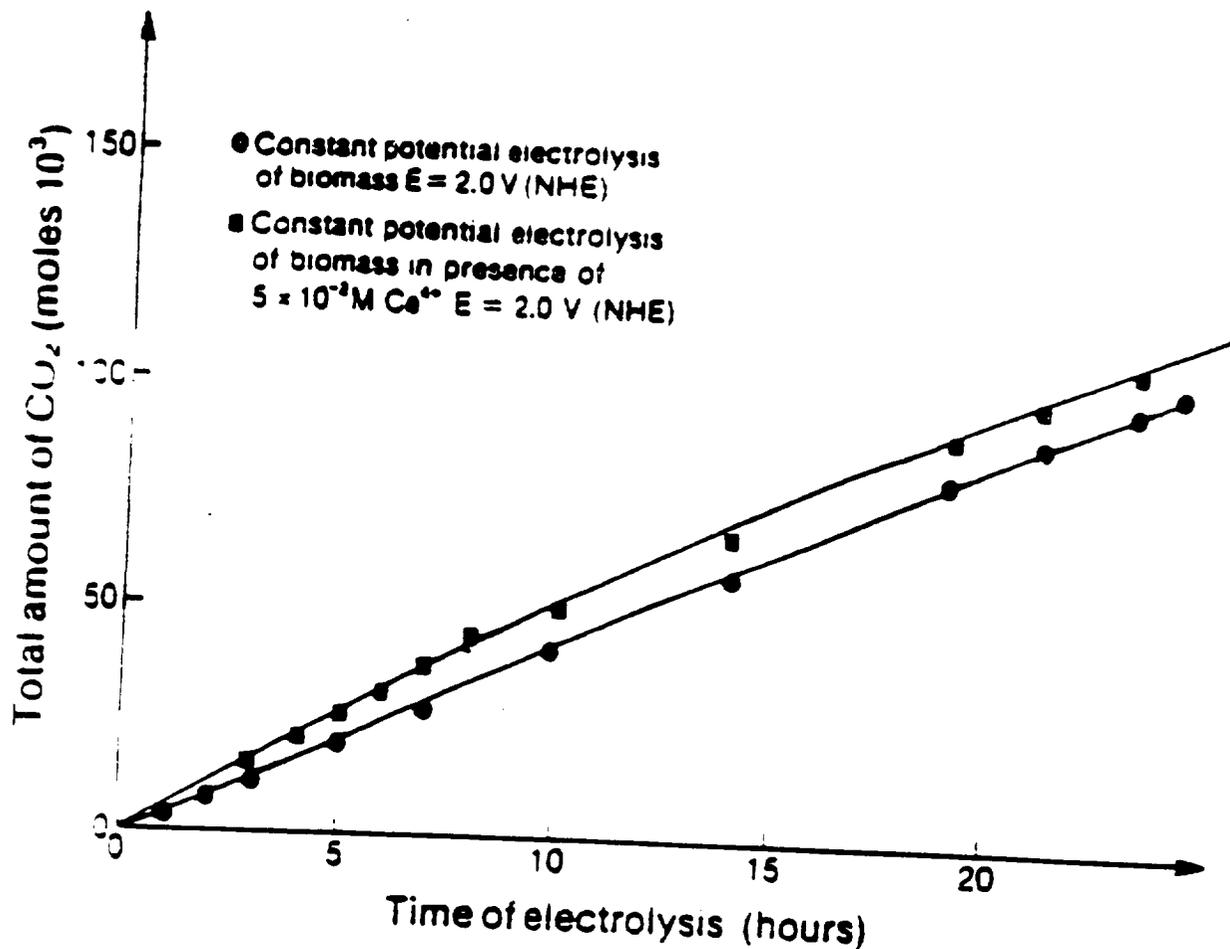
Figure 39: CO_2 production during biomass electrolysis in 5 M H_2SO_4 using a PbO_2 electrode at 80°C. Biomass concentration 14 g/liter.
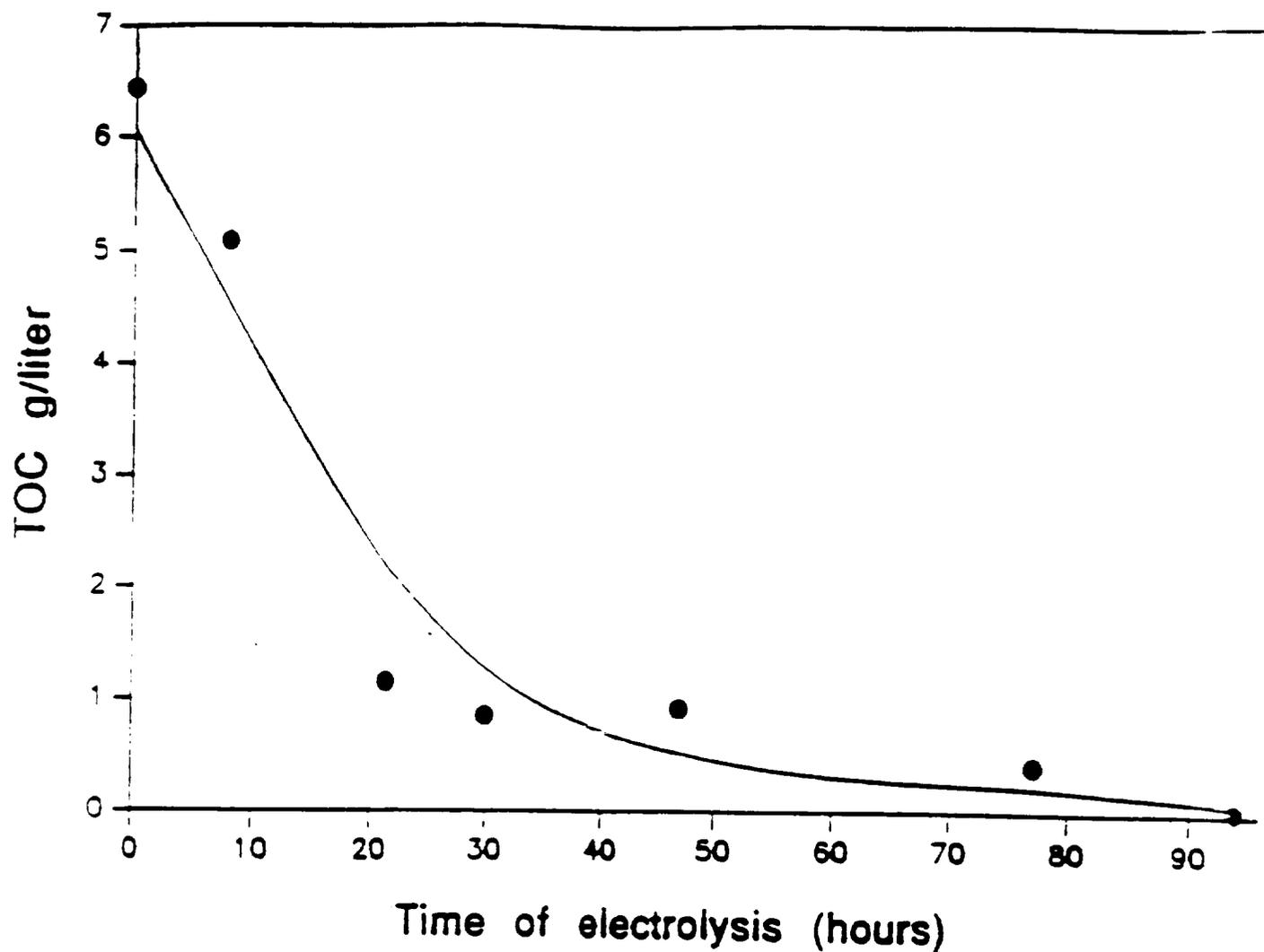
Figure 40: Total organic carbon variation with electrolysis time of artificial fecal waste in 5 M H_2SO_4 at 80°C. Artificial fecal waste concentration 14 g/liter. PbO_2 electrode area 20 cm^2.
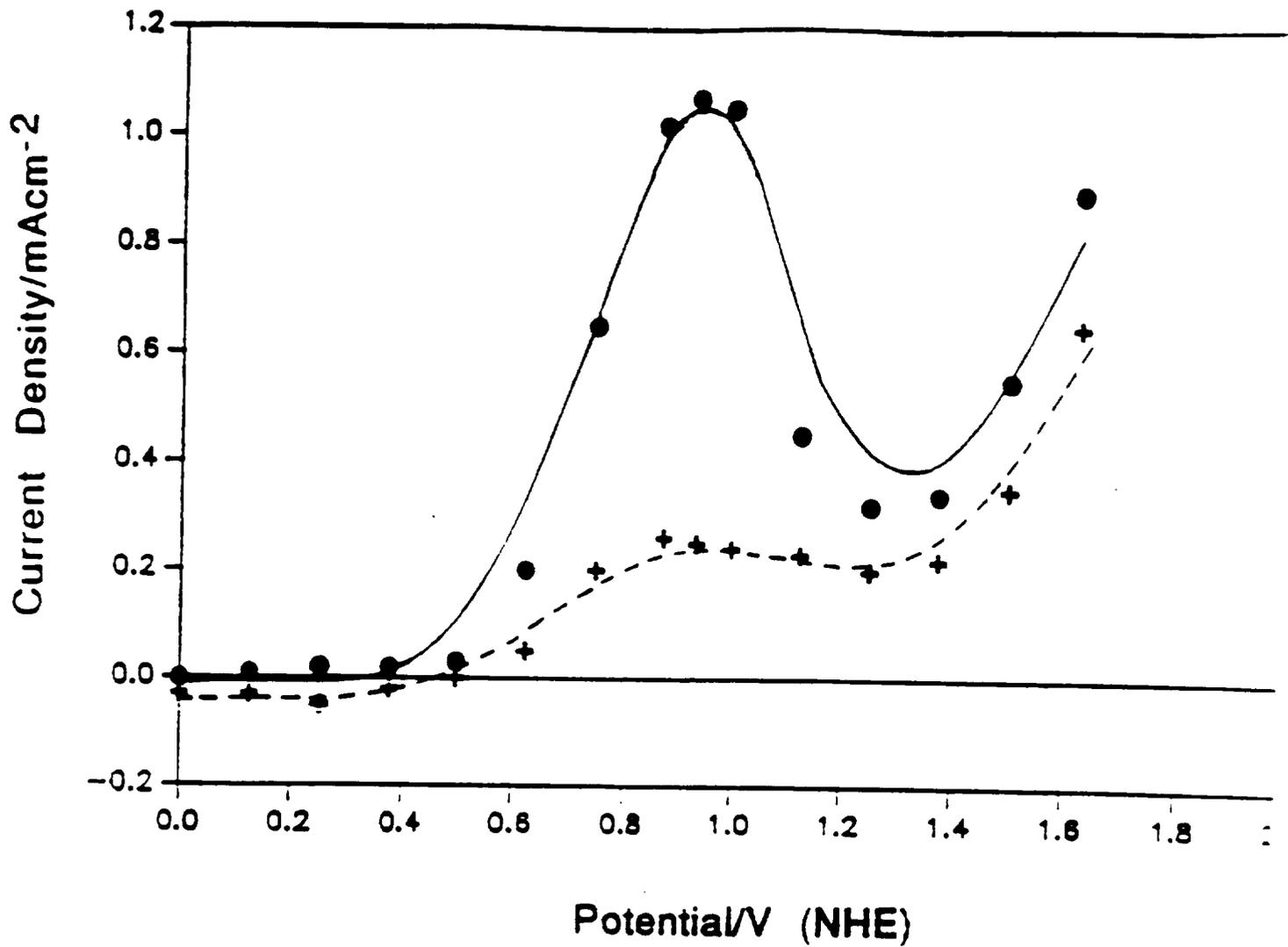
Fig 41 a

Figure 41: Cyclic voltammogram of a mixture of artificial fecal waste and
urine on Pt, at different time of electrolysis. Scan rate 10 mv/s.

(a) Before electrolysis pH = 6.77

(b) After 72 hour electrolysis pH = 2

(c) After 96 hour electrolysis pH = 1.5

Fig 41 b
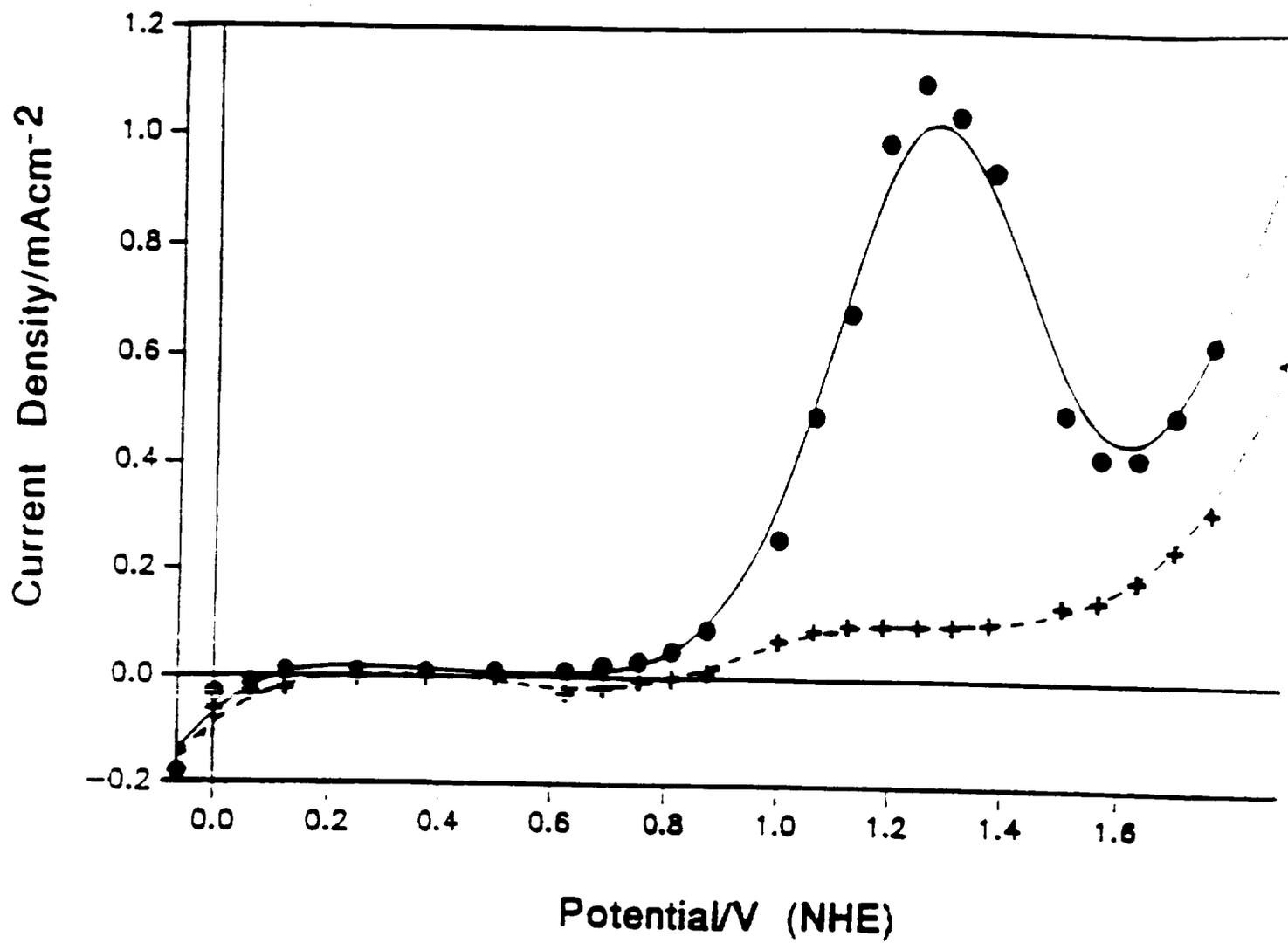
Fig 41 c
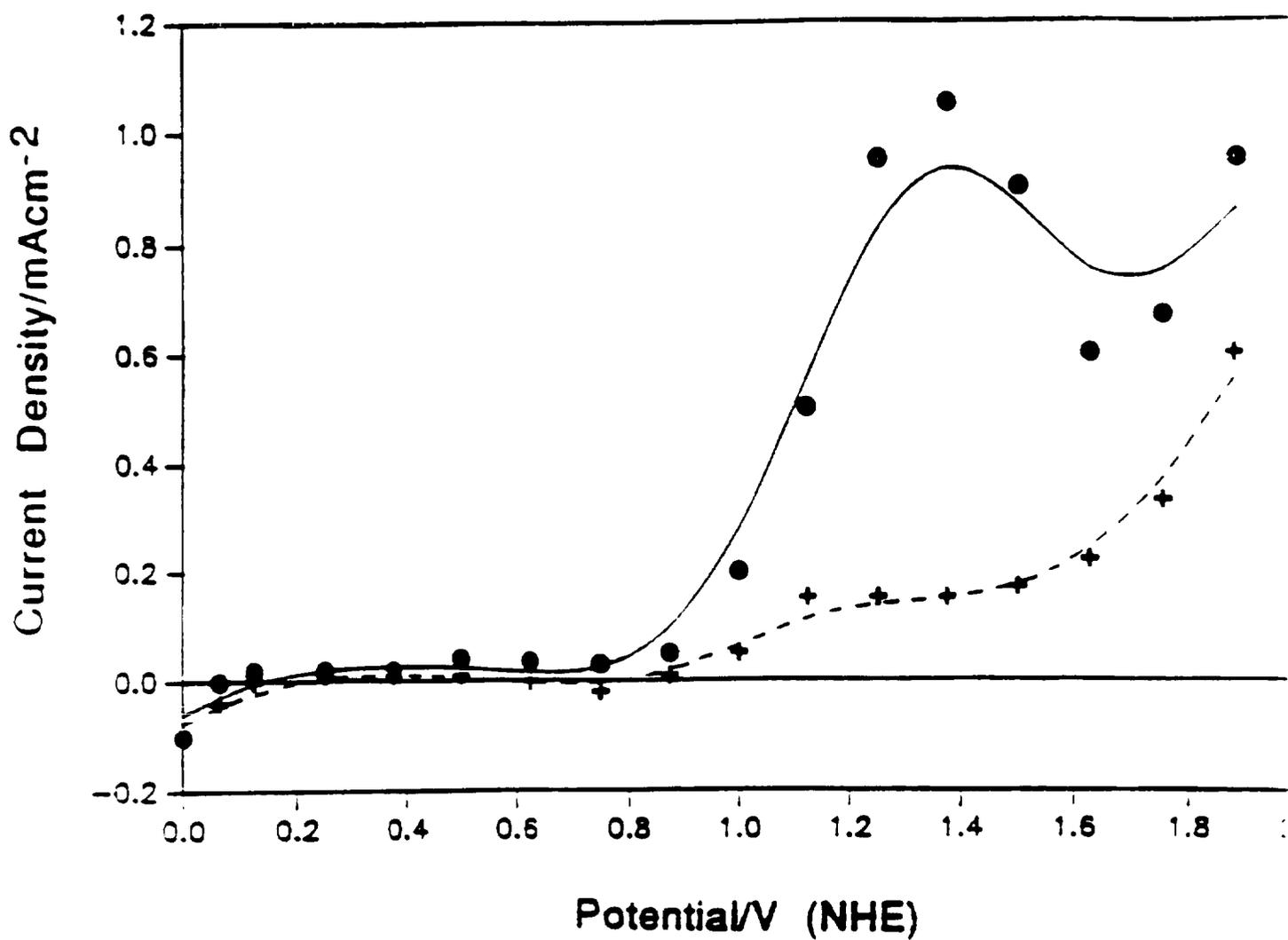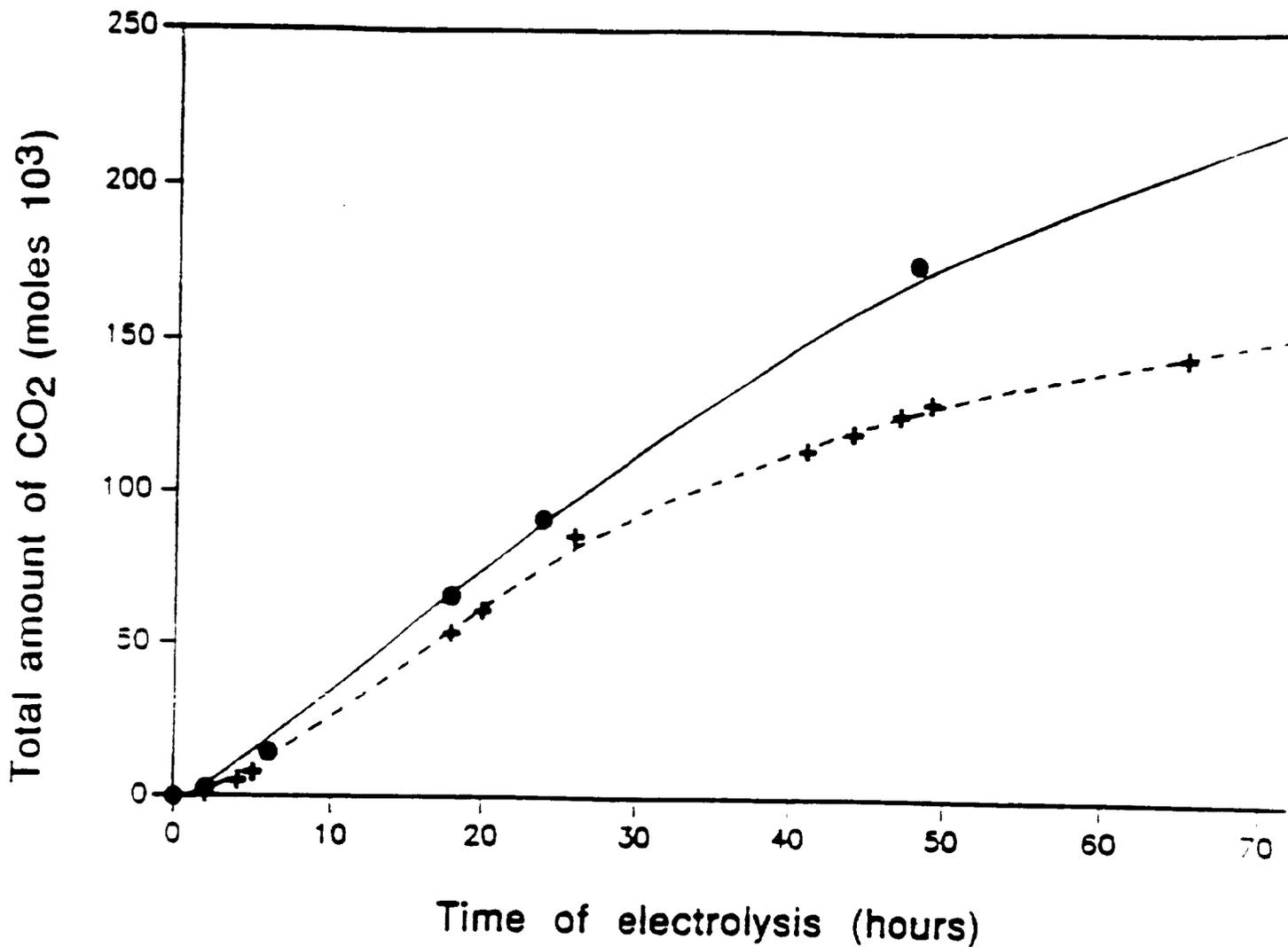
Figure 42: CO_2 production during artificial fecal waste electrolysis in urine using a Pt electrode (100 sq. cm.) at (+ 37°C) and (● 60°C). Artificial fecal waste concentration 13.3 3 g/liter. Current I = 800 MA.
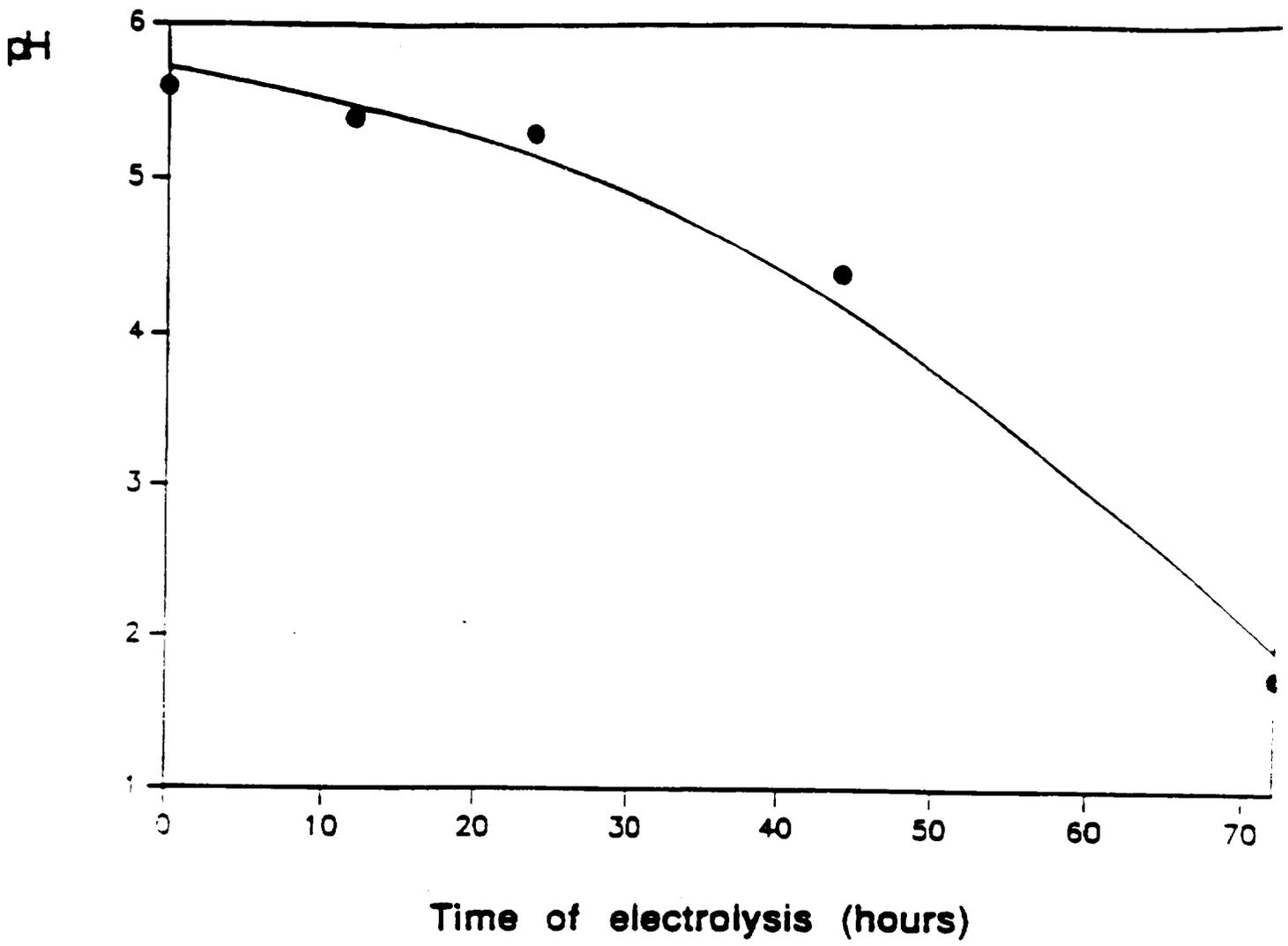
Figure 43: PH variation during artificial fecal waste electrolysis in urine using a Pt. electrode (100 cm^2) at (● 60°C). Artificial waste concentration 13.3 3 g/liter. Current I - 800 MA.
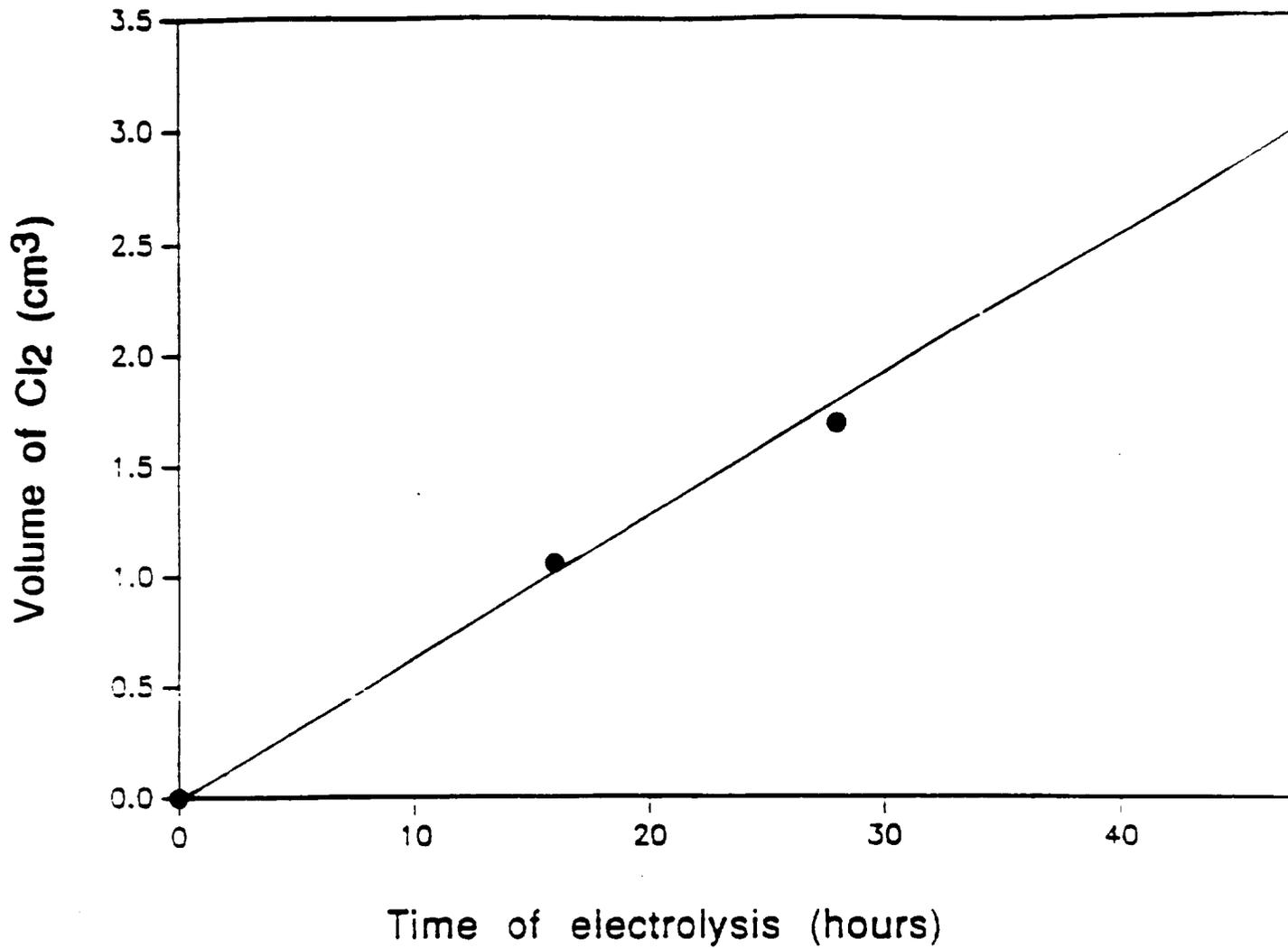
Figure 44: Chlorine production during artificial fecal waste electrolysis using a pt electrode (100 sq. cm.) at (● 60°C). Artificial fecal waste concentration 13.3 3 g/liter. Current I - 800 MA.
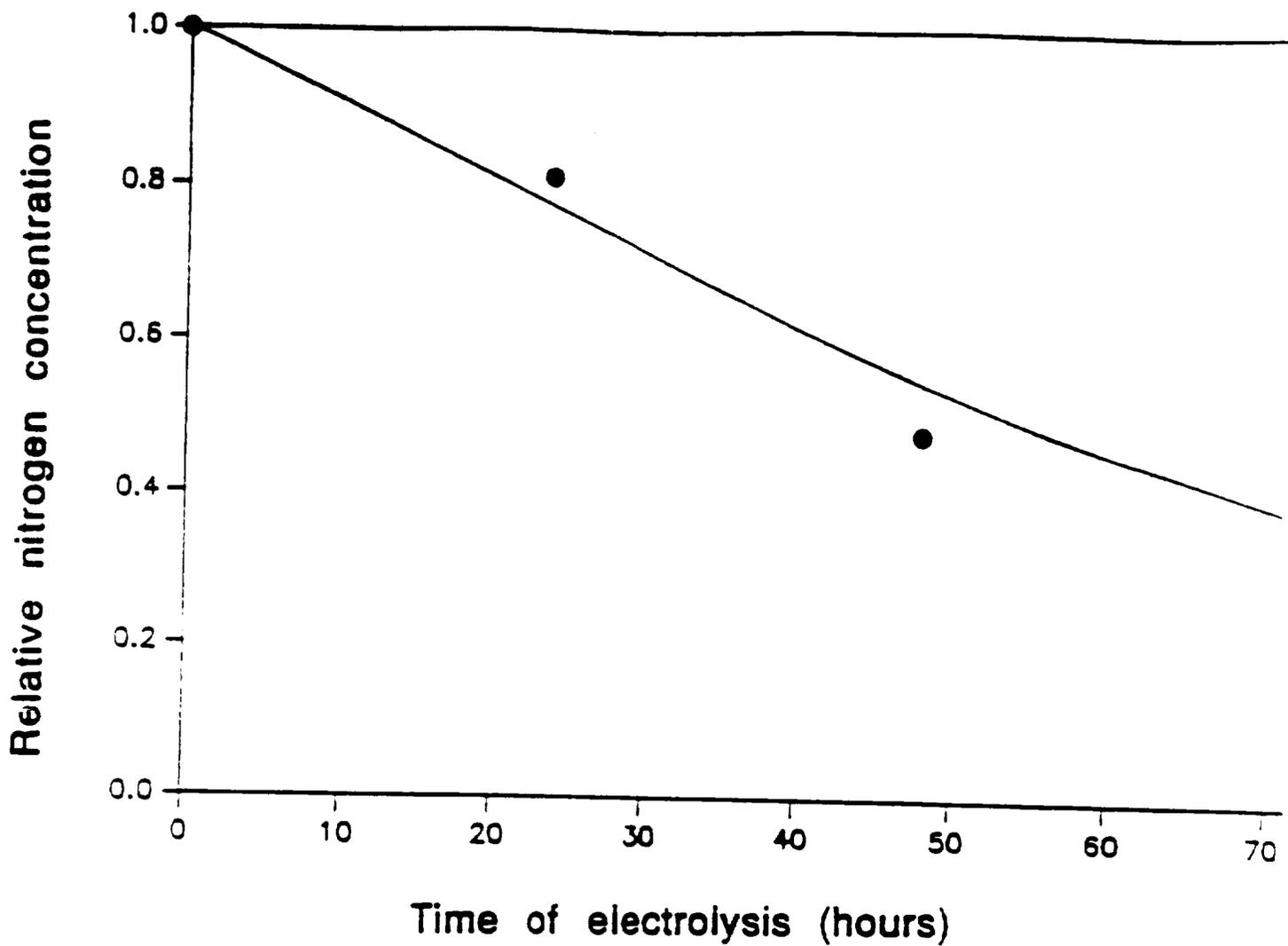
Figure 45: Total nitrogen content variation with electrolysis time of a
mixture of artifical fecal waste and uring at 60°C. Dry waste
concentration 13.3 3 g/liter. Platinum electrode area 100 sq. cm.
Current I = 800 MA.
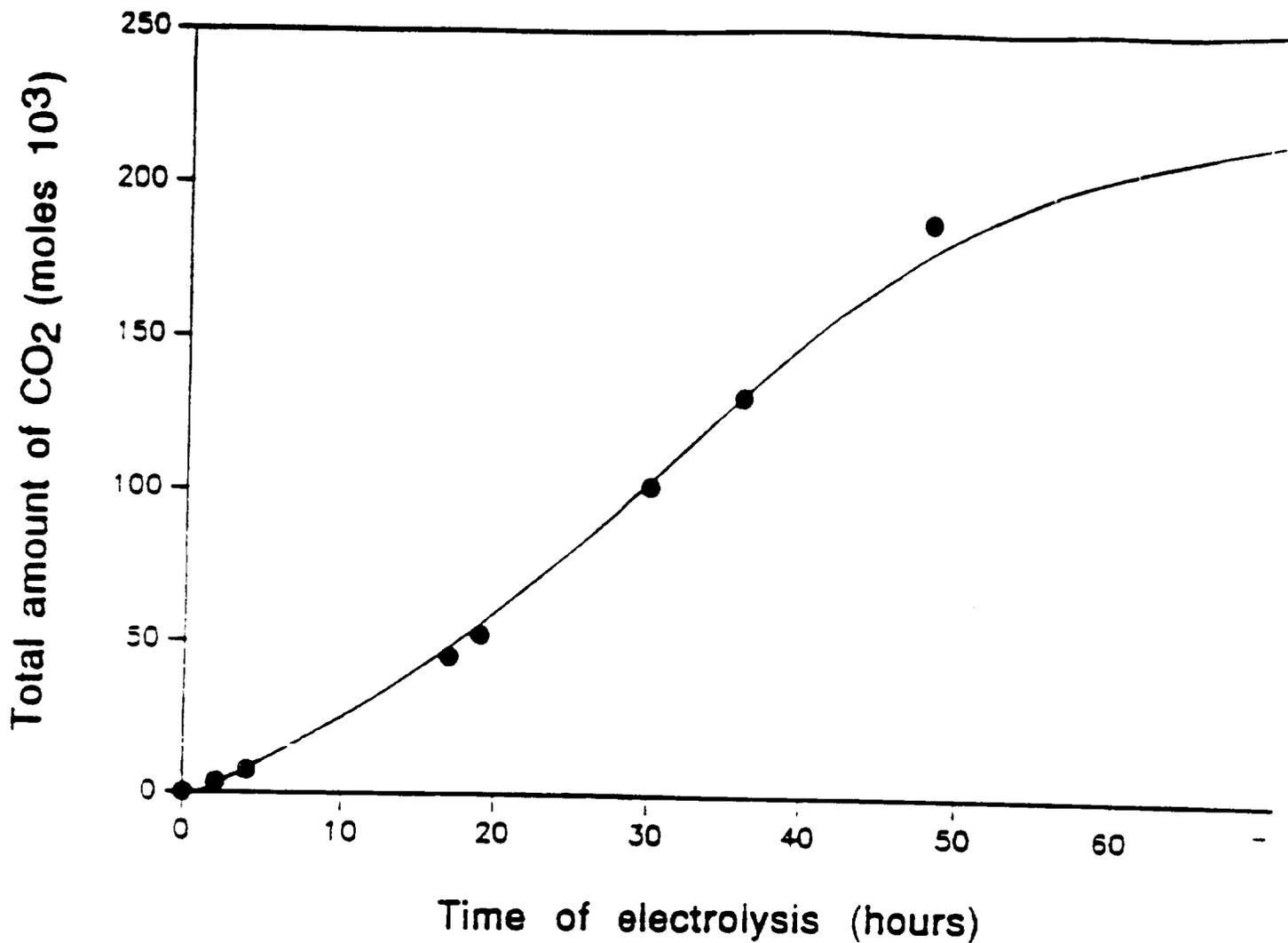
Figure 46: CO_2 production during artificial fecal waste electrolysis using a PbO_2 electrode at 60°C. Artificial fecal waste concentration 13.3 3 g/liter. Current I = 800 MA.
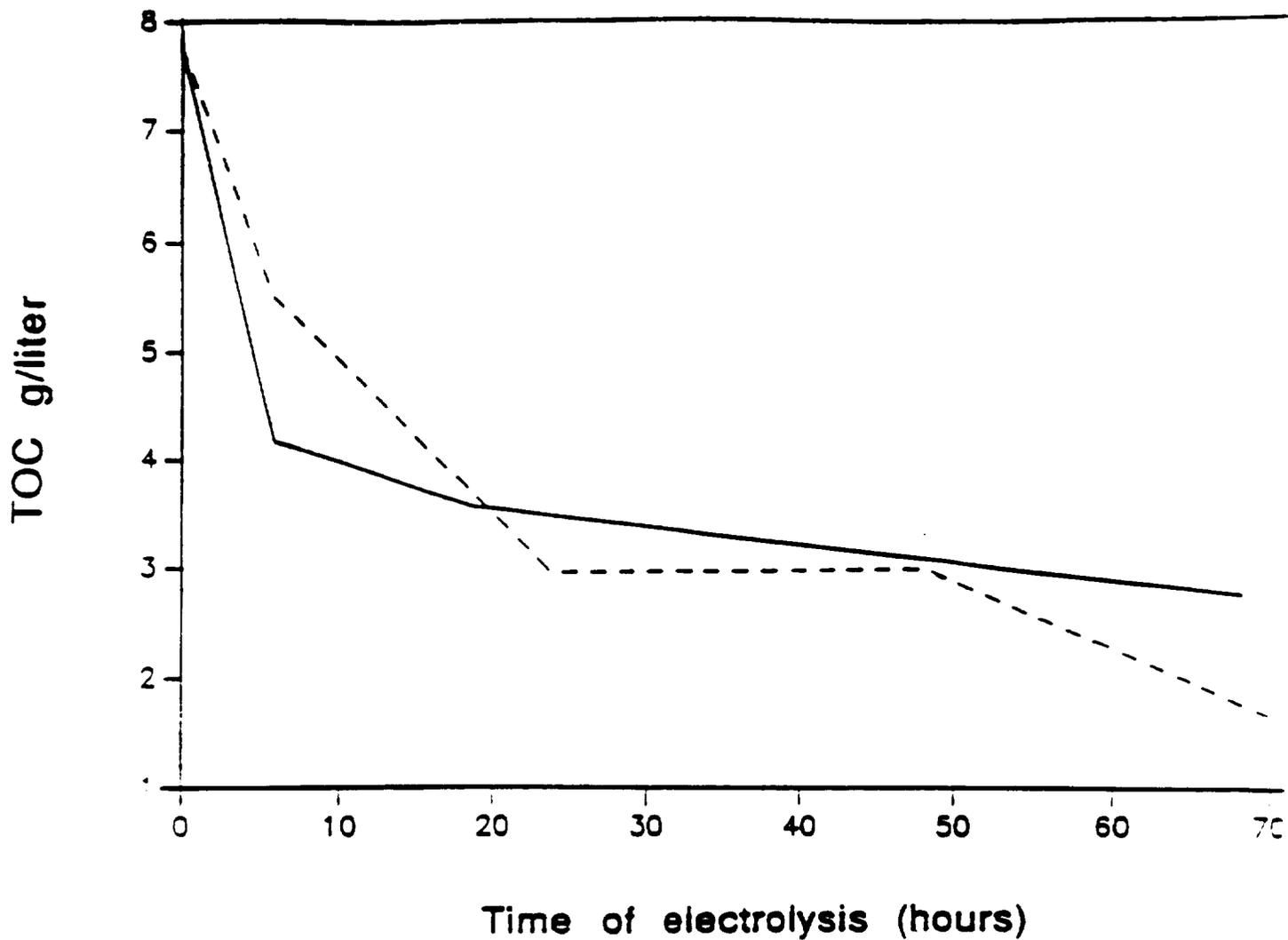
Figure 47: Total organic carbon variation with electrolysis time of a mixture of artificial fecal waste and urine at two different temperatures (37°C) (60°C). Dry waste concentration 13.3 3 g/liter. Pt electrodes area 100 sq. cm. Current I - 800 MA.
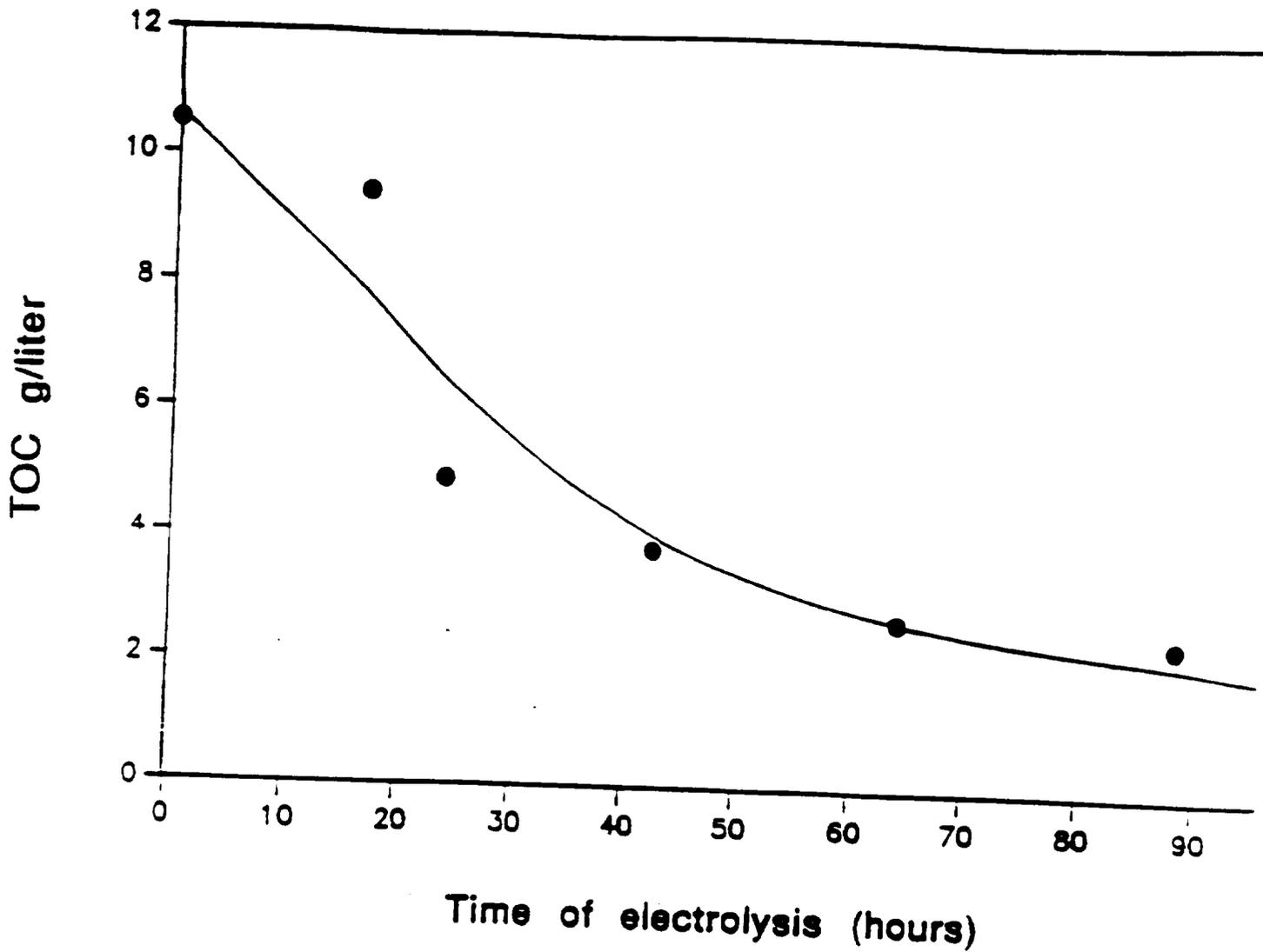
Figure 48: Total organic carbon variation with electrolysis time of a mixture of artificial fecal waste with urine at 60°C on PbO_2 electrode. Dry waste concentration 13.3 3 g/liter. Current I = 800 MA.

MILLILITER 0.04 N TITRANT
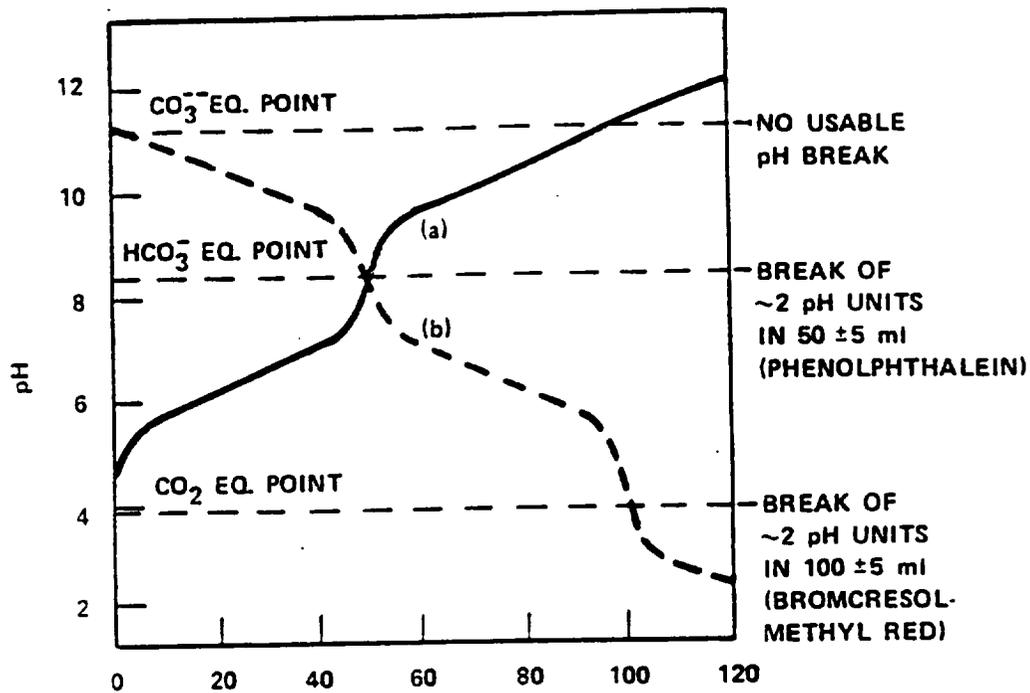
Figure 49 .. Titration curves for 50 cc of .04M H_2CO_3 with .04M NaOH (curve a) and 50cc of .04M Na_2CO_3 with .04M HCl (curve b).
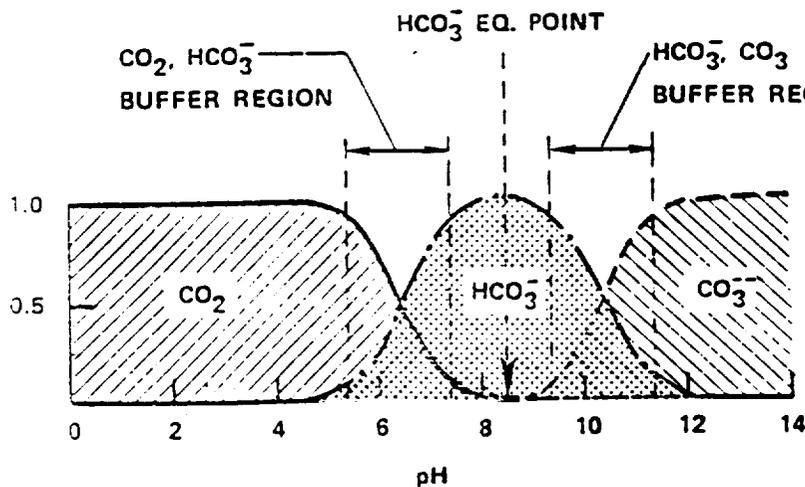

Figure 50 . Fractions of carbonate species as a function of pH.

Table 1

	E_o	$E_{p/2}$	Ref
Urea	-0.738(a)		
Glucose	-0.36		
Formate		-0.432	[38]
Mannitol	+0.02(a)		
Succinate	+0.11(a)		
Glutamine	+0.11(a)		
Butaraldehyde	+0.11(a)		
Casein		(E_p) +1.0(b)	[22]
Adenine		+1.25(c)	[38]
Uric Acid		+0.86(d)	[38]
Saccnaromyces cerevisae		(E_p) +0.98(e)	[39]

Peak or half wave potentials are signified by E_p or $E_p/2$ repectively.

(a) Calculated from $\Delta G_o f$ values given in Ref 40.

(b) 0.1M NaOH on Platinum.

(c) Aqueous buffer (pH 5.7) on platinum.

(d) 2M H_2SO_4 on graphite.

(e) 0.1M phosphate buffer (pH 7.0) on graphite.

32

Table 2

Solvent	Electrolyte	Anodic Limit
Acetic acid	NaOAc	+2.0
Acetone	$(nBu)_4NClO_4$	+1.6
Acetonitrile	$LiClO_4$	+2.5
Acetonitrile	$(Et)_4NBF_4$	+3.2
Dimethylformamide	$(nBu)_4NClO_4$	+1.6
Methylene chloride	$(nBu)_4NClO_4$	+1.8
Nitrobenzene	$(nPr)_4NClO_4$	+1.6
Nitromethane	$Mg(ClO_4)_2$	+2.2
Propylene carbonate	Et_4NClO_4	+1.7
Pyridine	Et_4NClO_4	+3.3
Sulfolane	Et_4NClO_4	+3.0
Tetrahydrofuran	Et_4NClO_4	+1.6

Table 3   Contents of Artificial Fecal Waste

Waste Component	Weight (kg)	% Of Total Dry Weight
Cellulose	0.60	33%
Torpulina	0.43	25%
E.coli	0.12	7%
Casein	0.17	10%
Oleic acid	0.37	20%
KCl	0.04	2%
NaCl	0.04	2%
CaCl$_2$	0.03	1%
Water	2.8	-

34